

**UNCLASSIFIED**

**AD 4 5 2 7 9 2**

**DEFENSE DOCUMENTATION CENTER**

**FOR**

**SCIENTIFIC AND TECHNICAL INFORMATION**

**CAMERON STATION, ALEXANDRIA, VIRGINIA**



**UNCLASSIFIED**

**NOTICE:** When government or other drawings, specifications or other data are used for any purpose other than in connection with a definitely related government procurement operation, the U. S. Government thereby incurs no responsibility, nor any obligation whatsoever; and the fact that the Government may have formulated, furnished, or in any way supplied the said drawings, specifications, or other data is not to be regarded by implication or otherwise as in any manner licensing the holder or any other person or corporation, or conveying any rights or permission to manufacture, use or sell any patented invention that may in any way be related thereto.



EFFECTS OF AIRFRAME GEOMETRY  
ON DOWNWASH PROBLEMS OF  
TANDEM DUCTED-PROPELLER  
VTOL AIRCRAFT

DATE Jan. 1964 REPORT NO. 179T80-6

Prepared Under Navy,  
Bureau of Naval Weapons  
Contract N0w61-0926-c

PREPARED

R. R. Pruyn  
R. R. Pruyn,  
Manager, Research Engineering

NO. OF PAGES

## ABSTRACT

A full scale half-model simulation of a dual tandem ducted propeller VTOL aircraft has been tested at heights of less than two duct diameters above sand and water terrain. Data on terrain transport, terrain caused aircraft damage, flow field measurements and ducted propeller performance were obtained. These tests were conducted at propeller disc loadings up to 60 pounds per square foot with various aircraft configurations and ducted propeller orientations. The dual tandem configuration was found to cause a significant increase in downwash problems compared to isolated propeller configurations previously tested. Reduced performance, severe engine and propeller damage and an oscillating aerodynamic interference were experienced. Several promising devices to alleviate downwash problems were evaluated.

## FOREWORD

This report was prepared by the Kellett Aircraft Corporation, Willow Grove, Pennsylvania for the Bureau of Naval Weapons of the U.S. Navy under contract N0w61-0926-c. The results of a full scale experimental investigation of the effects of airframe geometry on the downwash problems encountered by a tandem ducted propeller VTOL aircraft are presented.

The results and conclusions presented herein are based on work initiated in July 1961. The test program was concluded in May, 1963. The investigation was conducted under the direction of Mr. Richard R. Pruyn, Manager of Research for Kellett, Mr. James Jones was the Kellett project engineer.

The aid and suggestions of Mr. W. Koven and Mr. B. Stein of the Bureau of Naval Weapons are gratefully acknowledged. The assistance and supervision of these men has significantly contributed to the success of this program.

A motion picture film (16mm color sound) supplements this report and can be obtained from the Bureau of Naval Weapons. Since many of the conclusions drawn from the testing are necessarily based on qualitative evidence, this film is a valuable aid to the understanding of downwash problems.

## TABLE OF CONTENTS

	<u>Page</u>
ABSTRACT	ii
FOREWORD	iii
LIST OF ILLUSTRATIONS	vi
LIST OF TABLES	x
LIST OF SYMBOLS	xi
I INTRODUCTION	1
II TEST APPARATUS AND PROCEDURES	3
A. Test Facility	3
B. Test Conditions	6
C. Instrumentation	7
D. Test Procedure	10
E. Airframe Geometry	12
III DISCUSSION OF PROBLEM	14
A. Flow Field of Dual Tandem VTOL Aircraft	14
B. Mechanism of Particle Entrainment	15
C. Relation of this Program to State of Art	16
IV QUANTITATIVE TEST RESULTS	19
A. Flow Field Measurements	19
1. Upwash Data	19
2. Fuselage Pressure	19
B. Terrain Entrainment	22
1. Particle Cloud Height	22
2. Ducted Propeller Ingestion	24
3. Sand Collected Near Engines	25

## TABLE OF CONTENTS (Cont'd.)

	<u>Page</u>
C. Performance	27
1. Aerodynamic Interference	30
2. Effect of Operating Height	30
3. Effect of Terrain	32
4. Effect of Configuration	34
D. Evaluation of Alleviation Devices	35
1. Model Tests	36
2. Full Scale Tests	37
a. Ground Cover	37
b. Deflector Wing	38
c. Duct Inclination	39
V DISCUSSION OF QUALITATIVE RESULTS	41
A. Damage Due to Qualitative Terrain	42
1. Propeller and Duct Erosion	42
2. Power Plant Erosion	44
3. Airframe Damage	46
4. Effects on Ground Personnel and Supporting Equipment	47
B. Visibility	48
1. Effect of Configuration	49
2. Effect of Height, Over Water	49
3. Effect of Terrain Conditions	50
C. Evaluation of Operational Environment	51
VI CONCLUSIONS	54
VII RECOMMENDATIONS	57
VIII REFERENCES	60
APPENDIX I VISIBILITY METER DESIGN AND TESTING	62
APPENDIX II DUCTED PROPELLER PERFORMANCE PREDICTION	64

## LIST OF ILLUSTRATIONS

<u>Figure</u>		<u>Page</u>
1	General Arrangement-Downwash Test Rig, Tandem Ducted Propeller VTOL	71
2	Photograph of Downwash Test Rig Modified to Similate a Representative VTOL Airplane	72
3	Geometry of Ducts Used in Downwash Test Rig	73
4	Characteristics of Propeller Blades Used in Downwash Test Rig	74
5	Photograph of Test Rig with Water Test Pool	75
6	Sieve Analysis of Sand Terrain Sample	76
7	Photograph of Test Rig with Sand Terrain	77
8	Photograph of Particle Trap Located Inside Duct of Downwash Test Rig	78
9	Downwash Test Rig in Modified Configuration	79
10	Rotating Engine Inlet Screen (36 Mesh Wire Screen, 59 Percent Open Area)	80
11	Minimum Area Ground Covers for Full Scale Tests	81
12	Light Flexible Cover Deployment Test Rig	82
13	Terrain Deflector Wing or Flap (Short and Long Configurations)	83
14	Features of Downwash Flow for Dual Tandem Configuration	84
15	Flow Field Measurements Along Plane of Symmetry and Under Fuselage of VZ-2 Model (from Reference 10)	85
16	Variation of Dynamic Pressure With Height at Point Directly Above the Intersection of the Lateral Streamline and Side of Fuselage	86



LIST OF ILLUSTRATIONS (Cont'd.)

<u>Figure</u>		<u>Page</u>
17	Static Pressure Distribution on the Bottom Surface of the Fuselage, Modified Configuration	87
18	Effect of Longitudinal Inclination of Aft Duct on Fuselage Upload and Center of Pressure	88
19	Effect of Lateral Inclination of Forward Duct on Fuselage Upload and Center of Pressure	89
20	Dynamic Pressure of Upwash at Plane of Nacelles. (1.20 Dia. Above Ground)	90
21	Height Which Sand Cloud Attained for Various Surface Dynamic Pressures	91
22	Height at Which Water Spray Was Observed for Various Surface Dynamic Pressures	92
23	Effect of Disc Loading on Terrain Transportation	93
24	Sieve Analysis of Sand Particles Collected on Top of Fuselage for Various Disc Loadings	94
25	Sieve Analysis of Sand Particles Collected in Engine Nacelles for Various Disc Loadings	95
26	Portion of Typical Oscillograph Record of Ducted Propeller Operations Showing Aerodynamically Induced Oscillations of Thrust and Power	96
27	Effect of Operating Height on Performance Over Water (T-2 Configuration)	97
28	Effect of Operating Height on Performance Over Water (T-5 Configuration)	98
29	Effect of Terrain on Gas Producer Performance (T-2 Configuration)	99
30	Effect of Terrain on Aft Ducted Propeller Power Loading	100

LIST OF ILLUSTRATIONS (Cont'd.)

<u>Figure</u>		<u>Page</u>
31	Effect of Configuration on Aft Ducted Propeller Power Loading Obtained During Tests Over Water	101
32	Effect of Height and Configuration on Power Loading Obtained During Testing Over Sand	102
33	Effect of Inlet Screen on Power Loading at $h/D_e = 0.90$ for Modified Configuration	103
34	Effectiveness of Ground Cover in Preventing Particle Recirculation (Disc Loading = 50 psf)	104
35	Effectiveness of Deflector Wing in Preventing Particle Recirculation (Disc Loading = 50 psf)	105
36	Effect of Lateral Inclination of Forward Duct on Particle Recirculation (Disc Loading = 50 psf)	106
37	Effect of Longitudinal Inclination of Aft Duct on Particle Recirculation (Disc Loading = 50 psf)	107
38	Propeller Surface and Leading Edge Erosion Experienced During Tests Over Wet Sand ( $h/D_e = 1.48$ )	108
39	Photograph Showing Erosion of Streamline Strut used for Supporting the Engine within the Duct	109
40	Bottom Surface of Aft Propeller Blade Showing Failure of Neoprene Abrasive Covering After Five Minutes of Maximum Power Operation Over Sand	110
41	Sketch Showing Damage to Compressor Section Aft T53 Engine Downwash Test Rig	111

;  
LIST OF ILLUSTRATIONS (Cont'd.)

<u>Figure</u>		<u>Page</u>
42	First Stage Compressor of YT-53L3 Turbine Engine used to Power Aft Ducted Propeller Showing Damage Due to Sand Ingestion	112
43	Comparison of First Stage Compressor Blades of T-53 Engines Showing Damage Due to Sand Ingestion	113
44	Illustration of Zones used in Evaluating Operational Environment	114
45	Comparison of Predicted and Experimental Ducted Propeller Static Performance Data	115

## LIST OF TABLES

<u>Table</u>		<u>Page</u>
1	Evaluation of Operational Environment for Operations Over Fresh Water	67
2	Evaluation of Operational Environment for Operations Over Sand	67
3	Downwash Operational Environment Grading System	68
4	Evaluation of Terrain Stabilizing Chemicals	69
5	Evaluation of Ground Cover Material	70

### LIST OF SYMBOLS

$A_e$	Duct Exit cross sectional area, ft. <sup>2</sup>
$A_{fus}$	Fuselage bottom projected area, ft. <sup>2</sup>
$A_T$	Particle trap inlet area, ft. <sup>2</sup>
$C_o$	Particle drag coefficient
$D_e$	Duct exit diameter, feet
$d_s$	Density of sand-air mixture, lb. of sand ft. <sup>3</sup> of air
$h_e$	Duct exit height above ground (average of two ducts), feet
$h_{fus}$	Distance from bottom of fuselage to ground, feet
$L$	Fuselage lift, lb.
$q_N$	Dynamic pressure of downwash at duct exit, psf
$q_s$	Dynamic pressure at ground surface, psf
$S$	Terrain particle cross-section area, ft. <sup>2</sup>
$T$	Total thrust including propeller, duct, and residual engine thrusts, lb.
$T_1, T_2, \dots T_s$	Symbols for test configurations, specify longitudinal and lateral position of aft ducted propeller
$V_e$	Velocity of downwash at duct exit, fps.
$W$	Particle weight, pounds
$W_s$	Weight of sand collected, pounds per minute

## I INTRODUCTION

The development of high speed vertical take-off and landing (VTOL) aircraft has introduced new aircraft designs employing very high disc loadings. As a consequence of the resulting aerodynamic downwash, operational problems will be encountered when operating in the vicinity of certain types of terrain. Recognizing this problem, the Bureau of Naval Weapons has given continuous support to a Kellett Aircraft Corporation program designed to gain full scale operational experience in this area and thereby assist in the development of VTOL aircraft.

Kellett previously explored VTOL operational problems caused by downwash effects under U.S. Navy contract NOw60-0450-f, sponsored jointly by the U.S. Navy, Bureau of Naval Weapons, and the U.S. Army Transportation Research Command. This experience was utilized to direct the subject program and to establish certain test conditions. For instance, sand and water terrain had proven troublesome and thus were chosen for further study. Also, the areas of engine and propeller damage, personnel and ground equipment environment, pilot visibility and aircraft concealment had been defined as problem areas. Based on this background, this program was established to determine the influence of airframe geometry on downwash problems as compared to the earlier isolated propeller testing.

This report describes the test bed and testing procedures. The quantitative and qualitative results obtained from the testing are presented and discussed. Conclusions are drawn as to the severity of downwash problems and the influence of these problems on future VTOL aircraft. Recommended programs leading to future VTOL aircraft which will be able to operate independent of the terrain are presented.

## II TEST APPARATUS AND PROCEDURES

### A. Test Facility

The downwash test rig consisted of a full scale half-model of a tandem ducted VTOL aircraft. Two YT-53 turboprop engines of 960 horsepower each drove the two ducted propellers of the model. Each engine was mounted coaxially within each duct and was directly connected to an eight foot diameter propeller. The ducted propeller location and airframe geometry was variable and one configuration simulated a representative VTOL aircraft. Dummy engine nacelles, a simulated landing gear assembly and a realistic fuselage nose section were included for this simulation.

In a steady-state hovering attitude, the VTOL aircraft possesses both lateral aerodynamic and lateral geometric symmetry. Thus, an aerodynamic reflection plane was established along the longitudinal axis of the aircraft enabling a four propeller aircraft to be simulated with the use of two ducted propellers and a longitudinal half-fuselage. A physical reflection plane 20 feet high and 80 feet long, was erected which was sufficiently large to prevent any significant flow around it in the subsequent testing. Figure 1 shows the general arrangement of the test rig and Figure 2 is a photograph of the test rig modified to simulate a representative VTOL aircraft. The use of the reflection plane



effected a considerable economy in the construction and operation of the test rig.

A longitudinal half-fuselage was mounted on the reflection plane. The airframe was designed to simulate a transport aircraft with a box-like fuselage and rear loading provision. A short stub wing was provided between the fuselage and the aft duct. The fuselage and wing were fabricated using panels of aluminum skins fastened to wooden frames and attached in such a manner that the panels could be readily replaced if damaged.

The engine-ducted propeller units consisted of Hamilton Standard three-bladed propellers cut to an 8 foot diameter and Lycoming YT53-L-3 turbo-prop engines. The duct design was developed by Kellett and was based largely on unpublished model test data obtained from the David Taylor Model Basin. The duct geometry is given in Figure 3. The engines were mounted within a duct centerbody with streamlined connecting tubing used to insure minimum aerodynamic drag effects. Two load cells were mounted on each ducted propeller unit to measure total lift which is composed of propeller, duct and residual engine thrusts. Each unit was mounted on the modified boom end of a movable crane. The cranes were capable of positioning the duct exit at heights from 6 feet to 12.5 feet above the terrain and offered virtually unrestricted lateral placement. The engine operating controls, which were

electrically operated, and the instrumentation read-out equipment were installed in a control house located 75 feet from the reflection plane.

The propeller blade characteristics are shown in Figure 4. The pitch of the blades was a 31.5 degree setting at a section located  $3\frac{1}{2}$  feet from the propeller axis. This pitch setting was held constant for all testing. It enabled disc loadings (based on the duct exit area) from 5 psf to 60 psf to be attained.

To reduce aerodynamic interference, the crane which supported the forward ducted propeller was located behind the aerodynamic reflection plane. The same arrangement was not possible for the aft propeller because of the stub wing extending between this duct and the fuselage. Consequently its boom axis was oriented parallel to the reflection plane with the crane housing located well away from the test site. With this arrangement of the cranes the forward duct could be tilted laterally and the aft duct longitudinally. A tilt mechanism driven by an electric motor was provided.

The terrain sample was contained in a rectangular watertight pool 70 feet by 87 feet, as indicated in Figure 1. The average depth of the water in the pool was 24 inches and that of the sand 10 inches. Edge effects were minimized by the construction of an aerodynamic and hydrodynamic fairing around the pool walls. Observations of the subsequent testing

confirmed that the pool size was sufficient to avoid any unwarranted boundary effects.

#### B. Test Conditions

Each test condition was defined by the following parameters:

1. Height of duct exit above ground level
2. Propeller thrust axis inclination
3. Aft duct location
4. Disc loading (Nominal total thrust divided by duct exit area)
5. Terrain type

Each parameter was varied individually and in combination with parameters. Duct exit heights of 8 and 13 feet were tested. The forward duct axis was tilted to  $\pm 10$  degrees from vertical and the aft duct axis to  $\pm 15$  degrees from vertical. Five different aft duct locations were included in the testing. Disc loading was set at 30, 40 or 55 pounds per square foot and the terrain was either sand or water. Almost every possible variation of these parameters was included in the testing.

The first series of tests were conducted over water. Photographs of the test arrangement for operations over water and of a full power test run over water are presented in Figure 5.

To simulate hovering over sand, the test pool area was filled with sand to an average depth of 10 inches. The

sand sample consisted of particle sizes ranging between 200 and 5000 microns. The particle size graduation determined by a standard sieve analysis of sand test samples, taken before and after the test runs over this terrain, is presented in Figure 6. The results shown, substantiate the observation that during the course of testing a great deal of the fine sand particles were blown away, changing the sand content. The sand had an average moisture of 11.8 percent by weight and an average density of 113 pounds per cubic foot. Photographs of the sand test configuration and a full power run over sand are presented in Figure 7.

#### C. Instrumentation

Instrumentation was designed and installed as part of the test rig to ensure that data obtained would fully describe the performance and test conditions for each run. The data obtained were either recorded with an oscillograph or read from a meter. The readout equipment was mounted in the control house located so that the responsible test engineer was aware of the variation in significant parameters during the entire test run.

The following data were recorded by an oscillograph:

1. Total thrust (sum of propeller, duct and residual engine thrust)
2. Torque
3. Propeller rotational speed (rpm)
4. Duct tilt angle

These quantities were measured with an eighteen channel automatic bridge balance and calibrating unit and recorded on an eighteen channel oscillograph.

Two load cells were located on each duct to measure the total of the propeller, duct, and engine residual thrusts. A potentiometer type of differential pressure transducer was used to measure engine torque. Engine torque was read on a meter as well as the oscillograph so that this data was immediately available to the responsible test engineer.

Propeller rotational speed of each engine was recorded by relaying the output signal from an engine mounted tachometer generator to a transistorized rectifier which supplied a signal to the oscillograph as well as driving a tachometer indicator. The duct inclination angle was measured by a rotary potentiometer located at the pivot point of each duct. This signal was read on a meter as well as on the oscillograph.

Additional engine data was read from gages located on an instrument panel in the control house. This data included:

1. Power turbine rotational speed (measured in of maximum rpm)
2. Engine exhaust gas temperature
3. Oil temperature
4. Oil pressure

A substantial amount of aerodynamic pressure data was gathered during the course of testing. For this purpose static and total pressure probes were placed under the fuselage, at the duct inlet, in front of the dummy nacelle engine intakes, and at various elevations along the side of the fuselage between the fore and aft ducts. The probes were connected with flexible plastic tubing to banks of multiple tube manometer boards where the pressure was read and recorded. These pressure measurements gave a quantitative picture of the downwash flow field.

Both motion pictures and still camera exposures were made of the test rig in operation. Two 16mm motion picture cameras were used, being remotely operated from the control house. One was located in the dummy cockpit to enable the effect of downwash on a pilot's vision to be evaluated while the other camera was located at a remote distance from the test bed, giving an overall view of the affected area. These films illustrate the nature of the downwash problem. To effectively trap the high energy sand particles passing through the duct, the traps shown in Figure 8 were devised. These traps provided a smooth path for the particles to enter and be trapped while allowing the air to escape. Sand was also collected from the top of the fuselage and inside the dummy engine intakes.

Samples of various materials were located on the reflection plane in the area under the fuselage. The samples

included bolts, hoses and various plates as can be seen in Figure 7.

A diligent effort was made to ensure that the measurements made during testing were valid. The equipment used was carefully selected and periodically recalibrated.

#### D. Test Procedure

The testing procedure for all of the test runs was reasonably well standardized. Although variations were introduced in certain cases, the sequence of test operations can generally be described as follows:

1. The duct exits were set at the desired height.
2. Motion picture cameras were loaded and set.  
Initial oscillograph readings were taken with the ducts still in the vertical position.
3. The duct axes were set in the horizontal position required for engine startup.
4. The engines were started and brought to idling speed.
5. The cameras were started and the propeller thrust axis tilted from horizontal to the desired test position.
6. The engine rpm was increased at a uniform rate until the desired turbine rpm was obtained.
7. Test personnel noted significant downwash effects and the flow field resulting from the disturbance

of the terrain for later correlation with the motion pictures.

8. When a steady state test condition was obtained and held for approximately 60 seconds, the engine rpm's were reduced to ground idle, the propeller thrust axis tilted to the horizontal position and the engines and cameras stopped, terminating the test. The average total time per test run was 3 minutes. The tilting of the duct axis to the desired position required 40 seconds, increasing the rpm from ground idle to the test setting required 20 seconds and the test rpm was held for 60 seconds. The time required to reduce the rpm to ground idle was about 15 seconds and the tilting of the duct axis back to the horizontal position necessary to stop the engines required 40 seconds.
9. Eroded areas of the terrain were measured. Damage to the propeller, engine, duct and fuselage was noted and significant findings photographed.
10. Sand samples were collected from traps installed within the ducts and the dummy engine nacelles.
11. Damage to test samples which were placed on the reflection plane under the fuselage between the two engines, was noted and photographs taken when warranted.



### E. Airframe Geometry

The variations in airframe geometry tested consisted of Basic configurations and a Modified configuration. These variations were also tested with duct tilt and with a few alleviation devices.

Basic configuration details are shown in Figure 1. Five locations of the aft ducted propeller were tested. These configurations were identified as T1 to T5 depending on the duct location as shown in Figure 1. The engine inlets were unprotected for these tests. Propeller protection was minimal consisting only of a readily replaceable vinyl tape. The fuselage was quite simple for these tests and included no appendages except a stub wing.

The Modified configuration included those appendages required to simulate a representative VTOL airplane. This configuration is shown in Figure 2, which illustrates the more representative fuselage and the addition of a dummy engine nacelle and a simulated landing gear. The design details of the modification are shown in Figure 9. A fillet was also added to the test rig which simulated the connection of the forward duct to the fuselage as can be seen in this figure. It should be noted that there was no attempt made to simulate engine flow. However, the location of the inlet cleanout ports over the stub wing as shown in Figure 9 caused a small flow to be induced through these nacelles.

An engine inlet protection device and better propeller blade protection were also added to the test rig when the change was made to the Modified configuration. The inlet screen was mounted on the propeller hub and rotated to reduce terrain particle clogging. This screen is shown, from the engine inlet side, mounted on the propeller in Figure 10. Heavy neoprene strips were used to cover the entire lower surface and leading edge of the propeller blades as may also be noted in this figure.

The full scale alleviation devices tested in this program included ground covers and a deflector wing or flap. Ground covers consisted of square canvas tarpaulins of the size and in the positions shown in Figure 11 and a light weight deployment cover. The deployable cover was of Mylar material and was deployed manually. The test crew deployed the cover by pulling ropes attached to the corners of the cover as shown in Figure 12.

The deflector wing was a horizontal surface which filled the space between the forward and aft ducts. This device was only tested with the Modified configuration. As shown in Figure 13, two spans of this wing which were tested; a long configuration of 10 foot span and a short configuration of 4 foot span.

### III DISCUSSION OF PROBLEM

It has been found that the presentation of data obtained in this program is considerably eased once a general discussion of the problem is presented. This discussion will be limited to a qualitative consideration of the flow field and an evaluation of particle entrainment; including an estimate of the influence of disc loading.

#### A. Flow Field of Dual Tandem VTOL Aircraft

In general, when an air jet strikes the ground it loses its vertical velocity and the energy is converted to a pressure that accelerates the air flow in all directions away from the impingement area. Where two or more lift devices are used in proximity to each other their respective jets upon meeting one another and the ground create an additional stagnation point. Generally, a plane of symmetry can be found in the flow which contains this additional stagnation point. The plane of symmetry acts as a solid wall through which no flow can pass because of the aerodynamic mirror image on the other side. Downwash which is directed toward this plane must go either upward or diverge to either side to escape. It is this upflow that has been found to be the primary contributor in the entrainment and transportation of particles.

The dual tandem configuration causes a distinctive flow pattern which aggravates downwash problems as compared

to a configuration with a single lifting device. The significant features of this flow field are illustrated in Figure 14 and include a longitudinal streamline which is coincident with the longitudinal plane of symmetry of the aircraft. Similarly, a lateral streamline is formed, but since the aircraft does not have fore and aft symmetry, the lateral streamline is curved. The intersection of the longitudinal and lateral streamlines at the ground surface is a stagnation point.

The downwash leaves the propellers in a downward and radially outward direction. The interference between the flow from adjacent propellers causes the longitudinal and lateral streamlines and also causes a significantly large upflow in the area which is enclosed between the propellers. The upflow region surrounds the fuselage and can carry terrain and debris from the ground to the aircraft.

#### B. Mechanism of Particle Entrainment

It has been found by testing, as discussed in Reference 1 and in this report, that the mechanism by which terrain particles become transported by the downwash is initially by bouncing. Large particles such as debris, lumber, weights, etc., have been seen to bounce along the ground propelled by the downwash. These particles have been noted to bounce to significant height by colliding with the ground or other stationary obstacles. Similar motions have also been noted in the movement of smaller particles such as sand.

The significance of this method of entrainment is that the height that a particle can reach depends only on the energy which it can achieve on the ground, and chance.

A simple, first order, analysis to estimate the maximum value of kinetic energy which the terrain particles can obtain is presented in Reference 2. From this analysis it is estimated that terrain particles can achieve a kinetic energy of about 0.5 ft-lbs at a disc loading of 60 to 100 psf. Thus, if these terrain particles achieve a reasonably elastic collision with a properly oriented obstacle they can bounce to a height of about 50 feet.

The entrainment of terrain in the downwash is considerably aggravated by regions of upflow. Water spray and other small particles can be carried aerodynamically by the downwash and recirculated to cause many problems. As will be discussed later in this report, multi-lift-device VTOL aircraft can cause upflow areas which are of diameter can be supported aerodynamically. These upflow regions catch particles which bounce from the ground and have been found to transport large quantities of terrain to engine and propeller areas of VTOL aircraft.

#### C. Relation of this Program to State of Art

There is presently an accelerating accumulation of the body of knowledge on the VTOL downwash problem. While a review of this knowledge is not an objective of this program,

it is of value to briefly relate the present program to this knowledge. Some of these data are also used for comparison in later sections of this report.

The earliest well-documented findings on downwash recirculated terrain were presented in Reference 3. This work was followed by the isolated propeller and jet model tests of References 4 and 5. Some of the effects of configuration on the downwash flow field were measured in model tests of Reference 6. Full scale isolated propeller downwash experience was obtained in Reference 1.

Full scale operational experience on downwash problems was also obtained when the relatively lightly loaded Army-Vertol VZ-2 aircraft was damaged in flight as reported in Reference 7. While inadvertently passing over an area which contained loose gravel, this aircraft sustained severe damage to the wooden skin and aluminum abrasion strip surfaces of its rotating components.

Full scale engine ingestion problems with helicopters have been experienced as reported in Reference 8. In this reference, the loss of power encountered by HSS-2 helicopters during ASW missions is discussed indicating the problems of salt water operations. The HSS-2 has a disc loading of only 6.2 psf. However, the recirculation was caused by the effects of a large toroidal vortex which surrounded the hovering helicopter. The size and intensity of this toroid is probably

a function of the weight of the aircraft and not the configuration. Therefore, it would be expected that similar small particle recirculation would also occur with VTOL aircraft of the same weight. This particle recirculation was reported to be greatly aggravated by the effects of the wind which may be indicative of possible increase of VTOL problems during landing or take-off.

Full scale downwash flow field data are available in References 9 showing some effects of configuration. The upflow region between two propellers is mentioned in this reference, but no data were obtained. However, data on the upflow region and other effects of configuration are shown in Reference 10. Rather detailed flow field data are available for tilt-wing VTOL models in this reference. An example of these data is shown in Figure 15 reproduced from this reference.

The present program is mainly related to the accumulated knowledge in that the small amount of full scale test experience has been expanded. This program was conducted with the hitherto unexplored dual-tandem configuration which is represented by the X-19A and X-22A aircraft. The X-22A aircraft is discussed in Reference 11. In the present program, some flow field measurements of the upflow region were obtained and are compared with the existing data. Propeller, engine and airframe damage and downwash environment evaluation follows the precedent of Reference 1.

#### IV QUANTITATIVE TEST RESULTS

In this section of the report, data on the flow field and fuselage pressures are reported, the effects of downwash on performance are summarized and several downwash alleviation devices are evaluated.

It was planned that quantitative measurements of visability would also be obtained in this program. However, as discussed in Appendix I, the required instrumentation did not function in a reliable manner and therefore only a qualitative estimate of visability was obtained. All qualitative data are presented in the next section.

##### A. Flow Field Measurements

###### 1. Upflow Data

The intersection of the lateral streamline and the side of the fuselage had the greatest amount of upwash. Pressure data were obtained in this region at various heights above the ground. This data is presented in Figure 16 in non-dimensional form where the ratio of local dynamic pressure to disc loading is plotted as a function of height. The scatter indicated is believed to be caused by the random direction of upflow, a phenomenon observed during the smoke studies conducted.

###### 2. Fuselage Pressure

During the Modified configuration tests, local pressure surveys were made along the bottom surface of the



simulated fuselage. For this purpose static pressure probes were located at four lateral locations at each of five longitudinal positions along the bottom surface of the half-fuselage. Readings were taken at various disc loadings from 30 to 52 psf. The results are shown in Figure 17 where the data has been presented in non-dimensional form by plotting the ratio of static pressure to disc loading as a function of longitudinal station for each lateral position. The data indicates a sizeable upload on the fuselage can be anticipated. The negative region detected at the outboard edge of the fuselage nose indicates that the flow direction is down over the nose of the fuselage. The sudden drop in pressure at approximately 330 inches back from the nose is primarily due to the change in geometry of the bottom fuselage surface which rises abruptly from this station toward the aircraft tail.

Total fuselage lift,  $L$ , can be obtained by numerically integrating the pressure distribution on the bottom fuselage surface. For the Modified configuration, the following expression can be used to calculate the upload on the fuselage:

$$L = 0.242 (A_{fus}) \left( \frac{T}{A_e} \right)$$

where:  $A_{fus}$  = Projected fuselage area (ft<sup>2</sup>)

$\frac{T}{A_e}$  = Disc loading based on duct exit area (psf)

Fuselage pressures were also obtained with the ducts operating at inclined positions. The effect of duct inclination

on the fuselage upload and the center of pressure is shown in Figure 18 for the aft duct and Figure 19 for the forward duct. The center of pressure location is not strongly affected by duct tilting. However, the total fuselage lift which is not affected by tilting the forward duct increases considerably when the aft duct is inclined rearward. It should be noted that when one duct was tilted the other duct was held in a vertical position. The results, therefore indicate the effects of individual duct tilting only. However, it is believed that any inclination of the downwash toward the stagnation point under the aircraft will increase the fuselage upload.

Comparative aerodynamic pressure data obtained with the two-propeller VZ-2 aircraft are shown in Figure 15. Note in this figure that the flow between the rotors and under the fuselage is directed vertically upward and has a dynamic pressure of 0.5 of the dynamic pressure of the downwash. If this flow impinged in a solid surface, the stagnation pressure would be comparable to the "Plane D" measurements shown in Figure 17. The pressures on the bottom of the fuselage are equal to approximately 60 percent of the downwash dynamic pressures (since  $q_n = \frac{1}{2} T/A_e$ ). This comparison is particularly interesting since the VZ-2 is of such a different configuration than the configuration tested in this program.

Pressure surveys were also performed near the locations of the dummy engine intakes during the Modified configuration

testing. The intakes were located 1.20 exit diameters above the ground level. Figure 20 presents the data obtained and also defines the locations of the pressure probes. The probes were pointed vertically downward and thus the dynamic pressure measurements include only the vertical component of velocity. It is important to recognize that the dummy engine intakes did not provide the given mass inflow demanded by an actual engine. Thus, the pressure distribution obtained in this region under prototype test conditions will undoubtedly be radically different.

#### B. Terrain Entrainment

The transport of terrain by the downwash was measured by estimating the water spray (or sand) cloud height, collecting sand in one of the ducted propellers and by collecting the sand which remained on the fuselage following each test. These data are indicative of the ingestion and concealment problems. The sand terrain data were obtained only with the Modified configuration. Additional terrain entrainment data are presented later in this section of this report to evaluate alleviation devices.

##### 1. Particle Cloud Height

In tests performed over water and sand an opaque sand particle or water spray cloud was formed. The intensity and height of this cloud was a function of duct height and disc loading. The cloud was concentrated along the plane of the

longitudinal and lateral streamlines and in the upflow region. The water spray cloud was a rather good flow visualization medium and showed the recirculation of the terrain into the ducted propellers. A plume of water spray occurred over the upflow region which would be a serious concealment problem.

The height of the opaque cloud was estimated from motion pictures taken during the tests. These data are shown in Figures 21 and 22 for sand and water respectively, with comparative data from Reference 1, 4 and 5. To provide a basis for comparison all data are plotted against the maximum surface dynamic pressure,  $(q_s)_{\max}$ , as developed in Reference 4. The relation  $(q_s)_{\max}/q_N$  may be obtained from the experimental data of this reference as a function of duct exit height. For a ducted propeller  $q_N$  is equal to  $\frac{1}{2} T/A_e$ .

The sand test data shown in Figure 21 indicate that the height of the cloud is not as large as would be expected based on the referenced model tests. However, the referenced data is for dry sand whereas the data from this program is for wet sand. It is believed that the effects of configuration aggravate the terrain cloud height but due to the difference in sand wetness these data are inconclusive.

The water spray cloud data shown in Figure 22 are unexpectedly in fair agreement with the isolated ducted propeller data of References 4 and 5. All of these data indicate that the problem is significantly greater than indicated

by the isolated open propeller data of Reference 1. This result may indicate that the spray problem becomes less severe with a larger diameter thrust device but that this affect is cancelled by the aggravation of the problem by the effects of configuration. Thus, the dual tandem configuration produces a similar spray as a small model ducted-fan at the same maximum surface dynamic pressure.

## 2. Ducted Propeller Ingestion

It was found that the sand trap shown in Figure 8 collected an average of 16 grams of sand per minute of maximum thrust operation during tests at 50 psf disc loading. This data can be used to estimate the average sand density of the air being ingested by the ducted propellers. The trap had an inlet area,  $A_T$  of 0.087 square feet and the trap design allowed the air to flow through without significant restriction. Therefore the flow through the trap can be approximated by the momentum value of the downwash at the duct exit,  $V_e$ . This value is 145 fps at 50 psf disc loading. Thus, for a sand weight per minute of  $W_s$  the density (pounds of sand per cubic feet of air) of the sand,  $d_s$ , is as follows:

$$d_s = \frac{W_s}{60 V_e A_T}$$
$$= 0.000047 \text{ lb./ft.}^3$$

This value is similar to the maximum sand density of  $0.000057 \text{ lb/ft}^3$  which was measured on a helicopter hovering

in a sand pit as noted in Reference 3. It is noted in this reference that this sand density is similar to a desert sand storm. However, it is believed that much larger sand densities occurred near the fuselage of the test rig especially in the upflow region.

The measured sand density is significant when compared with engine ingestion tests. Serious damage can be expected if this sand density is ingested by a turbine engine. For example, as reported in Reference 12, YT-53 engines were tested with a fine particle sand with a varying sand ingestion program which resulted in an ingestion rate of approximately  $0.000005 \text{ lb/ft}^3$ . This ingestion rate which is 10 times less sand density as was measured in the downwash test caused extensive engine damage. The significance of this damage is underscored by the fact that the maximum disc loading attained in the downwash testing was only 50 psf.

### 3. Sand Collected Near Engines

During tests of the Modified configuration with an average duct exit height to duct exit diameter ratio,  $h_e/D_e$  of 0.90, sand samples were collected from the top of the fuselage and from the dummy engine intakes for several disc loadings. The effect of disc loading on the quantity and size of the sand particles collected is shown in Figures 23, 24 and 25. Figure 23 indicates that the quantity of sand collected is very strongly affected by the disc loading with the sand

collected increasing more than linearly with increasing disc loading. The effect of disc loading on particle size is unexpectedly small as shown in Figure 24.

In analyzing this data, it should be noted that the flow through the dummy engine intakes was very small during these tests since it was created only by an induced flow. The effect of engine inlet flow which will be experienced by VTOL aircraft is not shown by these data. However, it would be expected that the engine flow would entrain at least all of the sand which happened to collect on the fuselage in the present tests. Thus an engine ingestion rate of several pounds of sand per minute can be expected.

One of the downwash tests was conducted with a 20 knot, aft to forward wind. (All other tests were conducted with a wind of 5 knots or less). The effect of this wind may be noted from Figures 23 and 24. The quantity of particles was reduced while the percentage of large particles increased. It is felt that this result was due to the wind which scattered many of the finer particles away from the fuselage area.

The size of particles collected (as shown in Figures 24 and 25) was generally larger than those particles collected in other downwash programs. This could be attributed to the strength of the upflow region being sufficient to propel a major portion of the available particles to the region above the fuselage. From Figure 24 it may be noted that almost 100

percent of the sand collected was finer than 6400 microns (0.25 inch). To propel particles of this size the upflow must have a dynamic pressure which is greater than the weight to drag area ratio,  $W/CdS$ , of these particles. If it is assumed that the particles are roughly spherical and since the Reynolds number of the particles is on the order of 10,000 it results that

$$W/CdS \approx \frac{0.5 \times 10^{-3}}{(0.5)(3.2 \times 10^{-4})} \approx 3 \text{ PSF}$$

The upflow measurements of Figure 16 indicate that the dynamic pressure was at least  $(0.15) T/A_e$  or 4.5 psf even for the tests at 30 psf disc loading. The upflow region could therefore easily support any of the particles which were available from the ground.

It should be noted that at the higher disc loadings proposed for some VTOL aircraft, much larger particles can be expected to be carried to the fuselage areas. For instance, since the relation  $W/CdS$  is roughly proportional to the particle diameter, it would be expected that at least 13,000 microns (0.5 inch) size particles could be transported with a disc loading of 100 psf.

### C. Performance

The requirement of operation over unprepared terrain imposes unique problems on the VTOL aircraft. One of the most serious problems encountered is the effect of particle



recirculation on engine and propeller performance. The problem of particle recirculation was studied during the program and the influence of duct exit height, terrain type and airframe geometry were determined.

In the test configuration the turbine engine intake was inside the propeller duct. This location was noted, from visual observation, to be an area of intense recirculation. Thus the results presented herein may represent the worst engine intake location.

In utilizing the hovering performance data of this report, it should be noted that this data was obtained as a by-product of tests conducted to obtain full-scale experience with downwash operational problems. For this reason, the experimental error on the performance measurements may be as large as ten percent of the maximum measured value. Also, the following test rig fabrication details may have a significant effect in performance:

1. The propellers used on the test rig were made for an AO-1 Mohawk aircraft. These propellers were cut to fit closely in the ducts of the test rig. The blade twist and camber of these propellers was considerably different than that which will produce optimum hovering performance.

2. The propellers of the test rig were operating at an extremely large pitch setting to provide a maximum thrust within the rpm limits of the engines. This large pitch setting

reduced the hovering efficiency. Typical ducted propeller VTOL aircraft will operate at a significantly higher rpm or will have a larger blade area and therefore should operate more efficiently.

3. The test data shown do not reflect the positive benefit of ground effect. There is very little ground effect on the ducted propeller performance; however, there is a significant upload on the fuselage due to the downwash. Based on fuselage pressure data, this upload will be approximately 3500 pounds for a typical aircraft (15,000 pounds gross weight,  $T/A_e = 76.5$ ). This upload is created with no increase in power and therefore, in ground effect the power loading data shown in this report should only be used with a thrust equal to the gross weight minus the upload.

As referred to in this section, performance is a measure of the lift force obtained at a given shaft power setting and therefore does not refer to engine performance. The total lift developed is the sum of propeller, duct and residual engine thrust. An attempt was made to differentiate between duct and propeller thrust by locating pressure probes at the duct inlet. However, the random flow pattern which exists at the inlet, thought to be caused by an aerodynamic interference phenomenon, induced such large scale oscillations in the measurements that useful duct inlet thrust data could not be obtained.

## 1. Aerodynamic Interference

The pressure oscillations noted in the duct inlet are believed to be part of an aerodynamic interference phenomenon associated with the general configuration tested. Low frequency vibrations of the ducts were also observed during test runs. An indication of the nature of these oscillations can be obtained from Figure 26, which is a typical oscillograph record of the data obtained during a test run. Low frequency oscillations of the thrust with amplitudes reaching nine (9) percent of the steady state value are evident in this data.

As described in an earlier section, the ducts were mounted at the end of crane booms for the testing. Thus, the stiffness of the duct support does not simulate that employed in an actual aircraft design. The crane is probably, in fact, a somewhat stiffer support. For this reason, no indication is available from the testing of the possible effect of reinforcement of the vibrations by resonance with the duct support structure. Such a reinforcement would serve to aggravate the existing vibration problem which is serious by itself.

## 2. Effect of Operating Height

During operation at low heights over water, the forward engine was able to generate only half of its potential thrust at the maximum power setting. The effect of duct exit

height is shown by Figures 27 and 28 which show that higher disc loadings were obtained at greater duct heights for the same gas producer speed. The results are presented for two different placements of the aft duct. At either location, (T-2 or T-5) the aft engine suffered only a small loss in performance. The loss in forward engine thrust was substantiated by the observation of a more dense water cloud recirculating into the forward engine and the inability of this engine to reach maximum rpm.

When the duct exit height to duct diameter ratio is increased to 1.30 the performance of both power units is significantly improved. This change can be attributed to less recirculation at this operating height and therefore less water ingestion.

The reason why a low operating height affects the forward engine more severely than the aft engine may be one of the following:

- a. Fuselage geometry provided a smoother flow path around the aft engine.
- b. The stub wing located inboard of the aft engine prevented water from flowing up and into this engine.
- c. Due to a faulty fuel control on the forward engine, it was not possible to bring both engines up to power simultaneously. Invariably, the aft

engine reached peak power first. This caused the plane of the lateral downwash streamline to form nearer the front duct than would be the case if each unit were producing the same downwash pressures. Since the upwash along this plane was the primary source of water ingestion, the forward engine undoubtedly received more than its share of recirculating water particles. This increased ingestion rate would, in turn cause a reduction in power and thereby produce less dynamic pressure in the vicinity of the forward duct. Thus a further shift in the location of the lateral plane was caused which aggravated still further the discrepancy in performance.

In all probability, each reason given contributed to the observed phenomenon. In any event, the data recorded should point out that water ingestion can cause a serious loss in performance and that the amount of water ingested is a strong function of the nature of the flow field.

### 3. Effect of Terrain

A comparison of tests conducted over sand and water show that operation over water is much more detrimental to engine efficiency while operation over sand can result in serious damage problems. The former is a short term problem while the effects of propeller and engine damage are cumulative.

The effect of water ingestion on engine efficiency is shown in Figure 29. This figure shows that for the same power setting and essentially the same duct exit height, fifteen (15) percent less disc loading is generated over water as over sand. Monitoring of exhaust gas temperatures indicated that while over water, the average operating temperature of both engines was 50°C. less than average temperature of 540°C. reached operating over sand. Since engine test cell data indicated that the normal operating temperature of the engines is 550°C., it is reasonable to expect that a drop from this temperature indicates an inefficient operating condition and thus a substantial loss of power. In summary, the serious effects of water ingestion on engine performance is well documented.

An unexpected and unexplained effect of terrain on ducted propeller performance is shown in Figure 30. Water ingestion apparently reduced the propeller performance as, for example, at a disc loading of 50 psf approximately 30 percent more power was required. Since the power is measured by a shaft mounted torque-meter this effect is not due to the engines. The explanations which can be offered are that separation of the inlet flow in the ducts of the test rig was aggravated by the increased mass flow due to the water, or this is some other effect resulting from pumping water. If the inlet flow was separated the duct thrust would be reduced.

#### 4. Effect of Configuration

To determine the effect of aircraft geometry various parameters were altered during the course of testing. A total of five locations of the aft duct and the effects of duct inclination were investigated. In addition, the Modified configuration was tested.

The effect of aft duct position on the power loading over water is shown by Figure 31. A definite increase in power loading is evident when the aft duct is moved closer to either the forward duct or the longitudinal reflection plane, as in the T1, T4, and T5 configuration. This increase in ducted propeller performance may be due to the increase in mass flow which results from the increased recirculation of these configurations. An optimum position of the aft duct was not determined.

Figure 32 is a comparison of power loadings over sand for the T2 configuration and the Modified configuration under similar conditions. The significant loss in performance indicated by the plot is believed due to:

- a. The increased propeller surface roughness caused by the addition of the abrasion strip.
- b. The increased particle recirculation resulting from lower height operations.
- c. Increased power required from the addition of the rotating inlet screen.

- d. Possible higher temperature of the recirculating air due to lower operating height.
- e. Increased duct aerodynamic interference due to lower operating height.

It is believed that performance data for the Modified configuration would have been reasonably similar to the T2 configuration had the test conditions been more nearly the same.

One of the unexpectedly large contributors to the reduction in the performance noted with the Modified configuration was the inlet screen. The effect of this screen on performance was isolated during single engine runs, the results of which are shown in Figure 33. This data indicates that approximately 25 percent of the power loss noted in Figure 32, can be attributed to the increase in shaft power required as a result of adding the screen.

The effect of duct tilting was also investigated with the test rig in the Modified configuration. It was found that in this configuration, duct tilt does not vary the power loading of the ducted propellers significantly. This result was unexpected especially in light of the apparent sensitivity of the ducted propeller performance as noted by the data of Figure 32.

#### D. Evaluation of Alleviation Devices

A substantial portion of the effort expended on the subject program was directed toward the development of devices



designed to alleviate the damaging effects of downwash entrainment. The testing included model tests for initial evaluation of alleviation devices and full scale tests of promising concepts. Tilting of the ducts was also investigated to determine if this maneuver could significantly improve the downwash flow field.

The evaluation of these methods of alleviating downwash problems has been based on the amount of recirculated sand which was collected. These data are not a direct measure of any particular downwash problem. However, this quantitative measure gives a relative evaluation of the amount of terrain available in sensitive areas to cause trouble. Based on this evaluation, the use of a terrain cover appears to be the most promising of the devices tested.

#### 1. Model Tests

To guide the full scale tests, a preliminary evaluation of devices and systems which could alleviate downwash problems was obtained by model tests. These tests were performed on soil stabilizing chemicals, downwash diverters and terrain particle traps. A two jet air ejector was used as the lift producing device. Disc loadings up to 20 psf based on nozzle exit area were attained.

The most promising systems investigated were the air dropable ground cover, air sprayed low density plastic foams, and airborne deflectors. A search of available material

suitable for sprays and ground covers was conducted. Tables 4 and 5 present the pertinent physical parameters of the various sprays and covers investigated.

These data indicate that a minimum size terrain cover can be made for a 35,000 pound dual tandem VTOL aircraft which has a weight of about 20 pounds. To protect the same area a spray would weigh about 80 pounds.

## 2. Full Scale Tests

### a. Ground Cover

Full scale tests were conducted to determine the effectiveness as well as the minimum size requirement of ground covers. Canvas covers of various sizes were placed directly under each duct. Weights were used to prevent the canvas from lifting during tests at full power. Figure 11 shows the ground cover test set up. Results of the tests are presented in Figure 34. Using the sand collected in the nacelles and the top of the fuselage as a criterion of particle recirculation, a minimum size effective cover should be approximately twice the duct exit area.

Small size ground covers, however, in a multi-lift device aircraft will multiply the problems of deployment and ground holddown. Tests were, therefore, performed with a lightweight Mylar sheet, large enough to cover the area under both ducts. Deployment of this cover was accomplished by folding the cover in accordion fashion and manually pulling

1

simultaneously in the directions indicated in Figure 12. For safety reasons this test was performed at ground idle power which corresponds roughly to a 6 psf disc loading. When fully extended the Mylar sheet sustained the downwash forces with a minimum of flapping or lifting.

The results of the full scale tests indicate that the terrain cover can be smaller than that indicated by the model tests. However, to provide the means of deployment and to provide the pilot with some margin for landing error, the cover must be made somewhat larger and heavier. These tests have shown that a cover can be deployed in the downwash. It is believed that it is practical to consider this device for operational aircraft with the pilot dropping the cover immediately before landing, waiting for it to deploy, then landing on its surface.

#### b. Deflector Wing

Two deflector wings, located on the fuselage between the two ducts as shown in Figure 13 were tested. The results of these tests are presented in Figure 35 where the amount of sand collected on top of the fuselage and inside the dummy nacelles is again used as a criterion to evaluate the effectiveness of the deflector wings. Although the sizes of the deflectors tested did not appear to prevent particle transportation to the top of the fuselage, the location of the deflectors directly under the nacelles provided adequate

protection for the engine intakes region. It should be noted, however, that the installation of the deflector wing eliminated the small flow through the nacelles previously induced by the downwash. It is reasonable to expect that the mass flow requirements of a turbo-prop engine installed within the nacelles would alter the flow conditions created by the addition of the deflector wing. Thus, it is reasonable to conclude that flaps or deflector wings must be more effective than those tested to obtain a reasonable reduction in engine ingestion.

#### c. Duct Inclinations

Altering the direction of an impinging jet has been considered as a means of downwash alleviation. During the course of this program tests were performed to determine the merits of jet inclination.

##### (1) Forward Duct Inclination

The forward duct was tilted laterally directing the impinging jet inboard (+10 degrees) or outboard (-10 degrees). This tilting affects the quantity of sand collected on top of the fuselage and inside the dummy engine intakes as indicated in Figure 36. The quantity of sand deposited on top of the fuselage is seen to be considerably reduced when the impinging jet is directed away from the longitudinal plane of symmetry. This same effect, however, is not evident in the sand collected in the nacelles.

The direction of the lateral streamline, located between the two ducts is believed to have a considerable

influence on the quantity of sand that was collected within the nacelles. The direction of the lateral streamline was directly dependent upon duct geometry and was found to change with variations in duct locations and duct inclinations. Since in the Modified configuration the lateral streamline happened to coincide with the nacelle intakes, any change from this geometry affected an improved flow pattern. This is evident from the amount of sand collected in the nacelles as shown in Figure 36. A peak value of 0.43 pounds of sand per minute in each inlet was collected at zero duct angle. Changes in duct angle to either plus or minus 10 degrees reduced this quantity considerably.

## (2) Aft Duct

The aft duct was tilted longitudinally directing the jet flow forward (-15 degrees) or aft (+15 degrees). The amount of sand collected on top of the fuselage and in the nacelles is shown in Figure 37 as a function of duct inclination,

The effect of relocating the lateral streamline on the quantity of sand trapped in the nacelles is again evident. Note that the quantity of sand collected on top of the fuselage is reduced when the aft duct is inclined to -15 degrees. By directing the impinging jet forward some jet mixing appears to occur with the forward jet, reducing the quantity of recirculating particles. Thus, the technique of duct tilting may be a desirable VTOL maneuver which will, at least partially, alleviate some of the downwash problems.

## V DISCUSSION OF QUALITATIVE RESULTS

In this section the damage due to terrain recirculation is reported, the visibility problem is discussed and the general operational environment is evaluated.

While it is always desirable to have a quantitative result to a program it is believed that the most important conclusions of this program are based on qualitative results. This, of course, results from the attempt of this program to obtain full scale operational experience with the dual tandem VTOL aircraft based on relatively inexpensive test rig experience. It is believed that this experience is a valid simulation of the dual tandem aircraft in steady hovering flight. This flight condition is probably one of the most serious as far as downwash problems are concerned and is typical of a small portion of each VTOL flight. However, the effects of the dynamic flight maneuvers of landing and take-off have not been evaluated and therefore the extent to which these results are applicable to the operational situation remains to be determined.

It should be noted that this testing indicates that the equivalent of at least 10 simulated landings and take-offs could be made before the unprotected test rig was seriously damaged by the sand terrain. This inherent damage absorbing capability can probably also be designed into a dual tandem

VTOL aircraft. Thus, it is possible that a war emergency VTOL aircraft operation can be conducted within this damage absorbing capability alone thereby requiring no compromise in the aircraft.

A. Damage Due to Qualitative Terrain

This section will report on the damage suffered by the propeller, engine and aircraft structure during testing over sand. Although some erosion occurred during tests over water these effects were not serious. It should be noted, however, that these tests were performed over fresh water and consequently the engines were not subjected to the encrustation and corrosive effects of salt water.

The testing over sand can be divided into two distinct portions. The Basic configuration (T1 to T5) tests consisted of an operating time of 8 minutes at a disc loading of 50 psf and one minute each at disc loadings of 30 and 40 psf. The engine inlet was not protected and the propellers had minimal protection during this testing. These tests were performed at a duct height to diameter ratio of 1.50. Modified configuration testing was then performed with engine inlet screens installed to protect the engine and an abrasion strip added to the propeller to reduce erosion. A total of fourteen minutes of testing were conducted in this configuration with a duct height to diameter ratio of 0.90.

1. Propeller and Duct Erosion

During the Basic configuration testing, the propeller

and duct experienced considerable damage from the recirculating sand particles. The propeller damage, shown by Figure 38, was most severe on the leading edge and the lower surface of the blades. It consisted of numerous nicks and pits ranging from approximately 0.003 inches in diameter by 0.003 inches deep to 0.10 inches in diameter by 0.032 inches deep. The damage to the aft propeller was more severe than that to the forward propeller. No damage was noted on the upper surface of the blades. A vinyl tape was applied to the leading edge of the blades to reduce the erosion but this failed to alleviate the problem.

To maximize performance of the ducted propeller a balsa rub strip was inserted in the ducts, maintaining a clearance of 0.06 inches with the propeller blade tip. This rub strip was eroded by sand particles which caused nicks in the balsa wood approximately 0.25 inches to 0.06 inches deep and 0.25 to 0.38 inches long.

The four steel streamlined struts, located across the duct to support the propeller and engine, suffered minor damage from the recirculating sand. A photograph of the erosion noted is included as Figure 39. The damage was confined largely to the rapid erosion of paint accompanied by a negligible amount of metal removed. However, this damage would be extremely serious if the struts were of aircraft construction.

There was some paint erosion on the heavy gage steel outside surface of the aft duct adjacent to the wing tip. The



deflection of recirculating particles by the wing is probably the major cause of this damage which probably would be serious with a light weight construction. Some erosion of paint from the surfaces of both ducts near the region of interaction also occurred. This was not as severe as the damage to the wing side of the aft duct, however.

The propeller abrasion strip installed for the Modified configuration testing provided only temporary protection from surface erosion. After five minutes of full power operation the covering was torn from the blades as indicated by Figure 40. This failure was probably caused by particles imbedding themselves under the strip and moving toward the blade tips under the action of centrifugal force. When the sand was forced between the strip and the blades over a sufficient area, the covering failed. No blade surface pitting was noted on the portion of blade which was covered by the strip.

Also during the Modified testing, the inner duct surface sustained severe pitting and gouging, particularly on the side closest to the planes of the longitudinal and lateral streamlines. There was considerably more pitting of the duct surface in the Modified configuration tests than was experienced in the earlier tests.

## 2. Power Plant Erosion

An external engine inspection following the completion of the Basic configuration testing revealed that the power

turbine blades and the region of the engine housing in the vicinity of the blades were highly polished. However, there was no pitting in this area and the blade tips were not rounded at the trailing edge, as might be anticipated. The first stage compressor blades had suffered extensive pitting and gouging particularly at the blade root section.

A more thorough inspection was conducted after removing the upper half of the engine compressor housing; as shown in Figure 41 this inspection revealed serious damage to all 5 stages of the compressor blades and also surface erosion of the stators. The blade erosion was particularly severe along the entire length of the leading edge of the first stage blades, especially at the root section where metal was eroded to a depth of 0.187 inches, probably by the impact of large sand particles drawn into the engine. Photographs showing the first stage compressor blades installed and a comparison of the blades after testing with the original blades are included as Figures 42 and 43, respectively.

The engine manufacturer recommended replacement of the first stage compressor blades prior to any further testing. Accordingly, the Modified configuration sand tests were performed after replacement of the first stage compressor blades.

The rotating engine inlet screen, installed for the Modified configuration testing, adequately protected the power plant. At the conclusion of testing, external inspection revealed that only minor nicks were sustained by the first stage compressor

blades, although the root section was highly polished. From Figure 6, the quantity of sand particles having a diameter less than the screen opening of 540 microns is only 35 percent of the total available particles. The screen undoubtedly stopped a sizable proportion of these smaller particles also. Furthermore, the impact forces which affect blade erosion are a function of particle size. Thus, it is reasonable to conclude that the screen reduced the blade erosion to a value considerably less than 35 percent of the damage suffered in the absence of this protective device.

### 3. Airframe Damage

The fuselage skin was damaged only on its bottom surface. Wet sand particles adhered to this area, accumulating during successive tests to thicknesses as great as 0.30 inches at the intersection of the longitudinal and lateral streamlines. As the sand dried it became very difficult to remove. Under the sand the Alclad skin was found to contain minute indentations approximately 0.002 to 0.003 inches deep. The same damage, although somewhat less severe, occurred to the bottom surface of the stub wing.

Representative samples of components used in landing gear assemblies were placed on the fuselage to resemble the geometry of a VTOL aircraft. These samples suffered slight damage during the testing. Miscellaneous samples of various materials were also placed under the fuselage during portions of the testing.

The significant damage noted to these specimens was pitting of plexiglas, erosion of paint and the sand blasting of all metal samples.

#### 4. Effects on Ground Personnel and Supporting Equipment

The instrumentation house, located sixty feet outboard from and in line with the forward duct, suffered some damage from the entrained sand particles. The house was a commercial steel sheetmetal prefabricated unit seven feet wide, ten feet long and seven feet high. All existing seams, normally weatherproof, had to be sealed to prevent particle penetration. The paint on the side of the house facing the forward duct became pitted and nicked by the sand. In time, the sheet metal began to rust in the area of the eroded paint. The window, through which the testing was observed, also became pitted and scratched. The 28 volt auxiliary power unit that supplied power for the instrumentation and engine operating controls, located beside the instrumentation house experienced damage similar to that suffered by the house itself.

The thirty-five ton Lorraine crane supporting the aft engine also sustained minor damage. The paint was pitted and eroded from the crane boom and also from the front of the crane cab. The crane operator's window was pitted and scratched to the extent that vision through it was impaired. The structure started to rust in the areas of the eroded paint. Considerable sand was trapped by the crane boom structure and the catwalks

and ledges protruding from the crane cab. Sand infiltrated through the doors, windows, and the crane boom cable openings in the cab. Under normal conditions these apertures are weatherproof.

Personnel standing within a radius of one hundred feet of each duct had to wear foul weather gear during the testing over water. Eye goggles became covered with mist making visibility poor. Personnel within the same radius during the sand test series and wearing protective goggles had to cover their face with a protective cloth. Although the face mask offered some protection, some of the sand particles still infiltrated under the mask.

#### B. Visibility

Loss of visibility is one of the more obvious consequences of particle entrainment and subsequent recirculation. It was found that pilot visibility will be restricted during operations over water and sand with the former presenting the more serious problem.

The evaluation of vision capability depends on the intensity of the reflected light and on the contrast and resolution of the view. However, these tests were conducted with similar bright sun illumination and with a background of high contrast objects. To aid in making this evaluation test personnel observations, remote camera coverage and a camera mounted in the simulated cockpit area were employed. (A contrast and intensity measuring visibility meter was also designed to obtain quantitative light data; but as described in Appendix I, the meter failed to give

consistent results). The cockpit mounted camera swept a 30 degree field of vision positioned midway between the longitudinal centerline of the aircraft and a perpendicular to it. This area was reported in Reference 9 as being the least congested with entrained particles, a fact substantiated by the subject testing.

#### 1. Effects of Configuration

There was no significant change in visibility noted as a result of configuration changes. In general, visibility conditions were considerably worse than would be expected from the isolated propeller testing due to the heavy concentration of particles entrained along the plane of the longitudinal and lateral streamlines. Also, terrain particles which are carried above the aircraft by the upflow region fall down over the front of the aircraft and reduce vision in this area. Changes in aircraft configuration which move the pilot away from the streamlines or which reduce the upflow will improve pilot's vision.

#### 2. Effect of Height, Over Water

The test rig was operated at two heights, corresponding to  $h_e/D_e$  ratios of 0.70 and 1.30. Although the lower operating height is, of course, most severe, visibility is seriously impaired at either height.

With an  $h_e/D_e$  ratio of 0.70, the pilot will lose visual contact throughout the major part of his field of vision, especially directly in front of the aircraft near the longitudinal streamlines. The 30 degrees swept by the cockpit camera was the least

congested with entrained particles. In this region, entrained particles did not rise more than one-half of a duct diameter above the ground until reaching a distance of about 80 feet from the fuselage. Even at this distance only very fine particles rose to significant heights. Within this region, the pilot will be able to distinguish the horizon, but no ground objects within a radius of 100 feet from the fuselage.

At the higher height, conditions were not as severe as at the lower operating height. Large objects were visible at 80 feet and there generally was a horizontal reference for pilot orientation, but only within the area swept by the cockpit camera. As noticed with the lower operating height, the planes of the aerodynamic streamlines contained so many terrain particles that visibility was essentially zero in these areas.

### 3. Effect of Terrain Conditions

As indicated in Reference 1, terrain yielding the most particles in a given volume will create the most severe downwash vision condition. Water, snow and sand were found to fall in this category. Although snow was not available, water and sand terrains were tested extensively during this program, and the effects of each on pilot's vision were evaluated.

Vision was considerably more limited during testing over water. In operating over water, a pilot can expect to encounter a severe loss of visual contact with terrain details, as well as a loss of a horizontal reference, particularly at he/De

ratios less than 1.0. During runs over sand, the quantity of entrained particles was considerably less by comparison. Large objects were visible beyond 40 feet and the pilot was constantly oriented with respect to the horizon. In every case, visibility through the planes of the longitudinal and lateral streamlines was almost completely obscured.

C. Evaluation of Operational Environment

To summarize the experience gained with the test rig, the grading system of Reference 1 has been used to establish operational environment evaluation tables. This effort is similar to the "Operational Limitations" tables of this reference and the same problem areas are evaluated. Namely:

Pilot Vision

Ground Personnel

Vision

Risk of Injury

Restriction of Motion

Ground Equipment Damage

Aircraft Damage

Loss of Concealment

This data is presented in Tables 1 and 2 for fresh water and wet sand respectively. The grading system is presented in Table 3. The general downwash area has been divided into three zones of varying downwash intensity for purposes of this study. The extent of these zones is shown by Figure 44.

Zone A is defined by a radius of 3 duct exit diameters



from the fuselage center. From data obtained and visual observations made during this program, it is felt that conditions for ground personnel within this zone will be unsatisfactory for disc loadings over 40 psf with duct height to diameter ratios less than 1.50. The possibility exists that serious injury will result to any person in this zone located within the regions of upwash along the planes of aerodynamic symmetry. Extrapolation of the dynamic pressure curve of Figure 16 to a height of 0.50 duct diameters indicates that dynamic pressure values of 1/3 the disc loading can be attained at ground level. Also, Figure 17 indicates that static pressures under the fuselage were approximately 1/3 of the disc loading. This dynamic pressure can therefore exert large forces on personnel. For example, Reference 13 reports that drag areas of an average man may range from 1.2 ft.<sup>2</sup> to 9 ft.<sup>2</sup>, depending on body position relative to wind direction. Thus, a 200 pound man can have a weight to drag area as low as 23 psf and therefore, he can be accelerated upward by the upwash if the disc loading exceeds 69 psf. If the disc loading is near 100 psf as proposed for some VTOL aircraft, this effect could be highly dangerous.

The maximum extent of Zone B is defined by a radius of 5 duct exit diameters from the fuselage center. Within this zone, personnel with protective gear may perform emergency operations. Equipment must be well secured, particularly at the planes of symmetry.

In Zone C, beyond a radius of 5 duct diameters, operating

conditions will be hindered only along the planes of symmetry. In this region, particles and debris may be transported as far as 10 diameters from the fuselage center, creating somewhat limiting conditions in this region.

## VI CONCLUSIONS

Downwash tests of a generalized dual tandem ducted propeller VTOL aircraft arrangement have served to point out the potential problem areas that exist when operating over essentially unprepared terrain. The extent to which these results are applicable to the operational situation remains to be determined. In general, the tests indicated that serious downwash problems can be expected with this aircraft.

The tandem configuration was found to cause a significant increase in downwash problems as compared to isolated propeller configurations tested previously. The most serious problems resulted from particle ingestion which caused unacceptable engine, propeller and airframe damage. This damage was aggravated by an upwash area located between the forward and aft ducted propellers near the sides of the fuselage. The upwash caused large amounts of terrain to be transported to the region above the fuselage. Quantitative data on the amount and size of sand particles transported to the fuselage indicate that engine inlet protection will be required.

The effects of variations in the dual tandem configuration were found to be small. Some effect of configuration on performance was noted. Terrain recirculation will be reduced if the propellers are either very close together or far apart so that the upflow region is reduced.

Current designs of tandem ducted propeller VTOL aircraft specify disc loadings of about 100 pounds per square foot with duct exit heights of less than one propeller diameter for a vertical take-off or landing maneuver. Although the testing reported herein did not include such extreme conditions, the following conclusions can reasonably be made for these operating conditions:

1. Operation over water and sand will cause severe vision problems to both the pilot and the ground crew.
2. Movement of personnel in the vicinity of the aircraft will be severely impeded. Face shields and protective clothing will be required. Personnel should not enter the upflow region.
3. Equipment in the immediate area of the operating aircraft must be restrained from motion in order to prevent injury to personnel and the aircraft.
4. Operation in proximity to unprepared cohesionless terrain, such as sand or dry snow will make concealment of the aircraft impossible.
5. An engine power loss due to ingestion will occur when operating over water at low altitudes.
6. Severe damage to unprotected engines, propellers, ducts and aircraft will result due to erosion and particle ingestion when operating over sand.
7. Ground coupled aerodynamic interference effects will reduce propeller performance, cause significant

oscillations in the propeller thrust and will provide a sizeable upload on the bottom of the fuselage.

Careful design and the development of specialized VTOL aircraft operational techniques probably can minimize many of the problem areas resulting from downwash. However, because of the severity of the operational environments studied, more direct methods of solution should be investigated. Further study should be made of alleviation devices such as ground covers, terrain stabilization and downwash deflectors.

Particular attention should be paid to the problem of engine particle ingestion. The resulting loss in performance and the blade erosion which occurs demand a solution to this problem. The development of engine inlet screens and the optimization of the inlet placement can greatly improve this serious problem.

## VII RECOMMENDATIONS

The full scale downwash testing conducted has uncovered problem areas which may impede the development and/or restrict the operation of a VTOL aircraft. In general, the approaches to the solution of downwash problems are the following:

1. Toughen Aircraft
2. Aircraft Redesign
3. Ground Preparation
4. Terminal Flight Maneuvers
5. Mission Analysis

Consequently, in order to aid the development of VTOL aircraft in general and the dual tandem aircraft in particular, it is recommended that work be initiated on the following programs:

1. The determination of the optimum engine intake location for the dual tandem configuration and the development of a suitable inlet particle separator.
2. The experimental investigation of the aerodynamic interference between ducts which was noted during the course of testing.
3. The development of surface-hardened blades capable of operating for extended periods of time in a severe downwash environment, such as sand.
4. An enlarged study of aircraft configuration effects to determine whether a significant alleviation of

the downwash problems can be obtained with this approach.

5. A detailed investigation of the effects of water intake on engine performance and endurance, with particular attention to the salt water corrosion problem.
6. Further testing and study of devices designed to alleviate downwash impingement problems.
7. The design and development of lightweight air dropable terrain covers.
8. The development of terrain stabilizing chemicals for application to the ground surface and means of applying same.
9. Further problem investigative tests should be conducted to higher disc loadings and with higher propeller tip speeds.
10. Systems analysis studies should be conducted to determine the terrain environment probability and to evaluate the damage resistance requirement for the VTOL aircraft when operating in severe environments.
11. The effects of landing and take-off maneuvers on downwash problems should be studied. Some maneuvers such as low speed translation or large vertical acceleration near the ground will probably aggravate

terrain recirculation. Maneuvers which alleviate downwash problems probably can be devised.

12. The effects of surroundings of prepared landing sites should be studied. Landing sites near large buildings will aggravate terrain recirculation due to the aerodynamic reflection on the building. Similar problems may exist on deck landing sites or on aircraft carriers.



# VIII REFERENCES

1. Pruyn, R. and Goland, L., "An Investigation of VTOL Operational Problems Due to Downwash Effects". Kellett Aircraft Corporation Report No. 179T80-2, June 1961. (Also Paper Presented at American Helicopter Society 18th Annual Forum, May 1962).
2. Pruyn, R., "The Impact of VTOL on Open Sea Rescue", Kellett Report, (Presented at Fourth Annual Symposium on Helicopter Open Sea Rescue, September 1963).
3. Watsen, E. A., "Amount of Dust Recirculated by a Hovering Helicopter", Kaman Aircraft Corporation Report No. R-169, December 1956.
4. Kuhn, R., "An Investigation to Determine Conditions Under Which Downwash from VTOL Aircraft will Start Surface Erosion from Various Types of Terrain", NASA TN D-56, September 1959.
5. Morse, A., and Newhouse, H., "VTOL Downwash Impingement Study Surface Erosion Tests", TREC Technical Report 60-67, Oct. 1960.
6. Newsom, W. A., Jr., "Effect of Ground Proximity on the Aerodynamic Characteristics of a Four-Engine Vertical-Take-Off-and Landing Transport Airplane Model with Tilting Wing and Propellers", NASA TN-4124, October 1957.
7. Pegg, R., "Damage Incurred on a Tilt-Wing Multi-Propeller VTOL/STOL Aircraft Operating Over a Level Gravel Covered Surface", NASA TND 535, 1960.
8. Stirgwolt, T. F., "Salt Water Ingestion by Gas Turbine Engines", Paper Presented at American Helicopter Society 17th Annual Forum, May 1961.
9. O'Bryan, T. C., "An Investigation of the Effect of Downwash from a VTOL Aircraft and a Helicopter in the Ground Environment", NASA TN D-977, October 1961.
10. Newsom, W. A. Jr., and Tosti, L. P., "Slipstream Flow Around Several Tilt-Wing VTOL Aircraft Models Operating Near the Ground", NASA TN D-1382, September 1962.
11. Paxhia, V. B. and Sing, E. Y., "Design Development of a Dual Tandem Ducted Propeller VTOL Aircraft", IAS Paper No. 63-30, January 1963.

REFERENCES (Cont'd.)

12. Anonymous, "First Test Results - Lycoming's Sand and Duct Program for the T-53 Gas Turbine Engine", Lycoming Brochure, October 1958.
13. Hoerner, S. F., "Fluid-Dynamic Drag", Published by Author, 1958.
14. Miller, N. J. and George, M. M., "Determination of Optimized Propellers for Ground Effect Machines", TRECOM Technical Report No.63-16, June 1963.
15. Grose, R. M., "Wind Tunnel Tests of Shrouded Propellers at Mach Numbers from 0 to 0.60", Report No.58-604, Wright-Patterson AFB, December 1958, ASTIA No.205464.

## APPENDIX I - VISIBILITY METER DESIGN AND TESTING

An attempt was made to develop a visibility meter for the purpose of quantitatively evaluating the effect of downwash impingement on pilot's visibility under the conditions tested. The meter was designed to be activated by light rays reaching the simulated cockpit area and thus give a measure of the downwash visibility problem. Unfortunately, as explained below, the meter did not function properly during the testing and thus the results obtained with it are unreliable and are omitted from this report.

The meter consisted of a photo cell, 16mm camera lenses, and a motor driven wobble plate with a first surface mirror mounted on the wobble plate. Light reflected from a half-black, half-white target would hit the wobble plate mirror which reflected the incoming light through the 16mm lenses onto the photo cell. Upon receiving light reflected from the white side of the target (but not from the black side) the photo cell would generate a voltage which would be transmitted to the recorder. The average value of the output signal was an indication of the light intensity and the amplitude of the oscillating signal was an indication of the resolution which could be detected between the white and black surfaces.

Under laboratory testing the meter worked well under all conditions. However, under actual test conditions the meter

did not respond as was anticipated from the laboratory results. This operational difficulty may be attributable to one or more of the following factors:

1. The large distance from target to photo cell.
2. The position of target and meter relative to the sun.
3. The diffused reflectivity of the water particles.
4. Terrain particles collecting on the cover glass of the visibility meter.

Even under the most severe downwash conditions, sufficient light was transmitted by reflection from the sand and water particles to maintain a reasonably high voltage at all times. Although this signal did vary and was recorded, the data obtained are not considered to be a valid indication of visibility loss in the cockpit area. The observations of test personnel and the close examination of the extensive film coverage were therefore used to reach conclusions regarding visibility under the various test conditions.

## APPENDIX II - DUCTED PROPELLER PERFORMANCE PREDICTION

In designing the downwash test rig it was necessary to estimate the performance which could be produced. An annular momentum blade element method with empirical corrections has been developed in Reference 14 for predicting ducted propeller performance. The predicted performance obtained with this method was in excellent agreement with the measured performance of the test rig. Since there is little ducted propeller performance data available and almost no correlation with theory, this performance method is briefly presented and the experimental comparison is discussed in this appendix.

The difficulty in predicting ducted propeller performance results from the momentum of the air which results from the thrust force on the inlet. As discussed in Reference 14, this effect is included in the following relation:

$$\frac{V_P}{\Omega R} \cdot \frac{\left[ (1 - X_P^2) \frac{dG_T}{dx} \left( \frac{A_P}{A_E} \right) \right]}{\left[ x \left\{ 1 + \left( \frac{A_P}{A_E} \right)^2 \right\} \right]} \left\{ 1 + \frac{T_S}{T_P} - \frac{A_E}{A_P} \left[ 1 + \frac{T_S}{T_P} \left( \frac{A_P}{A_E} \right) \left( \frac{k-1}{k+1} \right) \right] \right\}^{\frac{1}{2}} \quad (1)$$

In this equation the empirical factors  $T_S/T_P$  and  $k$  may be obtained from the test data of the above reference. At all propeller radii this equation must be solved simultaneously with the following blade-element thrust relation:

$$\frac{dC_T}{dx} = \frac{\sigma x}{2} \frac{x^2}{(1-x_p^2)} \left[ \left( \frac{V_P}{\Omega R_x} \right)^2 + 1 \right]^{\frac{1}{2}} \left[ C_l - C_d \left( \frac{V_P}{\Omega R_x} \right) \right] \quad (2)$$

The results are then radially integrated to obtain the thrust coefficient:

$$C_T = \int_{x=x_p}^{x=1} \frac{dC_T}{dx} dx \quad (3)$$

Similarly the propeller power coefficient is obtained as follows:

$$\frac{dC_P}{dx} = \frac{\sigma x}{2} \frac{x^3}{(1-x_p^2)} \left[ \left( \frac{V_P}{\Omega R_x} \right)^2 + 1 \right]^{\frac{1}{2}} \left[ C_{d_x} + C_{l_x} \left( \frac{V_P}{\Omega R_x} \right) \right] \quad (4)$$

And

$$C_P = \int_{x=x_p}^{x=1} \frac{dC_P}{dx} dx \quad (5)$$

This method was used to predict the downwash test rig performance assuming out of ground effect conditions. The agreement between predicted performance and test data as shown in Figure 45 is excellent with a value of  $T_s/T_p$  of 0.7 and  $k$  of -0.4.

The duct inlet used in this program (as described in Section III of this report) is similar to one of the inlets used in collecting the performance data reported in Reference 14. This shape was selected as typical of a duct designed to give good performance at high forward speeds. Performance data for a similar high speed duct from Reference 15 is also shown in Figure 45.

From the curve, the Kellett test data appears to be an extrapolation of the Reference 15 data to a larger power coefficient. This explanation is quite reasonable since the test rig propellers were operated at a high pitch setting to produce a maximum thrust within the rpm limit of the T-53 engines.

Additional symbols used in this appendix:

$A_p$	Propeller plane cross sectional area, square feet	
$C_d$	Airfoil section drag coefficient	
$C_l$	Airfoil section lift coefficient	
$C_p$	Propeller power coefficient,	$C_p = \frac{P}{A_p \rho (\Omega R)^3}$
$C_T$	Propeller thrust coefficient,	$C_T = \frac{T}{A_p \rho (\Omega R)^2}$
$k$	Inlet loss factor	
$T_p$	Propeller thrust, pounds	
$T_s$	Duct inlet thrust, pounds	
$R$	Propeller tip radius, feet	
$V_f$	Inflow velocity at propeller plane, feet/second	
$X$	Blade radius ratio, $X = r/R$	
$X_p$	Ratio of propeller hub radius to propeller radius	
$\rho$	Air mass density, slugs/cubic feet	
$\sigma$	Propeller solidity	
$\Omega$	Propeller rotational speed, radians/second	

OPERATIONS OVER FRESH WATER

TABLE 1: EVALUATION OF OPERATIONS

Disc Loading psf	Duct Height Ratio he/De	Pilot Vision	Personnel						
			Zone A			Zone B			Vision
			Vision	Injury	Motion	Vision	Injury	Motion	
50	0.70	U	U	U	U	L	T	L	T
	1.30	L	L	L	L	L	T	L	T
35	0.70	T	T	T	T	T	S	T	S
	1.30	S	T	T	T	T	S	S	S

\* May be unacceptable unless engine power under conditions of water surface

OPERATIONS OVER SAND

TABLE 2: EVALUATION OF OPERATIONS

Disc Loading psf	Duct Exit Height Ratio he/De	Pilot Vision	Personnel						
			Zone A			Zone B			Vision
			Vision	Injury	Motion	Vision	Injury	Motion	
50	0.90	T	U	U	U	L	L	L	L
	1.50	T	U	U	U	L	L	L	T
35	0.90	S	T	T	T	S	T	T	S
	1.50	S	T	T	T	S	T	S	S

\* Engine operation will be satisfactory on terrain if adequate inlet protection



# OPERATIONS OVER FRESH WATER

TABLE 1: EVALUATION OF OPERATIONAL ENVIRONMENT

Personnel							Equipment			Aircraft			Concealment
	Zone B			Zone C									
Condition	Vision	Injury	Motion	Vision	Injury	Motion	Zone A	Zone B	Zone C	Propeller	Engine	Airframe	
U	L	T	L	T	S	T	L	L	T	S	*L	S	L
L	L	T	L	T	S	S	L	S	S	S	*T	S	L
T	T	S	T	S	S	S	S	S	S	S	T	S	T
S	T	S	S	S	S	S	S	S	S	S	S	S	T

May be unacceptable unless engine can produce normal power under conditions of water spray ingestion.

# OPERATIONS OVER SAND

(Average moisture content of sand was 11.8%)

TABLE 2: EVALUATION OF OPERATIONAL ENVIRONMENT

Personnel							Equipment			Aircraft			Conceal- ment
	Zone B			Zone C									
ion	Vision	Injury	Motion	Vision	Injury	Motion	Zone A	Zone B	Zone C	Propel- ler	En- gine	Air- frame	
	L	L	L	L	T	T	L	L	T	U	*U	U	L
	L	L	L	T	T	S	L	L	T	L	*L	L	L
	S	T	T	S	S	S	S	S	S	T	*T	S	T
	S	T	S	S	S	S	S	S	S	T	*T	S	T

Engine operation will be satisfactory over sand terrain if adequate inlet protection is provided.



## Grading Code

U = Unacceptable  
L = Limited  
T = Tolerable  
S = Satisfactory

**TABLE 3**

**DOWNWASH OPERATIONAL ENVIRONMENT GRADING SYSTEM**

	<b>RATING</b>	<b>DESCRIPTION</b>	<b>PRIMARY MISSION ACCOMPLISHMENT</b>
<b>Normal Operation</b>	<b>Satisfactory, S</b>	The specified function can be performed unimpeded	<b>Yes</b>
<b>Emergency Operation</b>	<b>Tolerable, T</b>	Disturbance may be endured but is disconcerting and will reduce efficiency	<b>Yes</b>
	<b>Limited, L</b>	The specified function may be performed in a limited manner under emergency or combat condition (some damage may occur)	<b>Doubtful</b>
<b>No Operation</b>	<b>Unacceptable, U</b>	Based on present VTOL design and operational techniques and equipment, the specified function cannot be performed	<b>No</b>

TABLE 4: EVALUATION OF TERRAIN STABILIZING CHEMICAL

TRADE NAME CHARACTERISTICS	NOPLOFOAM H-201	LOCKFOAM P-502	ELVACET 81-900	ELVANOL 71-30	STAFOAM 1801
COMPOSITION	Semi-Rigid Fluorinated Hydro-Carbon	Semi-Rigid Urethane Foam Two-Part Mix	Polyvinyl Acetate Emulsion	Polyvinyl Alcohol	Polyurethane Foam Two-Part Mix
DELIVERY SYSTEM	Air Mix And Spray System	→		Pour in Place	Air Mix and Spray
DENSITY BEFORE DEL.	63	63	61	52	63
AFTER DELIVERY (Lb. /ft. 3)	0.9	2.0	-	-	2.0
TIME REQUIRED TO STABILIZE TERRAIN	25-35 Sec.	1 Min.	30 Min.	30 Min.	1 Min.
WEIGHT-AREA FACTOR (lbs. /ft. <sup>2</sup> )	0.15 (Tested)	0.22 (Tested)	0.48 (Tested)	0.41 (Tested)	0.19 (Estimated)
TERRAIN BONDING	Good	Good	Excellent	Fair	Good
FLAMMABILITY	Self Extinguishing	→		Non Flammable	Non Flammable
TOXICITY	Fumes Toxic when Settling Non-Toxic After Formed	→		Non Toxic	Irritating Vapors While Mixing
BEARING STRENGTH (PSI)	2.0 - 3.0	6.0	20.0	10.0	9.0
GENERAL INFORMATION	Requires No Preheat of 2 Part Mix. Terrain Temp. Should Be Above 40 <sup>0</sup> F	→		Forms An Excellent Surface Hard and Non Flammable	Delivery Difficult After Preparation Due to Precipitation Effect
					Temperature Limits of -60 <sup>0</sup> F to 200 <sup>0</sup> F

1

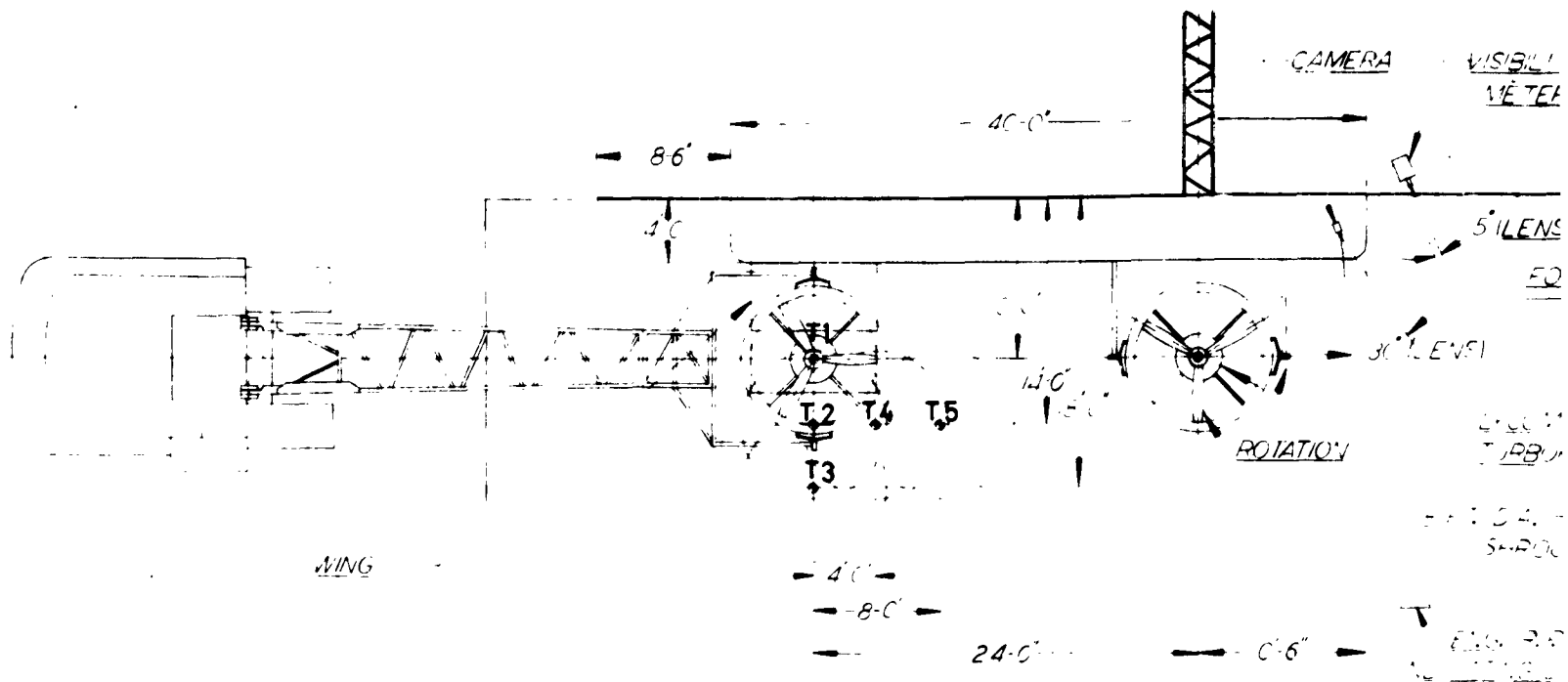
#### 4: EVALUATION OF TERRAIN STABILIZING CHEMICAL

KFOAM	ELVACET	ELVANOL	STAPOAM	RIGITHANE	RUBBATEX	ECCOFOAM	THICKOL
02	81-900	71-30	1801	334-328	173	FS	US-104-R US-104 C
1-Rigid thane Foam -Part Mix	Polyvinyl Acetate Emulsion	Polyvinyl Alcohol	Polyurethane Foam Two-Part Mix	Resin Foam Two-Part Mix	Water Base Coating	Open Cell Polyurethane Two-Part Mix	Low Viscosity Liquids Two-Part Mix
→	Pour in Place	Pour in Place	Air Mix and Spray	Air Spray	Pour in Place	Spray	Pour
	61	52	63	-	61	-	70.8
	-	-	2.0	1.9	-	2.5	70.8
in.	30 Min.	30 Min.	1 Min.	1 Min.	3 Hours	1 Min.	10 Min.
2 sted)	0.48 (Tested)	0.41 (Tested)	0.19 (Estimated)	0.17 (Estimated)	0.55 (Tested)	0.31 (Estimated)	0.63 (Tested)
1	Excellent	Fair	Good	Good	Fair	Fair	Excellent
→	Non Flammable	Non Flammable	Self Extinguishing	→	Non Flammable	→	Flammable at High Temperatures
→	Toxic if Inhaled in Large Quantities	Non Toxic	Irritating Vapors While Mixing	→	Non Toxic	Non Toxic	Non Toxic
	20.0	10.0	9.0	20.0	0.5	50	Approx. 100
→	Forms An Excellent Surface Hard and Non Flammable	Delivery Difficult After Preparation Due to Precipitation Effect	Temperature Limits of -60° F to 200° F	Requires Preheat of Chemicals	To Viscous For Spray Application	High Cost	Excellent Bonding and Strength Qualities- Burns Under Acetalene Torch

2

TABLE 5: EVALUATION OF GROUND COVER MATERIALS

Cover Materials	Screening	Films			Fabrics	Metallized Fabric	
	18 Mesh Screen	Mylar	Saran	Polyethylene	Fairprene	Mylar	Mylon Alum.
Specific Weight (lb/ft <sup>2</sup> )	0.28	0.072		.009	0.1	.007	.013
Terrain Protection	Fair	Good	Good	Good	Good	Fair	Good
Storage	6" dia. rolls x 10' wide	3' x 3' x 4" pkg.	3' x 3' x 4' pkg.	3' x 3' x 2" pkg.	3' x 3' x 1'	3' x 3' x 2"	3' x 3' x 3"
General Comments	Stiffness too great for use as air deployed system	Very tough material, good for ground troop movement	Problem with self clinging properly during deployment	Light-weight, not strong enough for troop movement	Good abrasion resistance	Problem with edge flapping	Cost is expensive
Weight Required for Dual Tandem Aircraft (4 - 12 ft. dia.), lb	500	128		16	179	13	25



1

ENCLOSURE

REFLECTION PLANE

PLAN VIEW

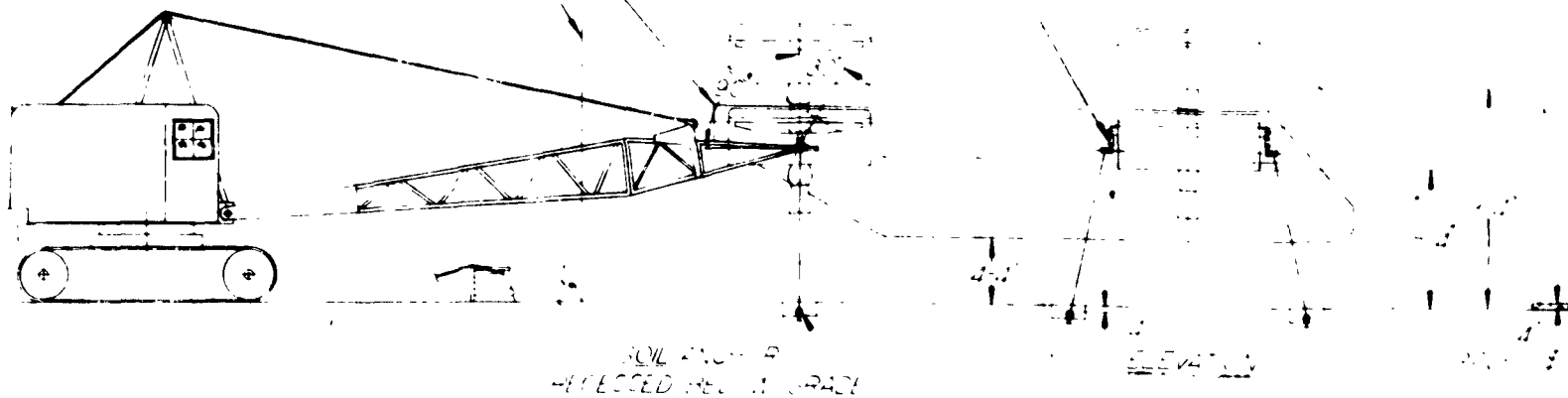
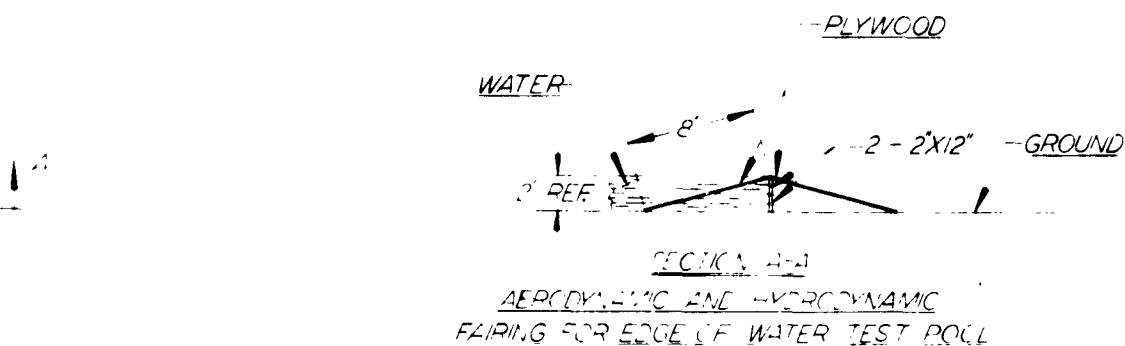




**FIGURE 1**  
**GENERAL ARRANGEMENT DOWNWASH TEST RIG**  
**TANDEM DUCTED PROPELLER VTOL**



EDGE OF WATER  
AND TERRAIN

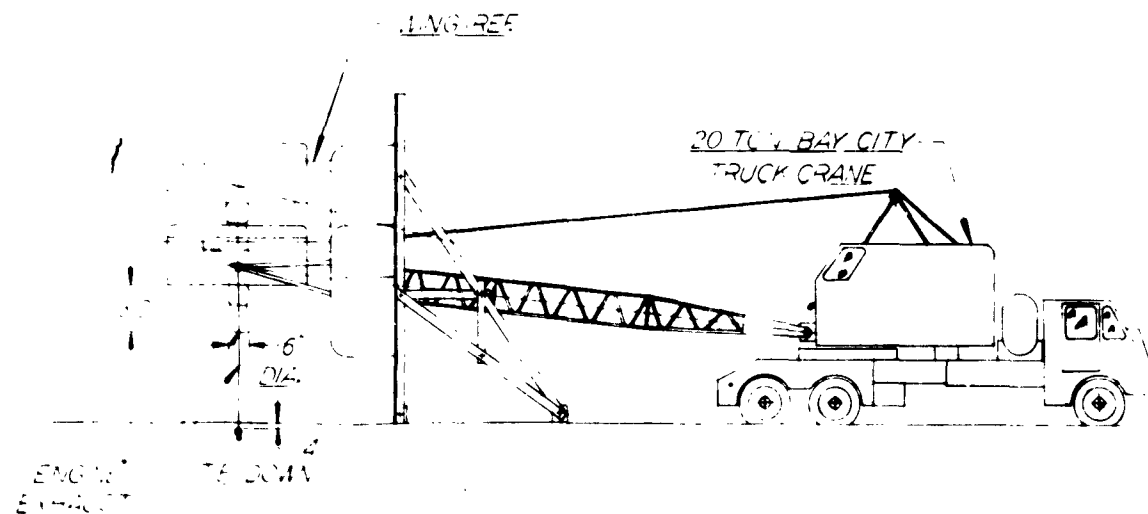






FIGURE 2. PHOTOGRAPH OF DOWNWASH TEST RIG MODIFIED TO SIMULATE  
A REPRESENTATIVE VTOL AIRPLANE



HAMILTON STANDARD PROPELLER 7063-6 (MODIFIED)

D BLADE DIAMETER IN FEET

h BLADE THICKNESS

b BLADE CHORD

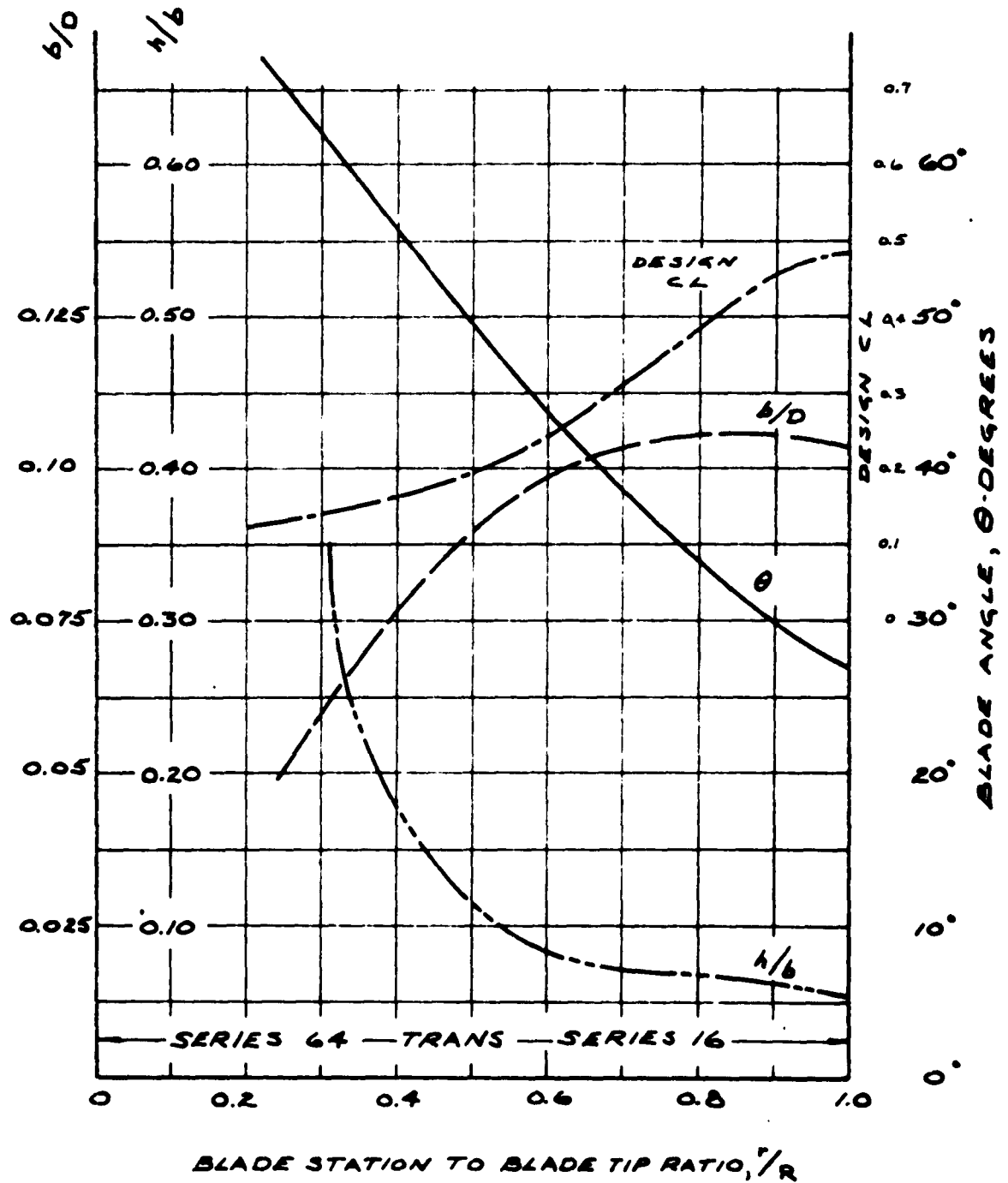


FIGURE 4. CHARACTERISTICS OF PROPELLER BLADES USED IN DOWNWASH TEST RIG



a) Side View of Test Rig,  $h_s/D_s = 1.30$



b) Three-quarter Aft View of Test Rig Operating at 60 psf Disc Loading

FIGURE 5. PHOTOGRAPH OF TEST RIG WITH WATER TEST POOL

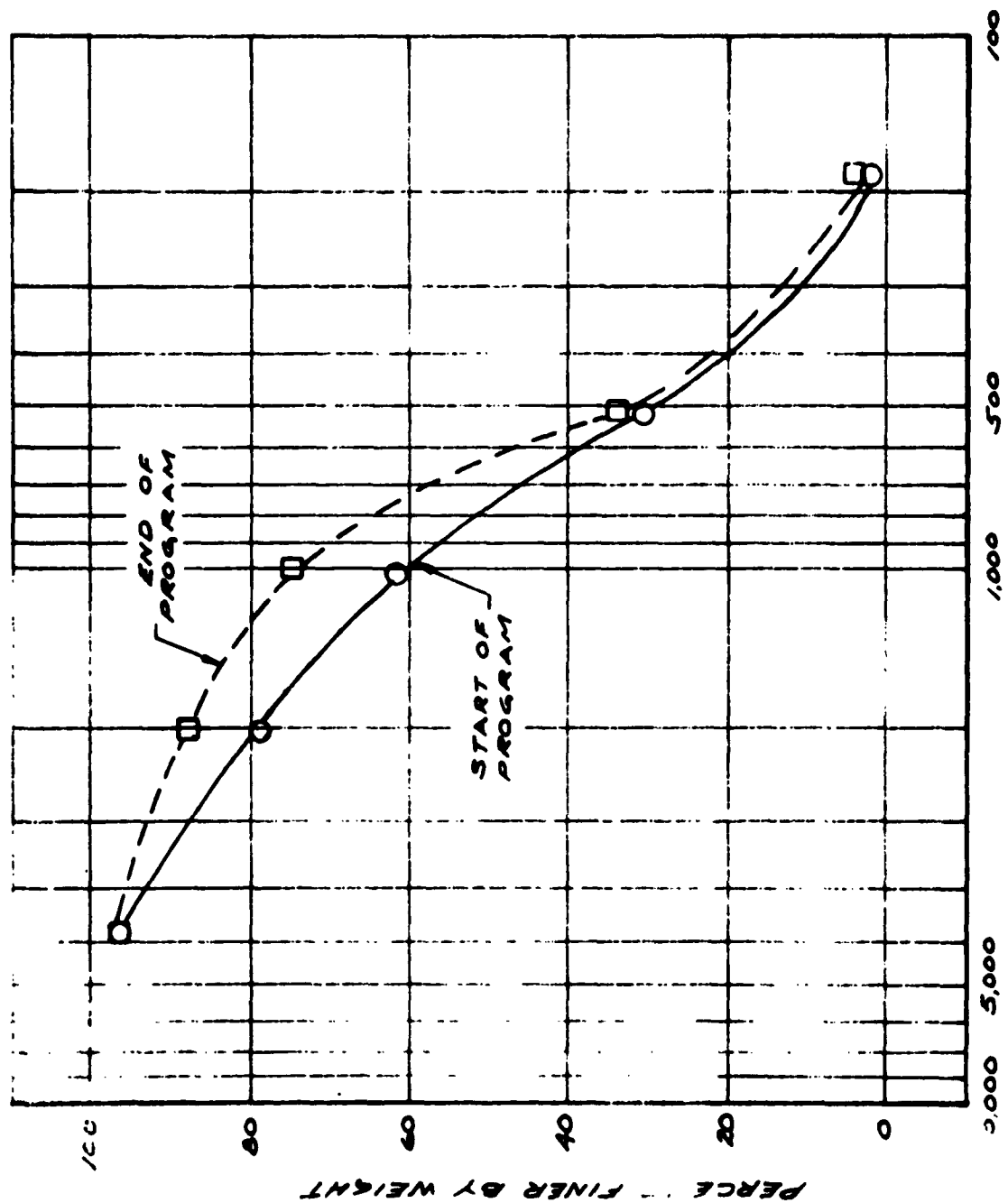
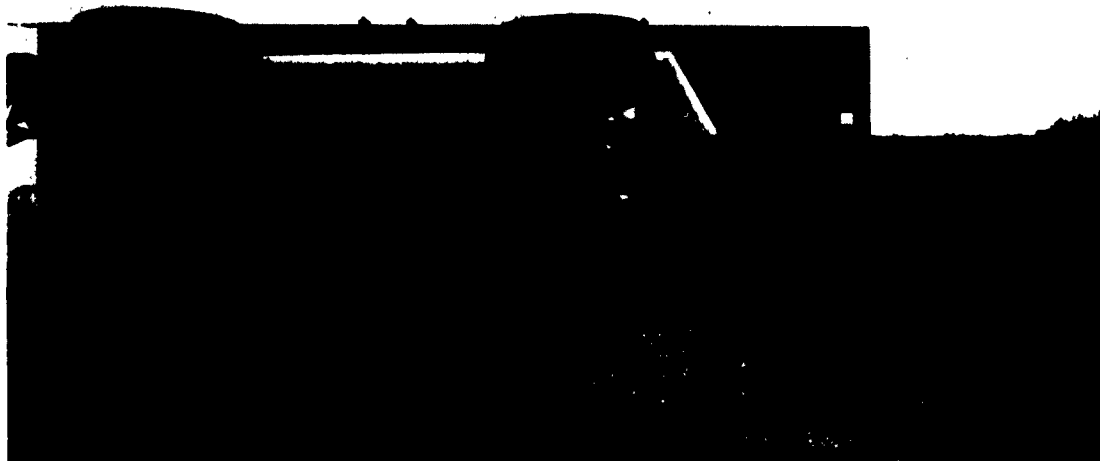


FIGURE 6. SIEVE ANALYSIS OF SAND TERRAIN SAMPLE



a) Side View of Test Rig,  $h_e/D_e = 1.50$

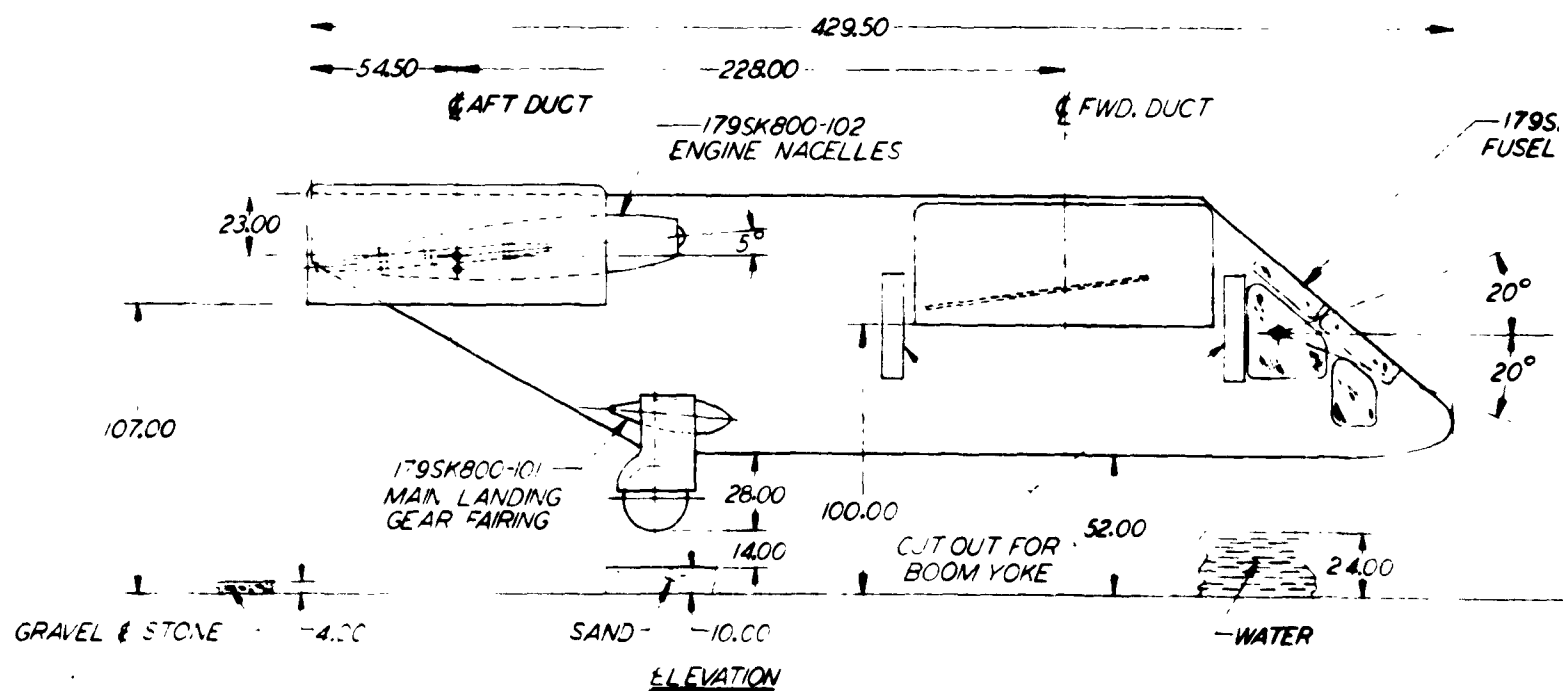


b) Three-quarter Aft View of Test Rig Operating  
at 60 psf Disc Loading

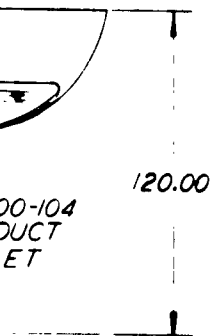
FIGURE 7. PHOTOGRAPH OF TEST RIG WITH SAND TERRAIN



FIGURE 8. PHOTOGRAPH OF PARTICLE TRAP LOCATED INSIDE  
DUCT OF DOWNWASH TEST RIG







**FIGURE 9. DOWNWASH TEST RIG IN MODIFIED CONFIGURATION**

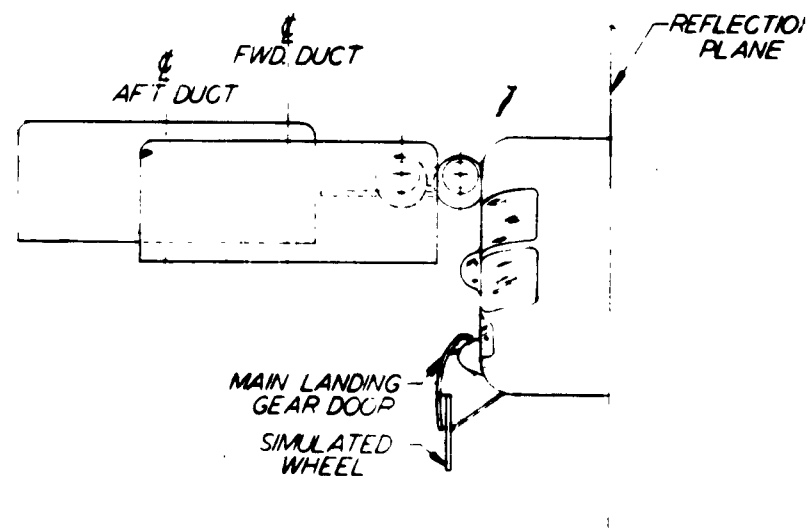
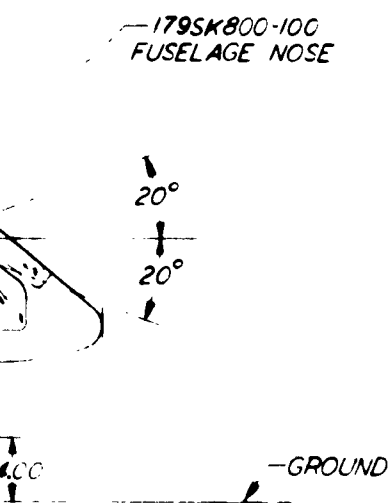
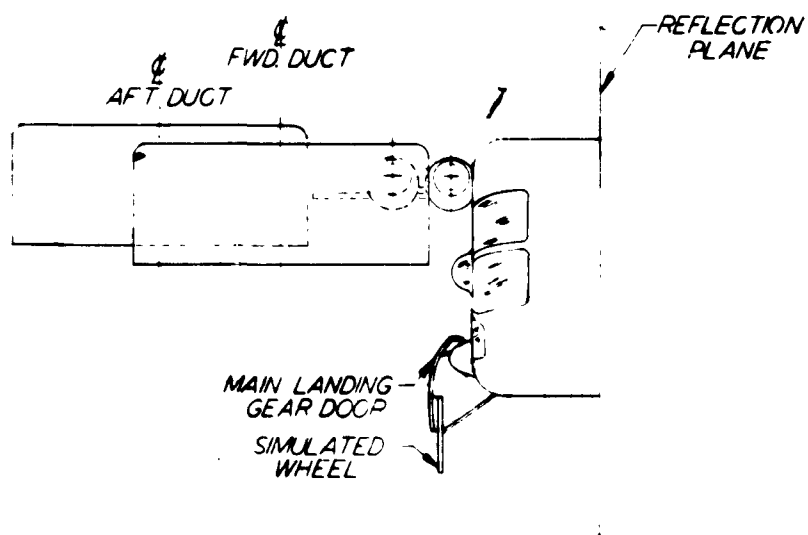


FIGURE 9. DOWNWASH TEST RIG IN  
MODIFIED CONFIGURATION



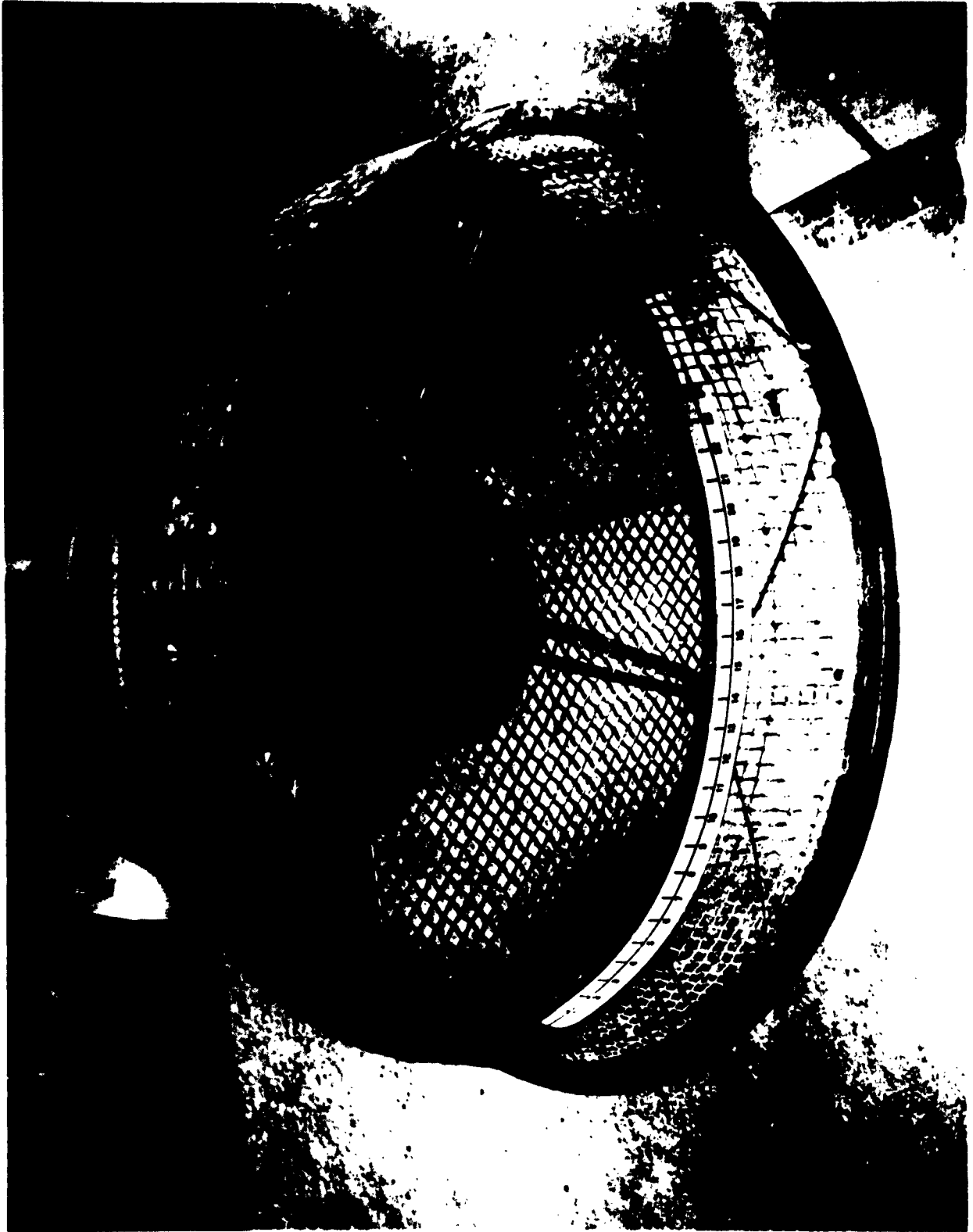


FIGURE 10. ROTATING ENGINE INLET SCREEN (36 MESH WIRE  
SCREEN, 59 PERCENT OPEN AREA)

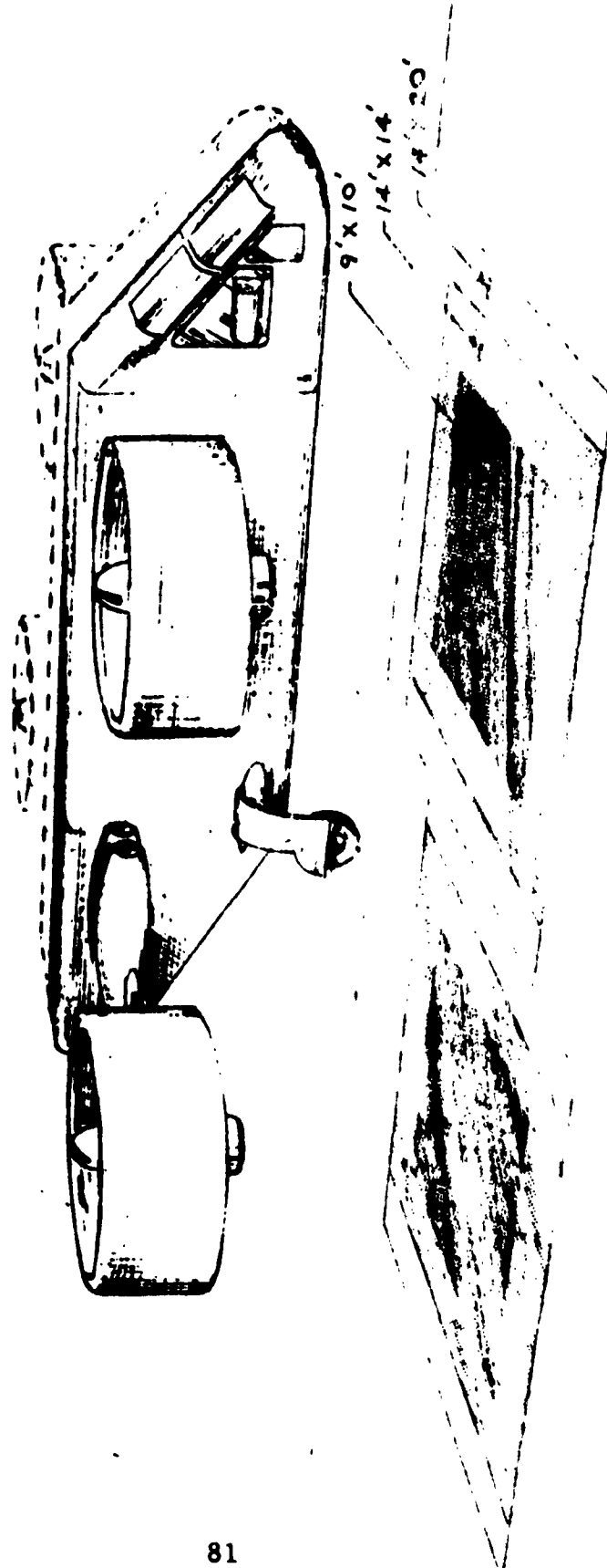


FIGURE 11. MINIMUM AREA GROUND COVERS FOR FULL SCALE TESTS

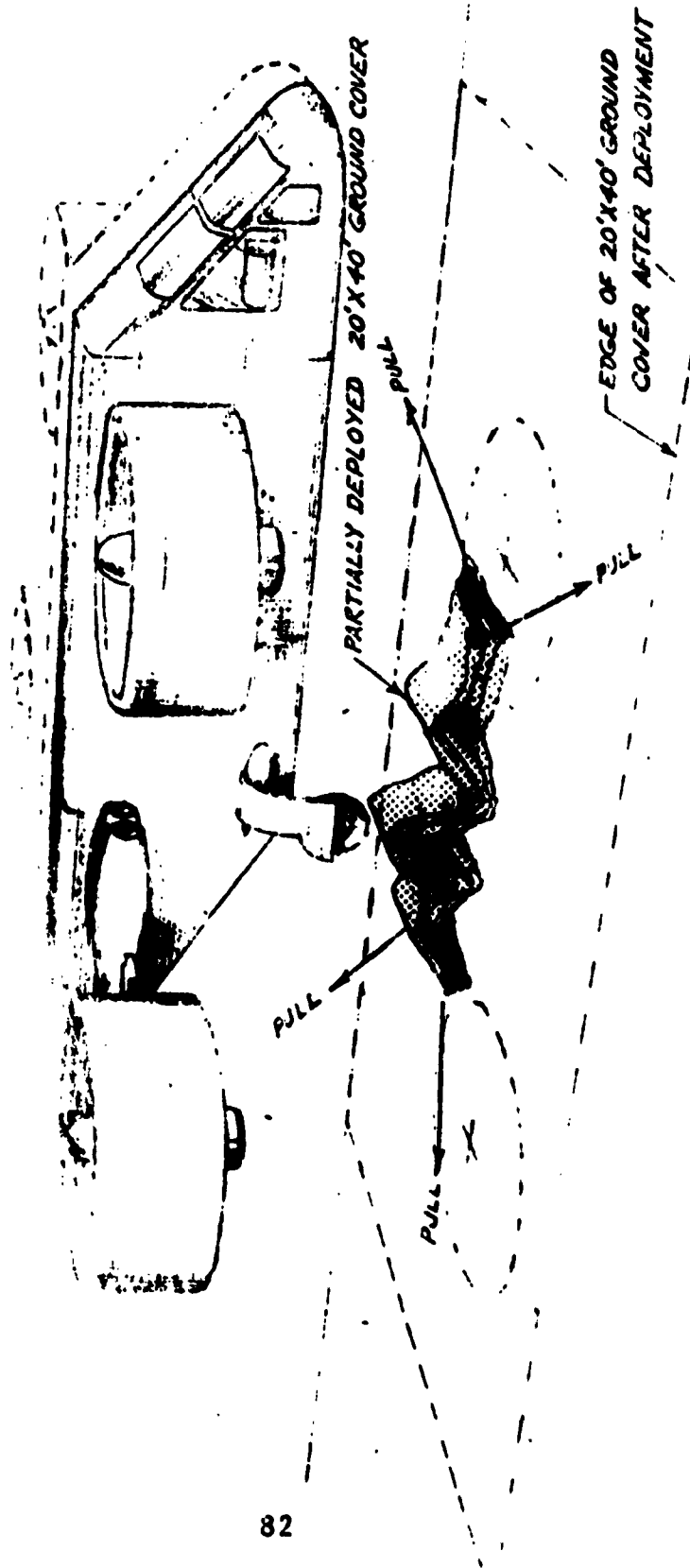


FIGURE 12. LIGHT FLEXIBLE COVER DEPLOYMENT TEST RIG

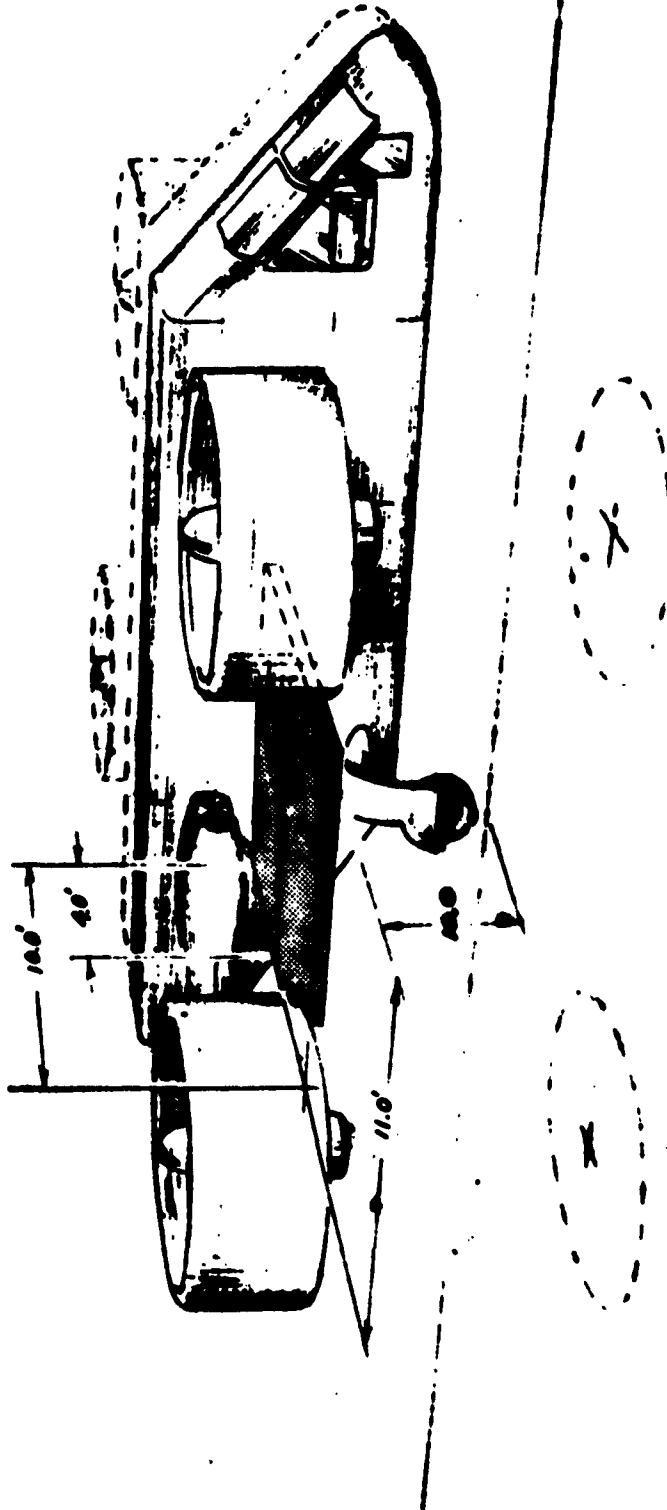
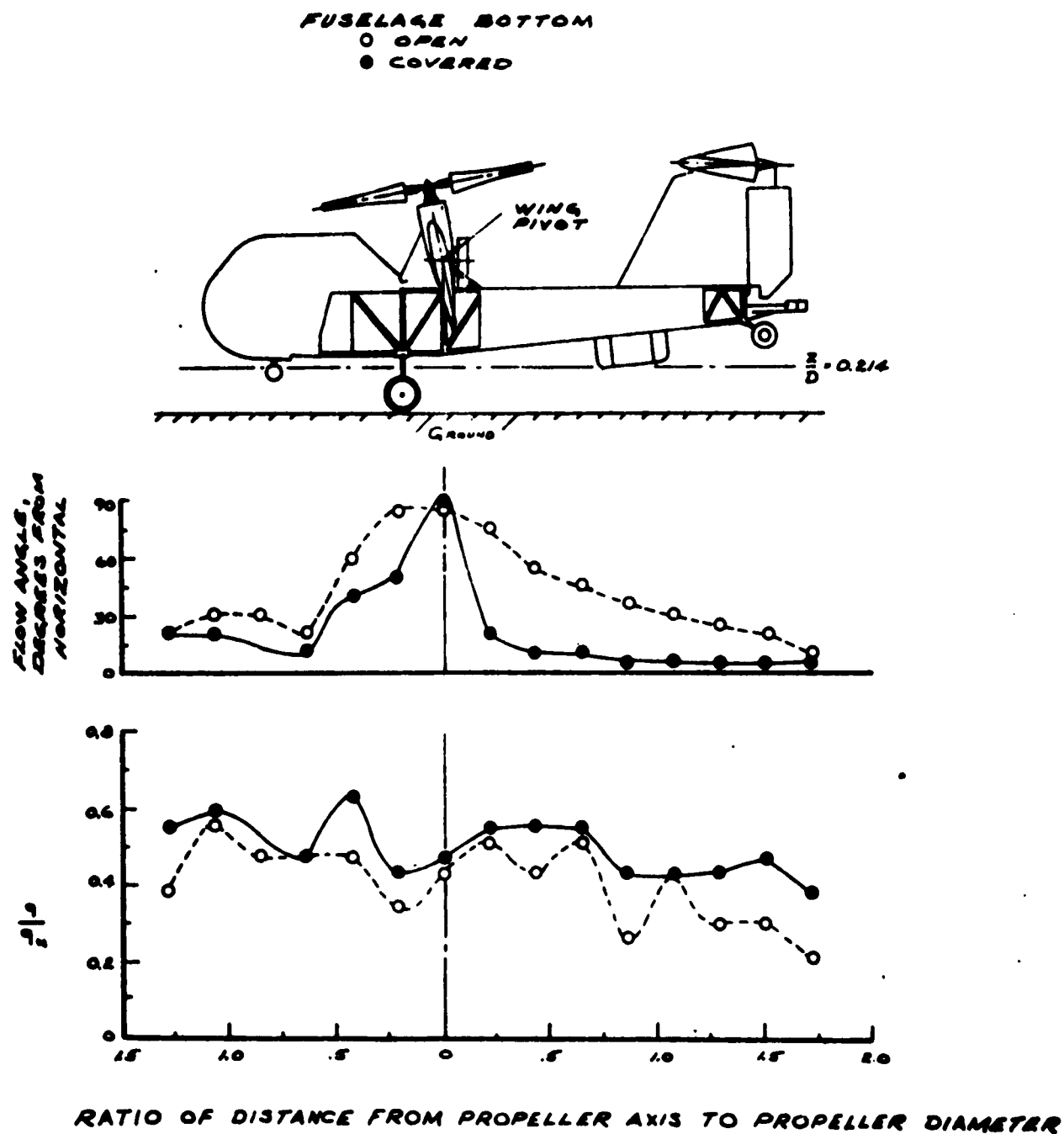


FIGURE 13. TERRAIN DEFLECTOR WING OR FLAP (SHORT AND LONG CONFIGURATIONS)

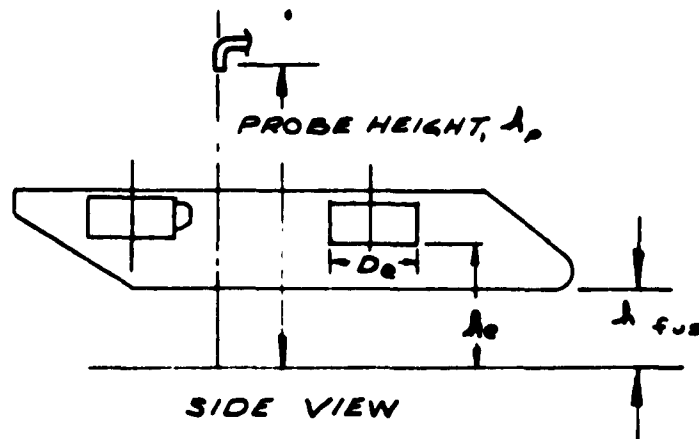


FIGURE 14. FEATURES OF DOWNWASH FLOW FOR DUAL TANDEM CONFIGURATION



**FIGURE 15. FLOW FIELD MEASUREMENTS ALONG PLANE OF SYMMETRY AND UNDER FUSELAGE OF VZ-2 MODEL (FROM REFERENCE 10)**





$$\lambda_e / D_e = 0.90$$

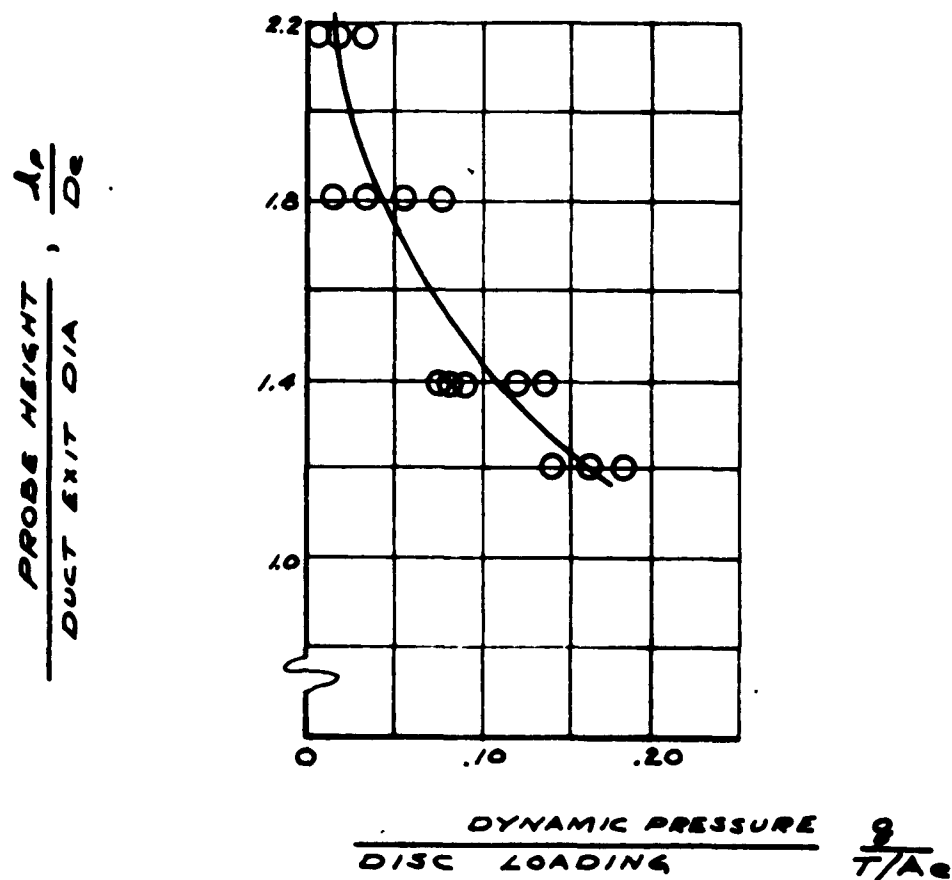


FIGURE 16. VARIATION OF DYNAMIC PRESSURE WITH HEIGHT AT POINT DIRECTLY ABOVE THE INTERSECTION OF THE LATERAL STREAMLINE AND SIDE OF FUSELAGE

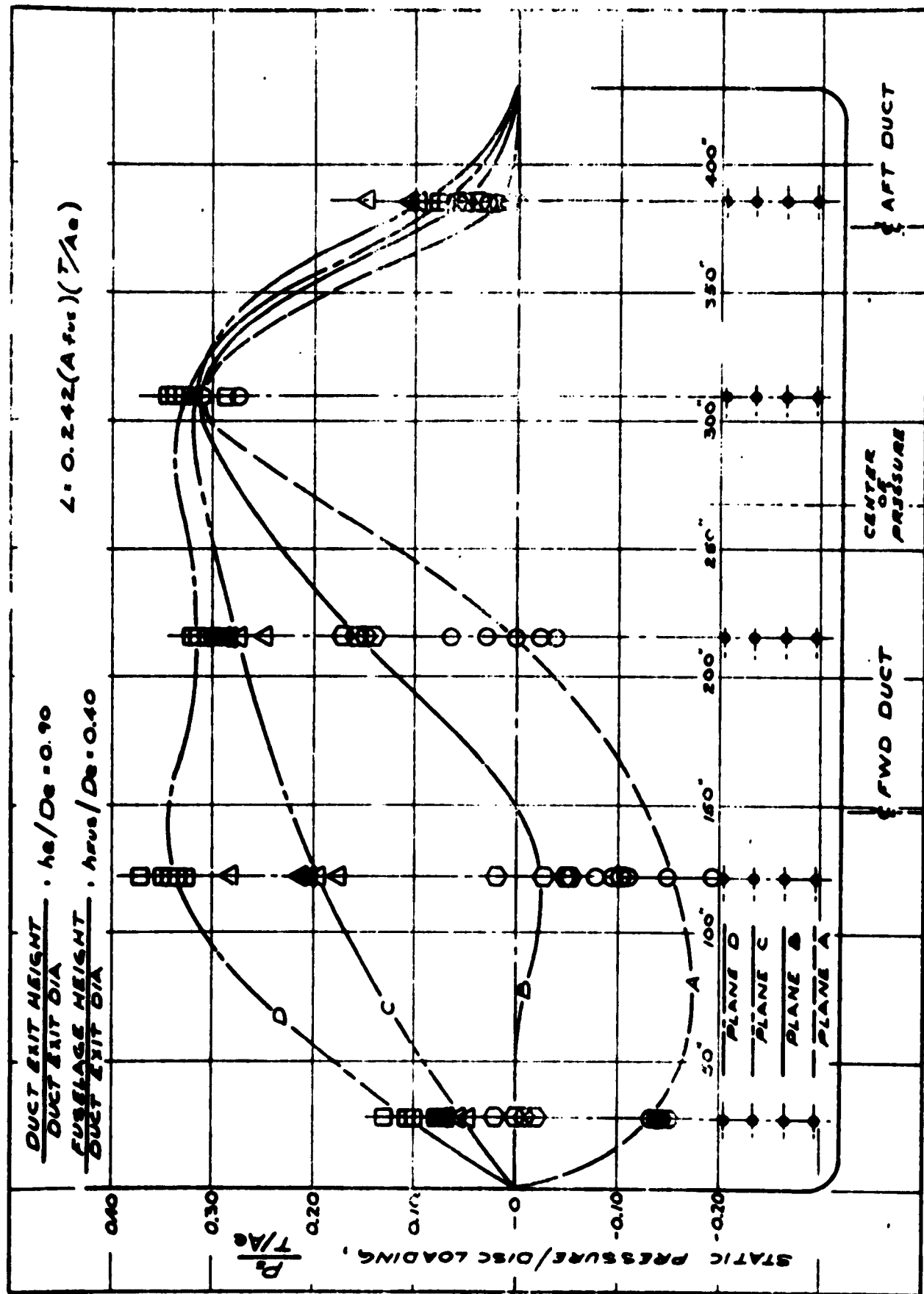


FIGURE 17. STATIC PRESSURE DISTRIBUTION ON THE BOTTOM SURFACE OF THE FUSELAGE, MODIFIED CONFIGURATION

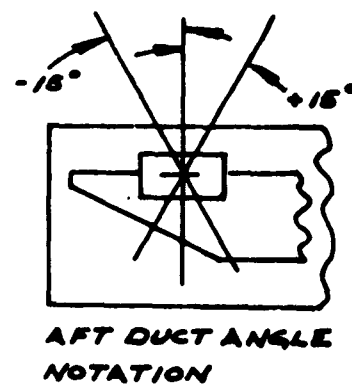
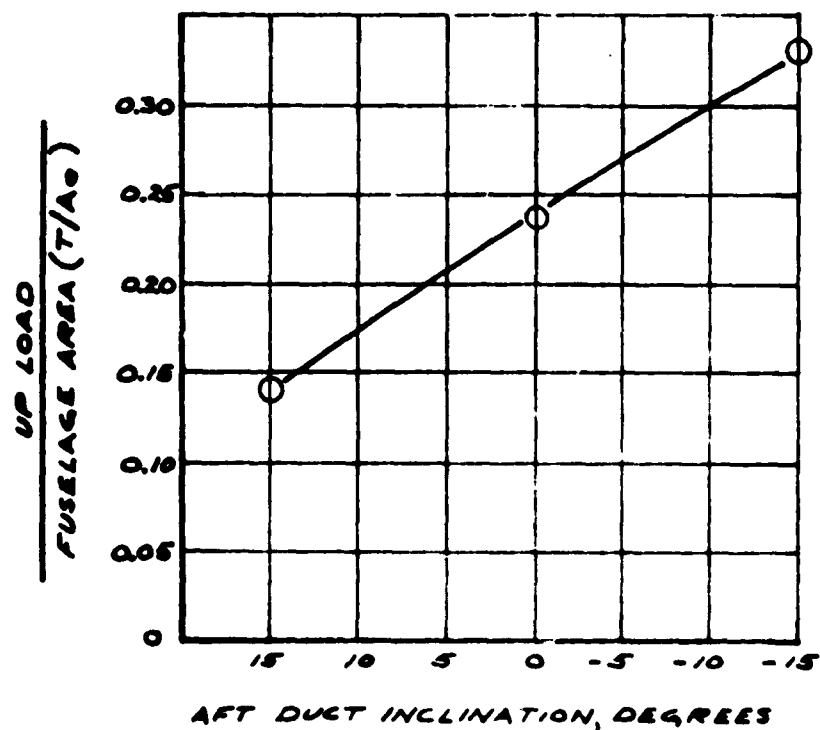
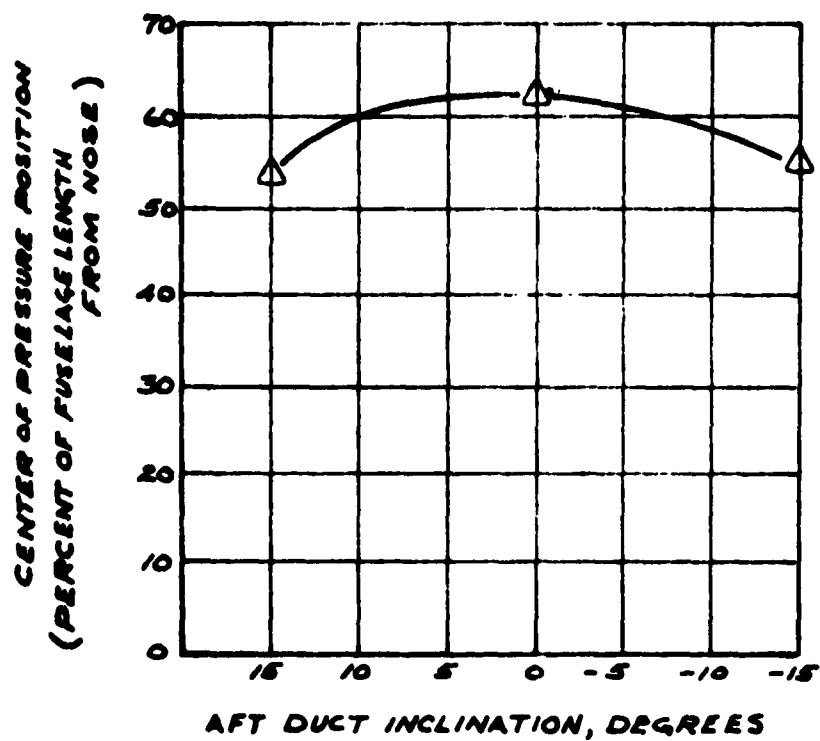


FIGURE 18. EFFECT OF LONGITUDINAL INCLINATION OF AFT DUCT ON FUSELAGE UPLOAD AND CENTER OF PRESSURE

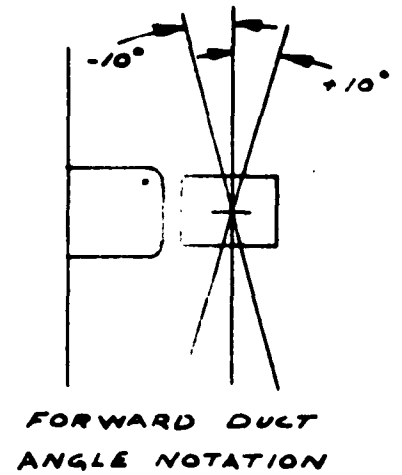
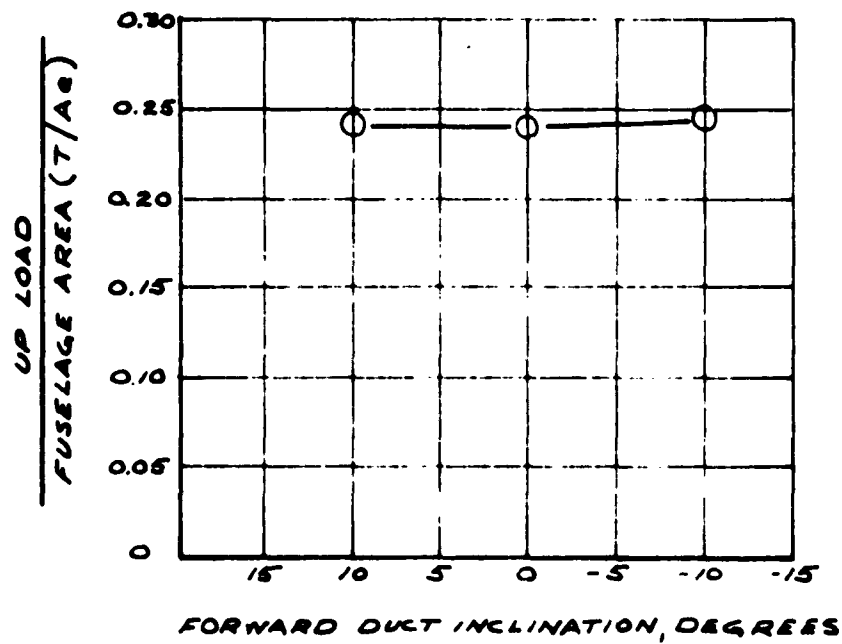
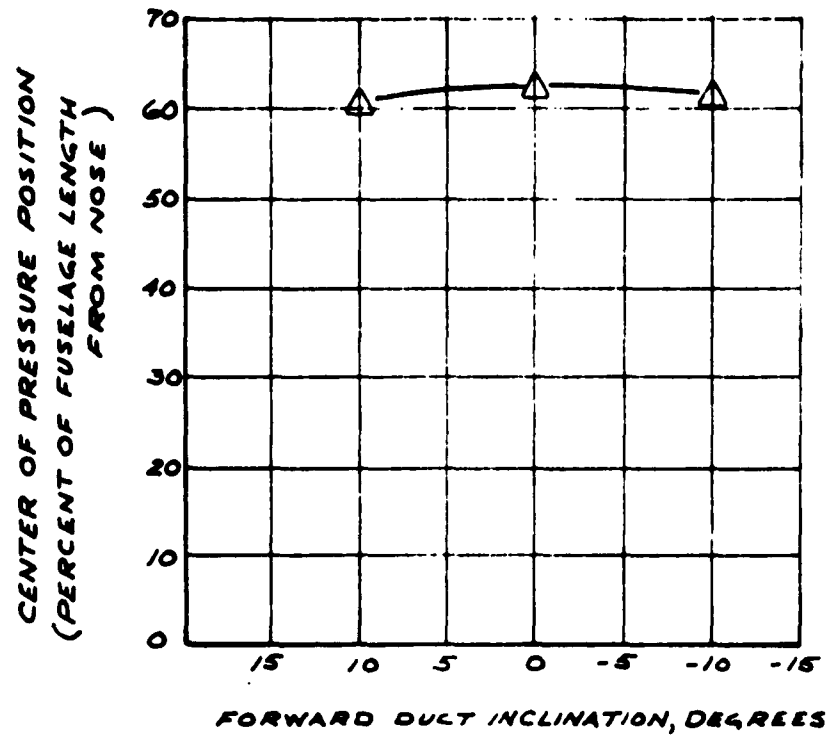


FIGURE 19. EFFECT OF LATERAL INCLINATION OF FORWARD DUCT ON FUSELAGE UPLOAD AND CENTER OF PRESSURE

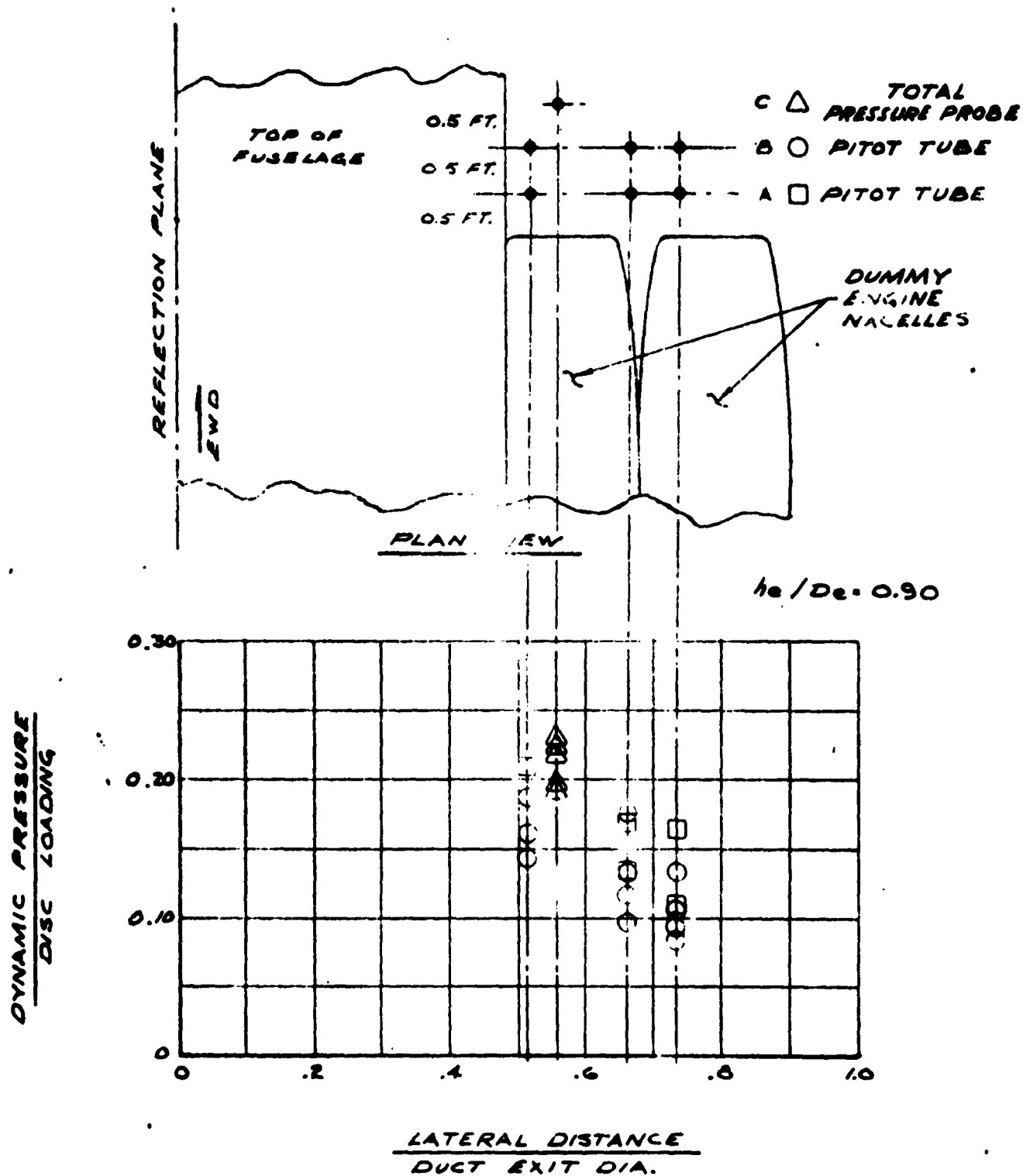


FIGURE 20. DYNAMIC PRESSURE OF UPWASH AT PLANE OF NACELLES.  
(1.20 DIA. ABOVE GROUND)

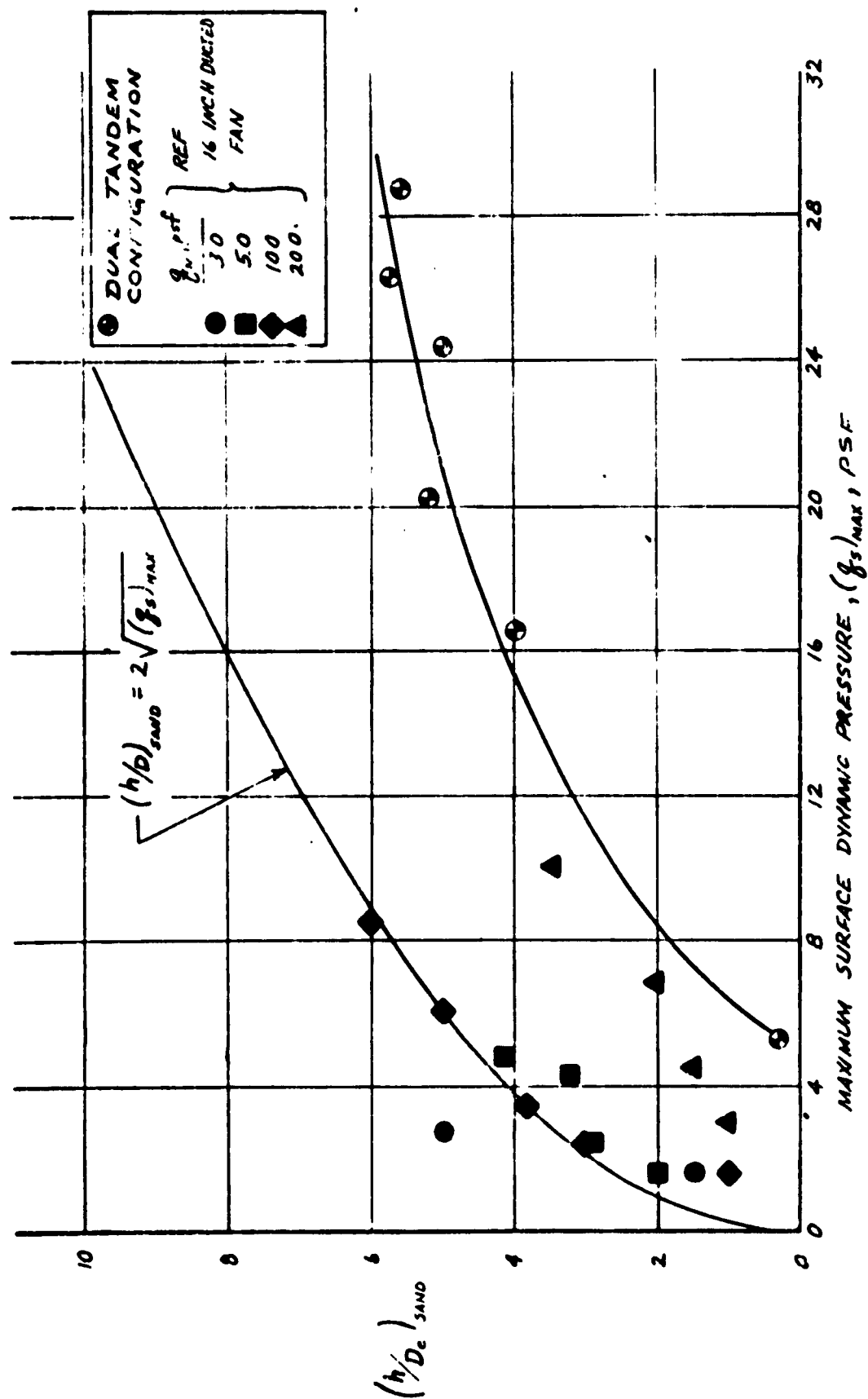


FIGURE 21. HEIGHT WHICH SAND CLOUD ATTAINED FOR VARIOUS SURFACE DYNAMIC PRESSURE

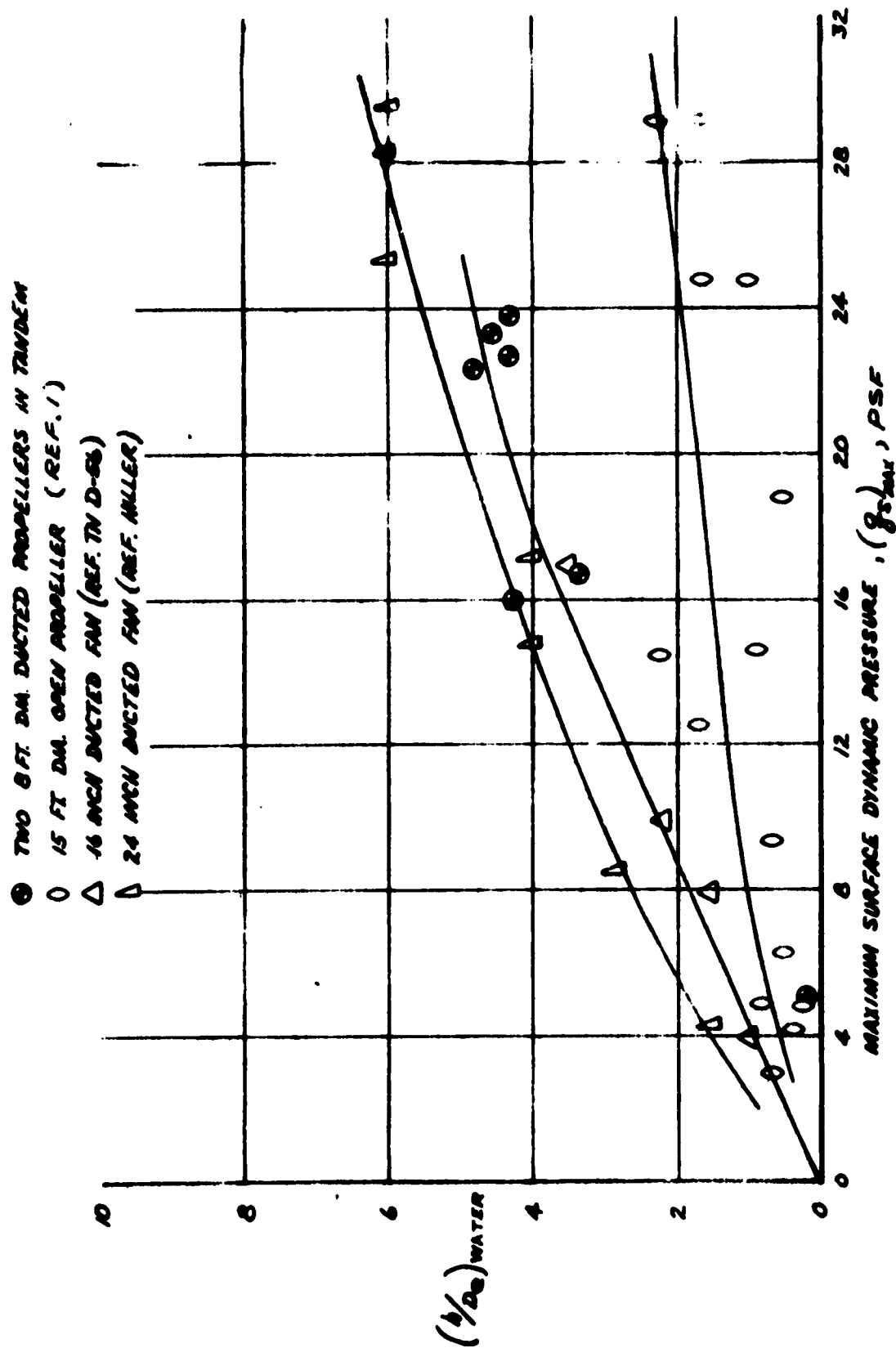


FIGURE 22. HEIGHT AT WHICH WATER SPRAY WAS OBSERVED FOR VARIOUS SURFACE DYNAMIC PRESSURES

NOTES : 1.  $\Delta \textcircled{1}$  DENOTE 20 KNOT WIND  
 RUNNING AFT TO FORWARD  
 2. TRACE OF SAND WAS  
 NOTED AT  $T/A_0 = 5 \text{ PSF}$

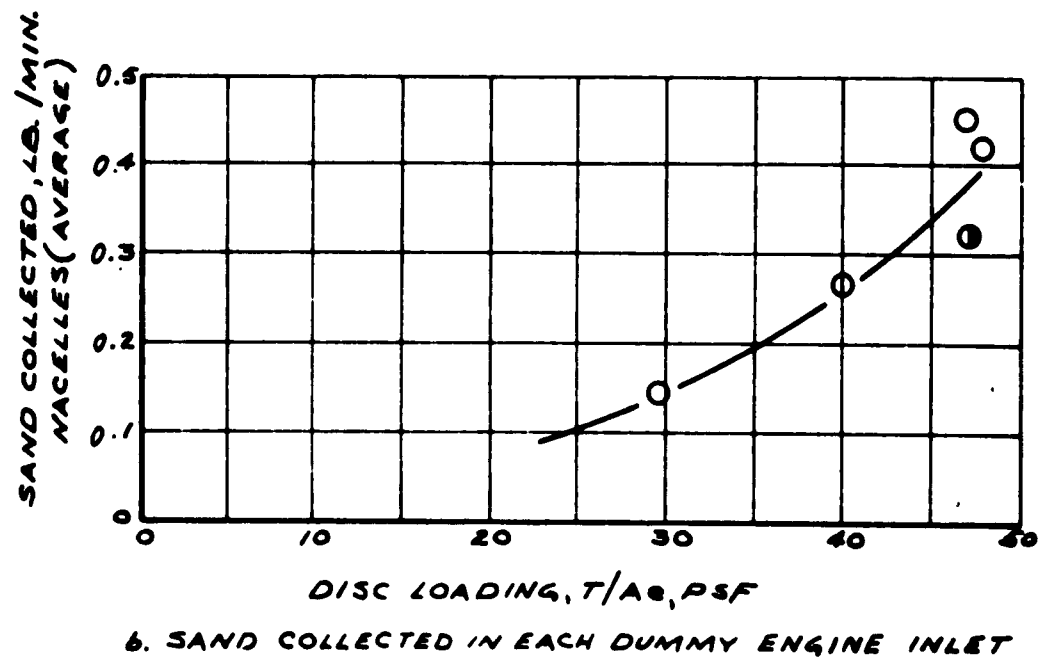
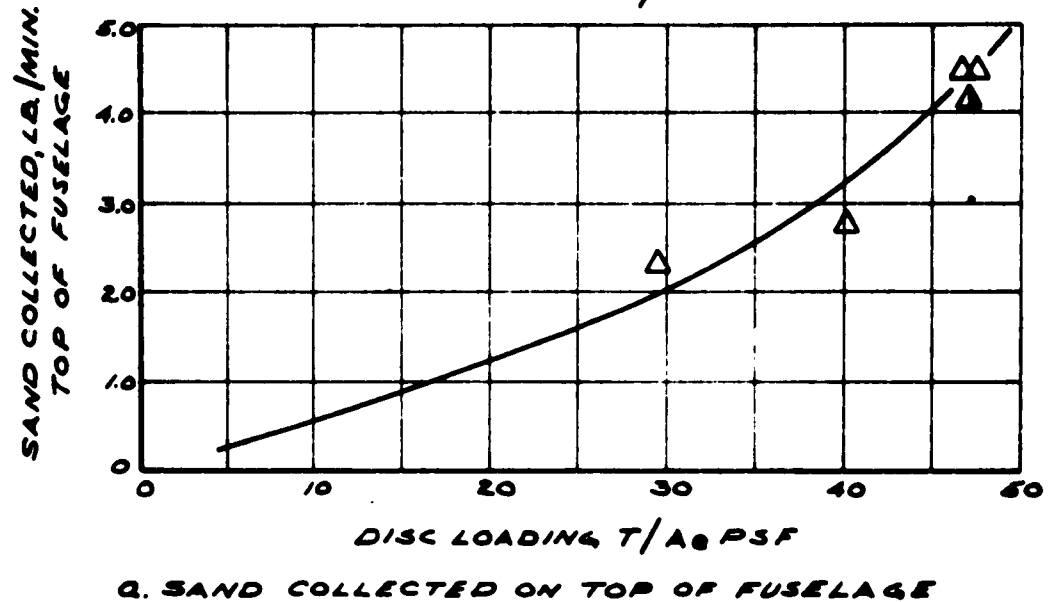


FIGURE 23. EFFECT OF DISC LOADING ON TERRAIN TRANSPORTATION



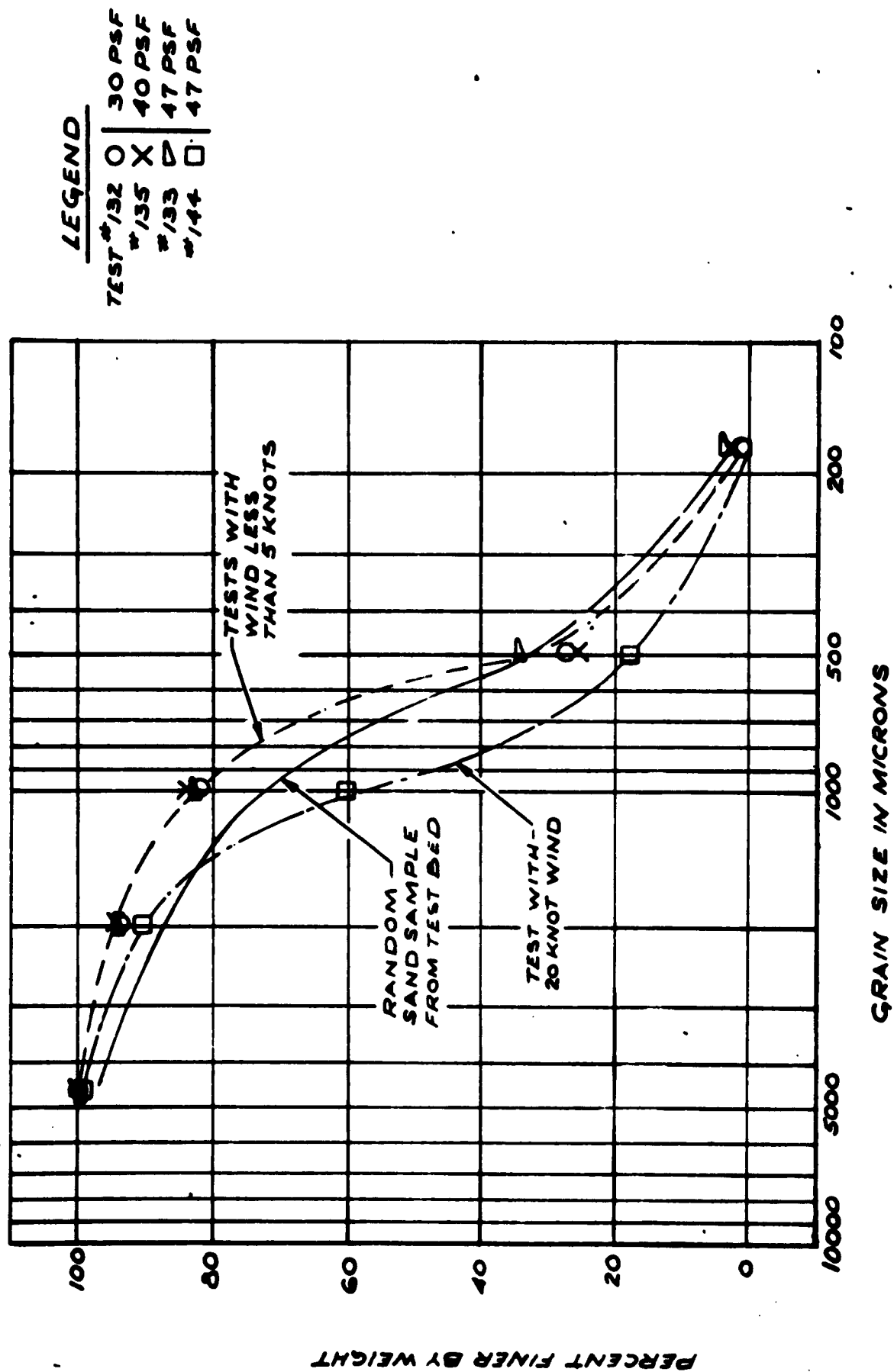


FIGURE 24. SIEVE ANALYSIS OF SAND PARTICLES COLLECTED ON TOP OF FUSELAGE FOR VARIOUS DISC LOADINGS

# **LEGEND**

SYMBOL	TEST NO.	DISC. LOADING	AFT DUCT INCLINATION ANGLE
○	132	30 PSF	0
×	133	40 PSF	0
△	133	47 PSF	0
□	144	47 PSF	0

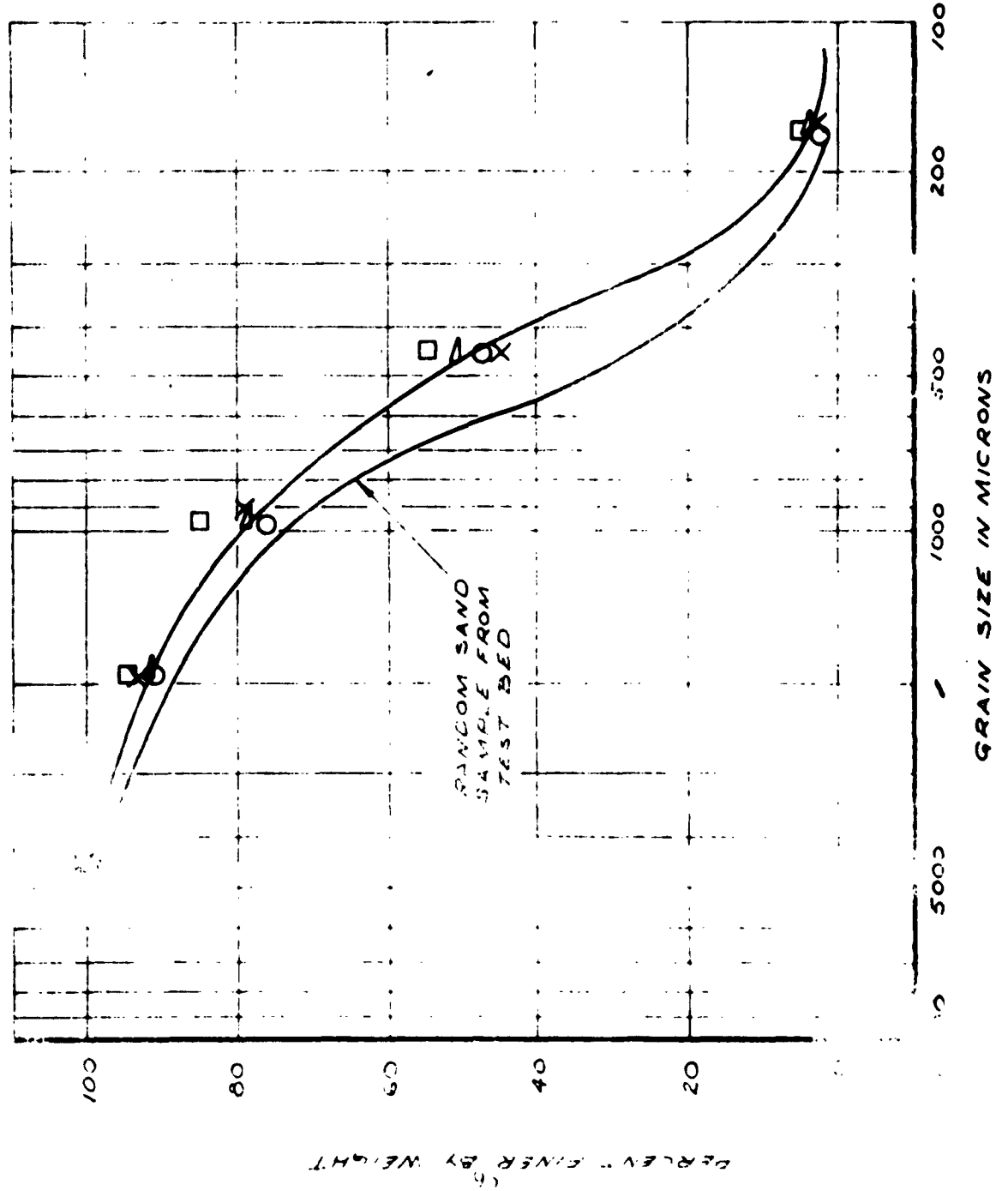


FIGURE 25. SIEVE ANALYSIS OF SAND PARTICLES COLLECTED IN ENGINE NACELLES FOR VARIOUS DISC LOADINGS

FT.LBS.

AFT TORQUE 3386

FWD. TORQUE 3105

TEST No. 133

MARCH 20, 1963

AFT PROP. 1540 RPM.

FWD. PROP. 1560 RPM.

THRUST

FWD. DUCT 1360#

AFT DUCT 1350#

FWD. DUCT 1240#

AFT DUCT 1910#

OSCILLATION OF PERCENT  
STEADY STATE VALUE

2.6 SEC.

PERIOD OF HIGHER FREQUENCY  
OSCILLATION 0.13 SECONDS.

FIGURE 26. PORTION OF TYPICAL OSCILLOGRAPH RECORD OF DUCTED PROPELLER OPERATIONS  
SHOWING AERODYNAMICALLY INDUCED OSCILLATIONS OF THRUST AND POWER

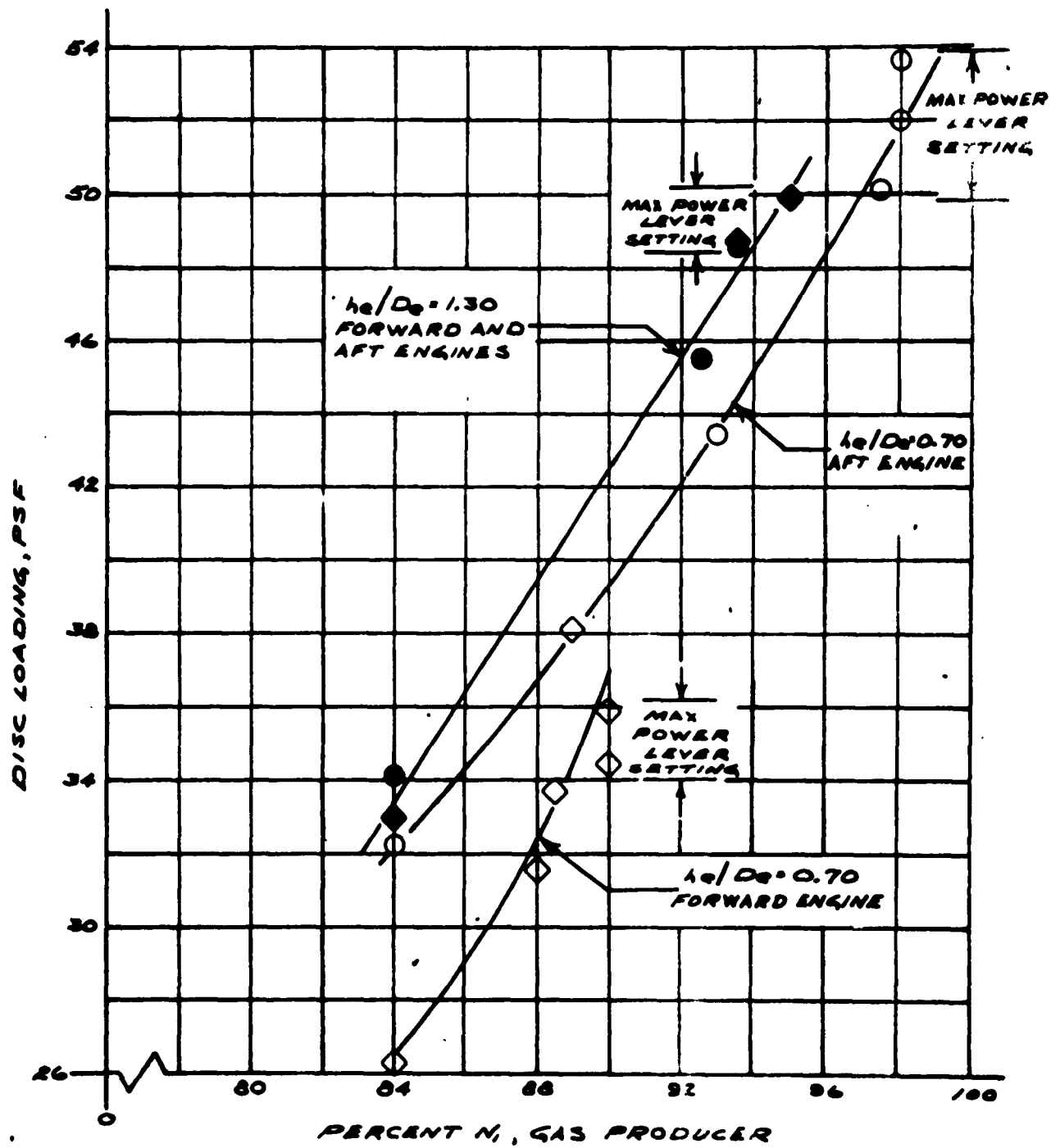


FIGURE 27. EFFECT OF OPERATING HEIGHT ON PERFORMANCE OVER WATER (T-2 CONFIGURATION)

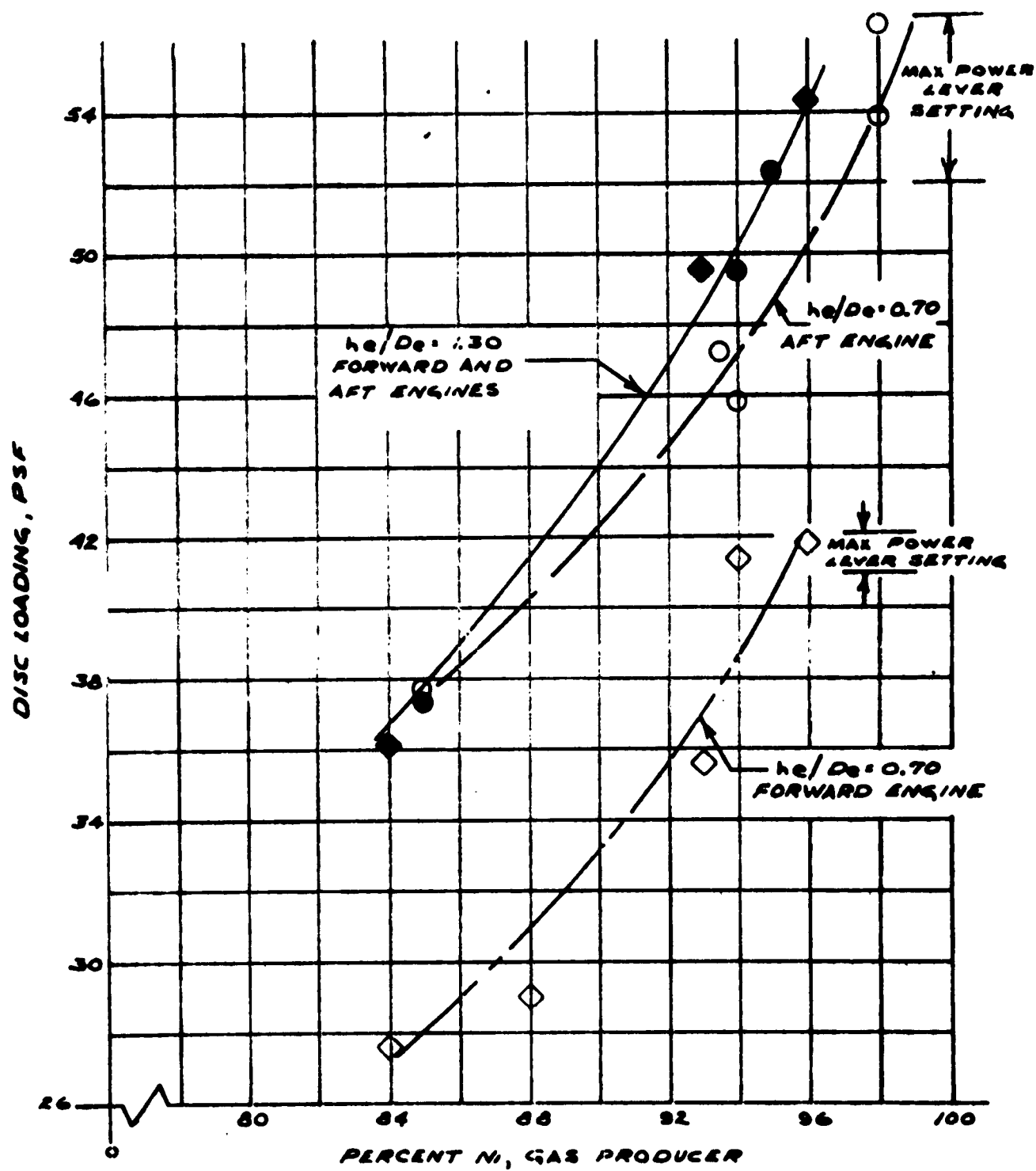


FIGURE 28. EFFECT OF OPERATING HEIGHT ON PERFORMANCE OVER WATER (T-5 CONFIGURATION)

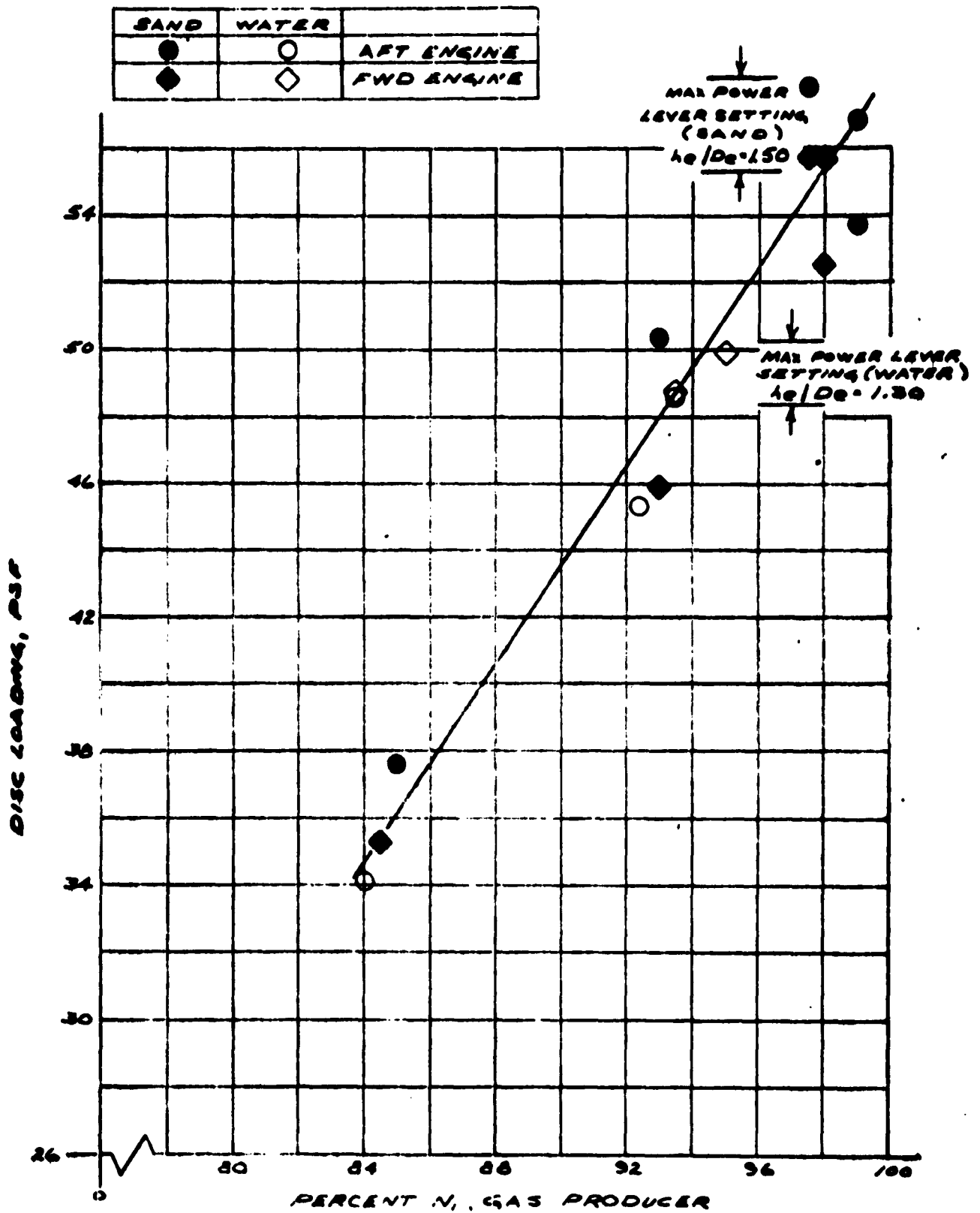


FIGURE 29. EFFECT OF TERRAIN ON GAS PRODUCER PERFORMANCE (T-2 CONFIGURATION)

CONFIGURATION	SYMBOL	
	SAND	WATER
$T_2$	■	□
$T_3$		◇

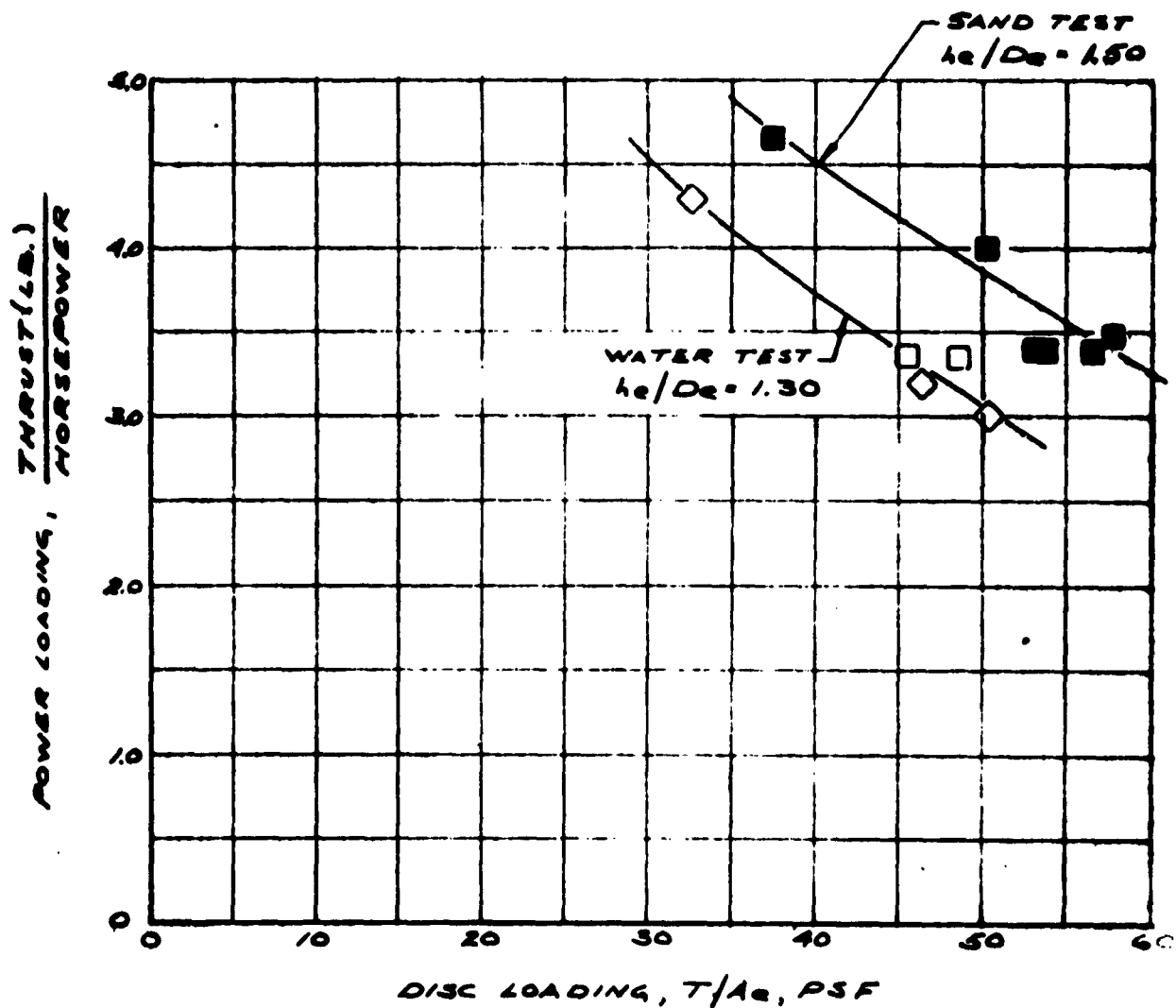


FIGURE 30. EFFECT OF TERRAIN ON AFT DUCTED PROPELLER POWER LOADING

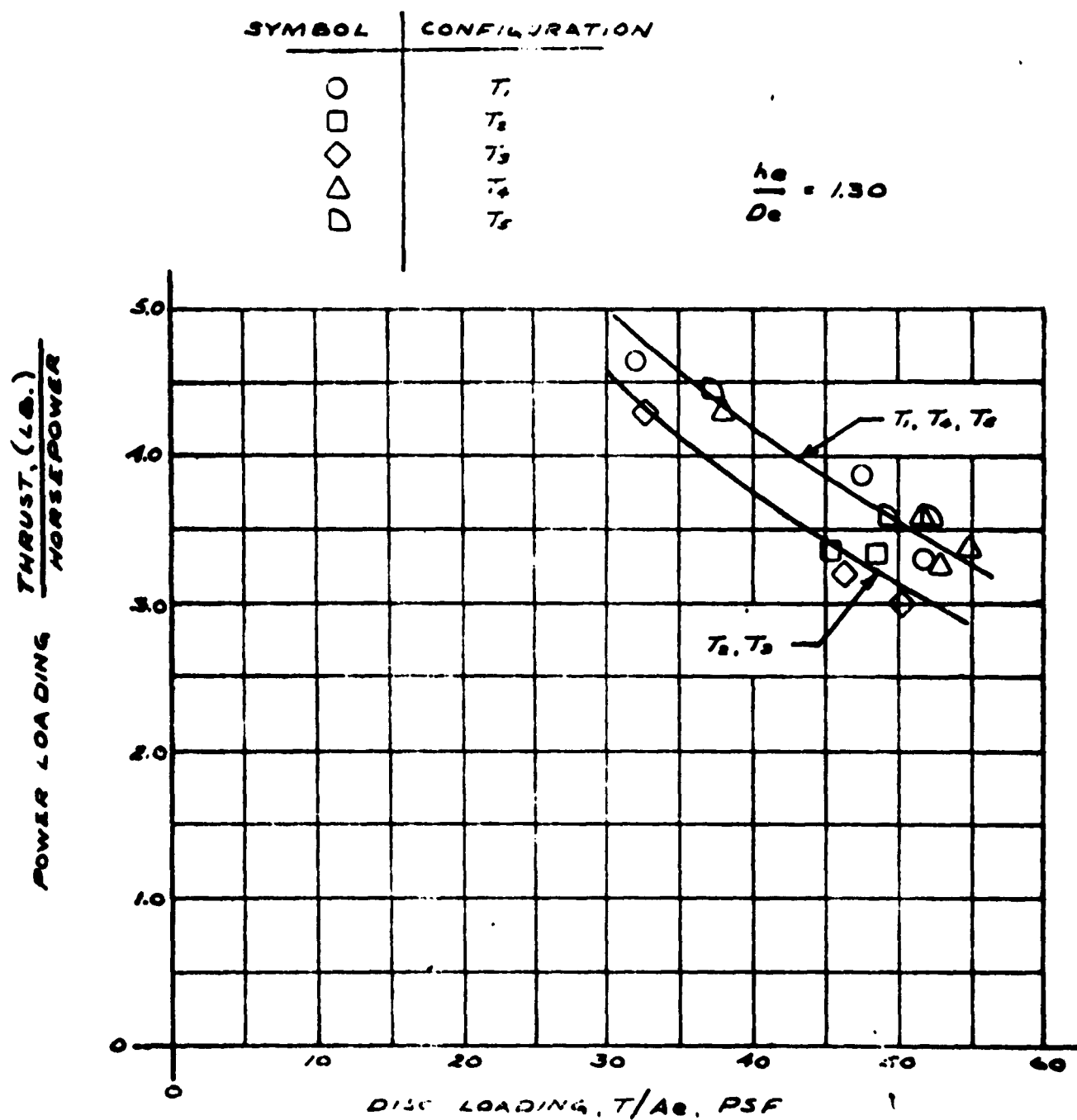


FIGURE 31. EFFECT OF CONFIGURATION ON AFT DUCTED PROPELLER POWER LOADING OBTAINED DURING TESTS OVER WATER



CONFIGURATION	FORWARD ENGINE	AFT ENGINE
MODIFIED	◇	○
T-2	—	●

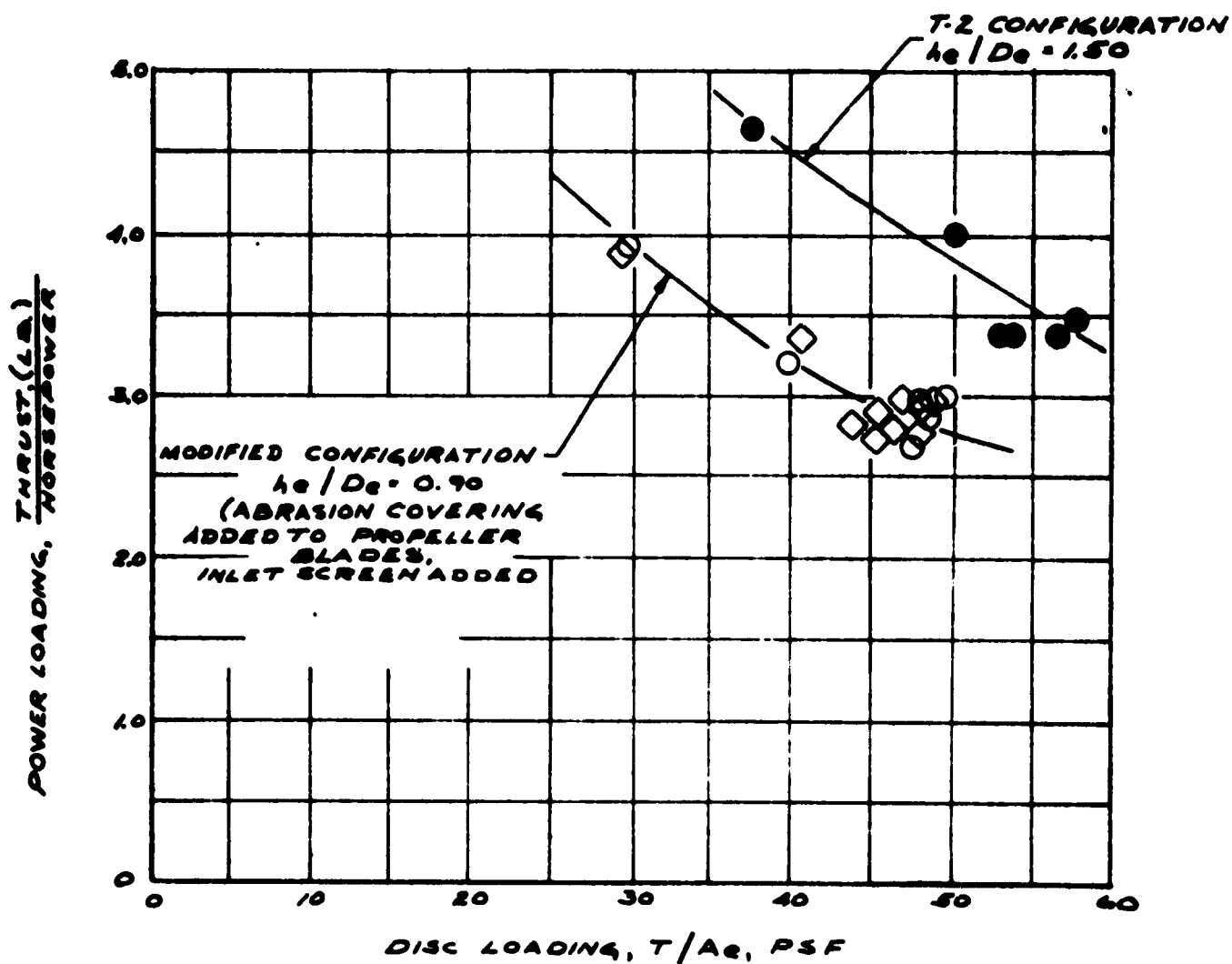


FIGURE 32. EFFECT OF HEIGHT AND CONFIGURATION ON POWER LOADING OBTAINED DURING TESTING OVER SAND

	FORWARD ENGINE	AFT ENGINE
SINGLE ENGINE RUNS WITH SCREEN	◇	○
SINGLE ENGINE RUNS NO SCREEN	◈	◉
DOUBLE ENGINE RUNS	◆	●

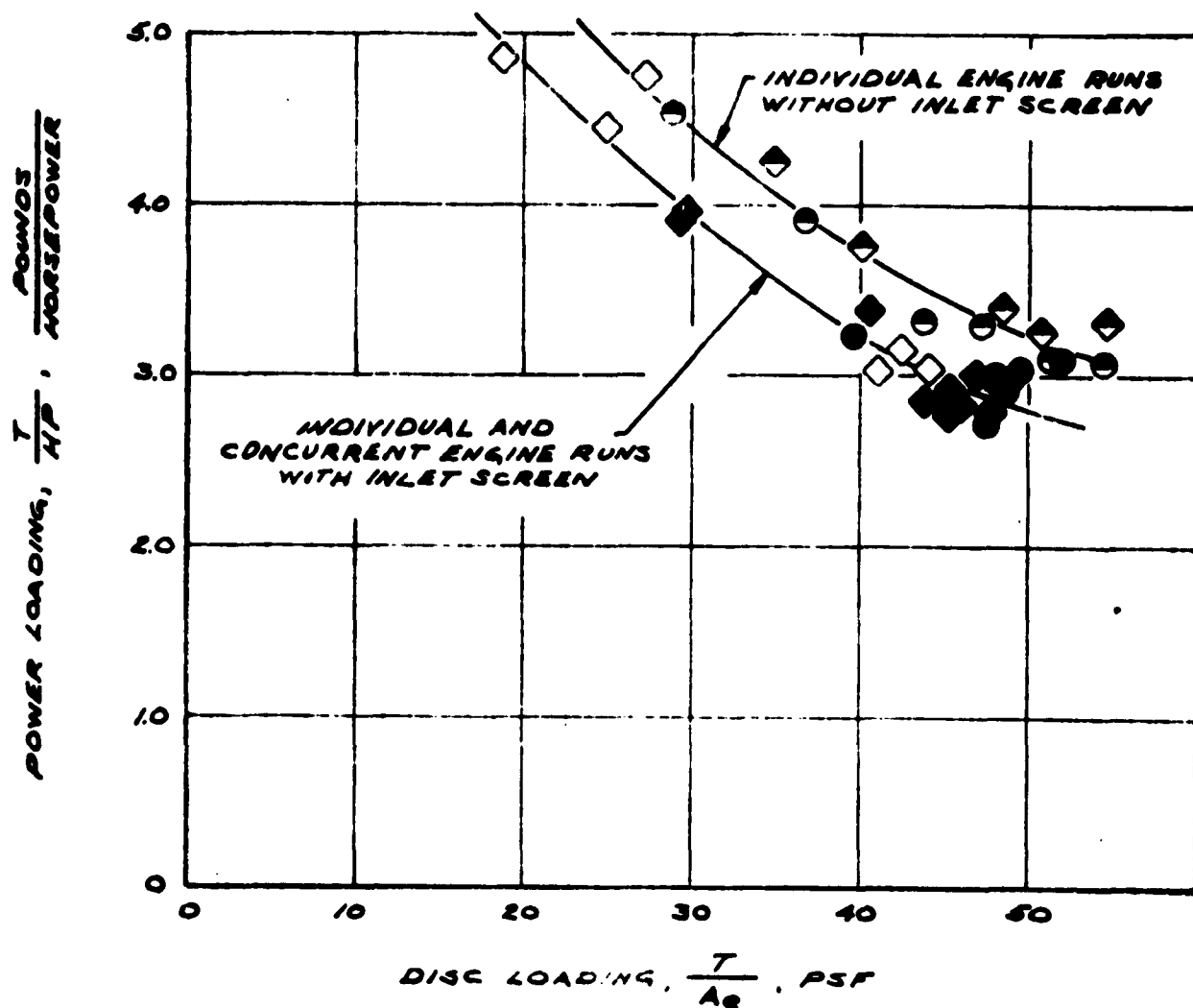
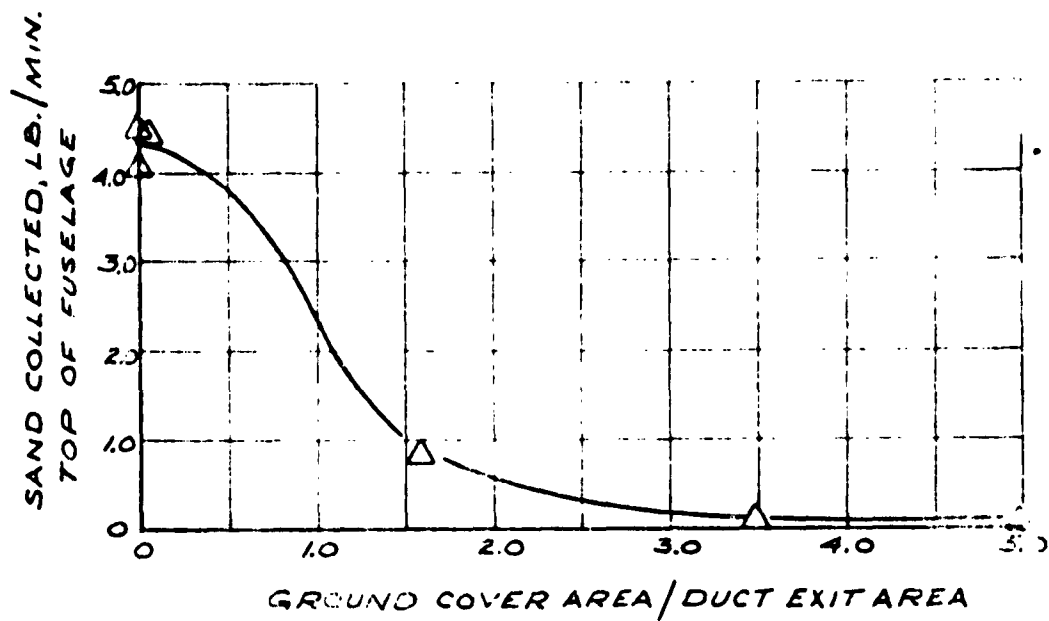


FIGURE 33. EFFECT OF INLET SCREEN ON POWER LOADING AT  $h_e/D_e = 0.90$  FOR MODIFIED CONFIGURATION



$$R_c/D_e = 0.90$$

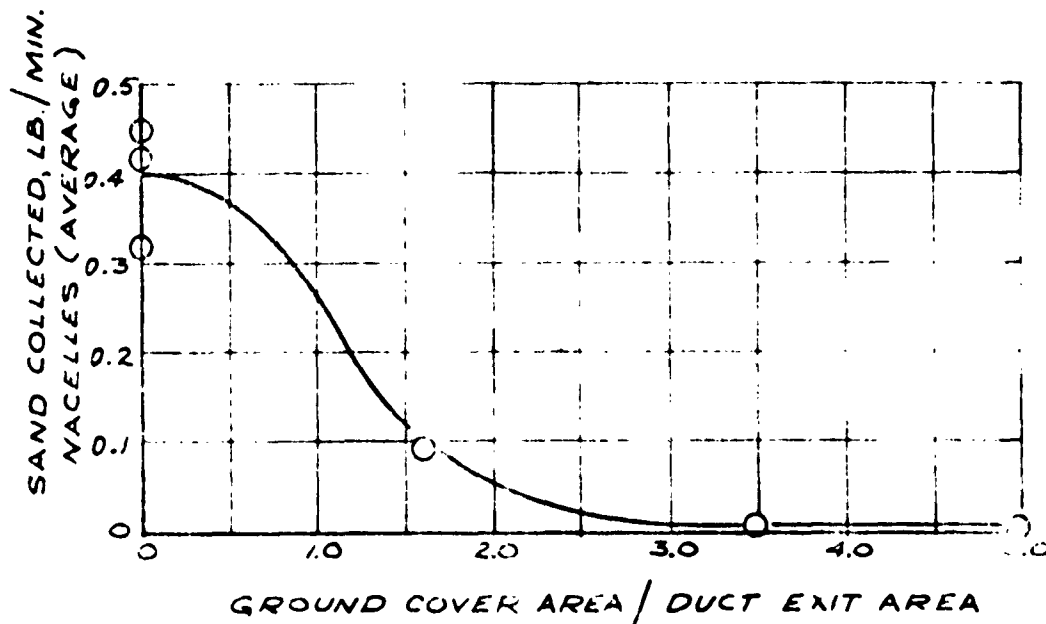
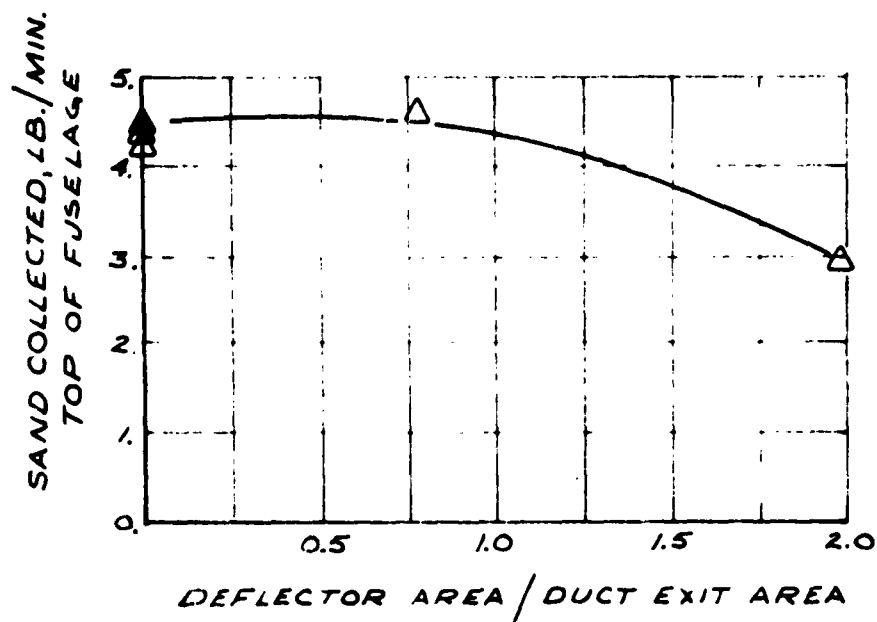


FIGURE 34. EFFECTIVENESS OF GROUND COVER IN PREVENTING RE-CIRCULATION (DISC LOADING = 50 PSF)



$$h_e/D_e = 0.90$$

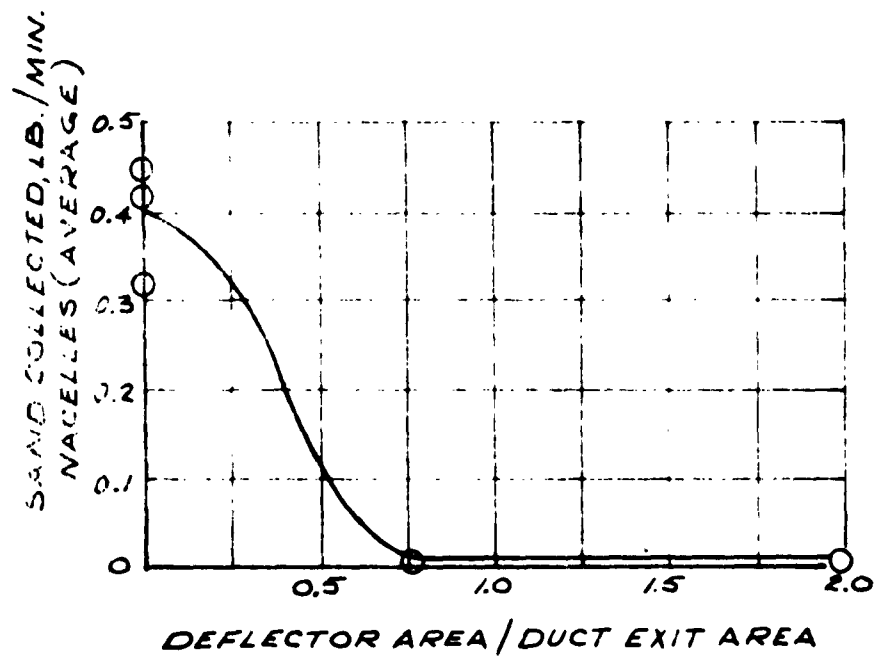
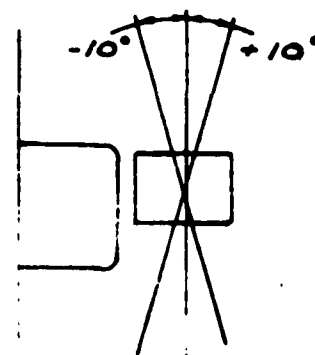
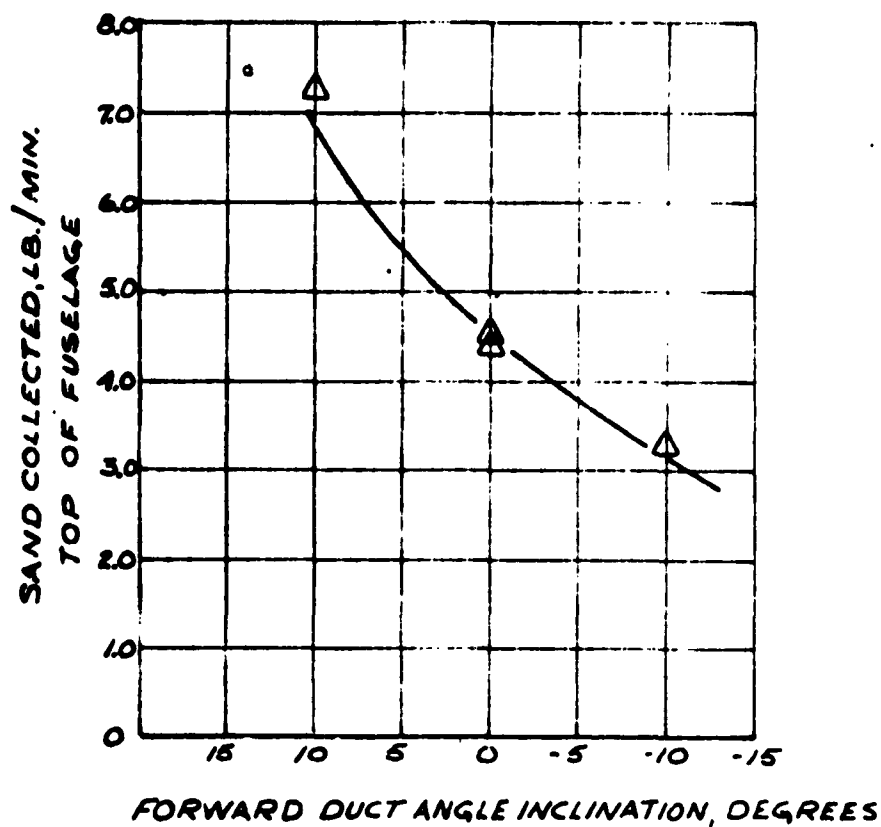
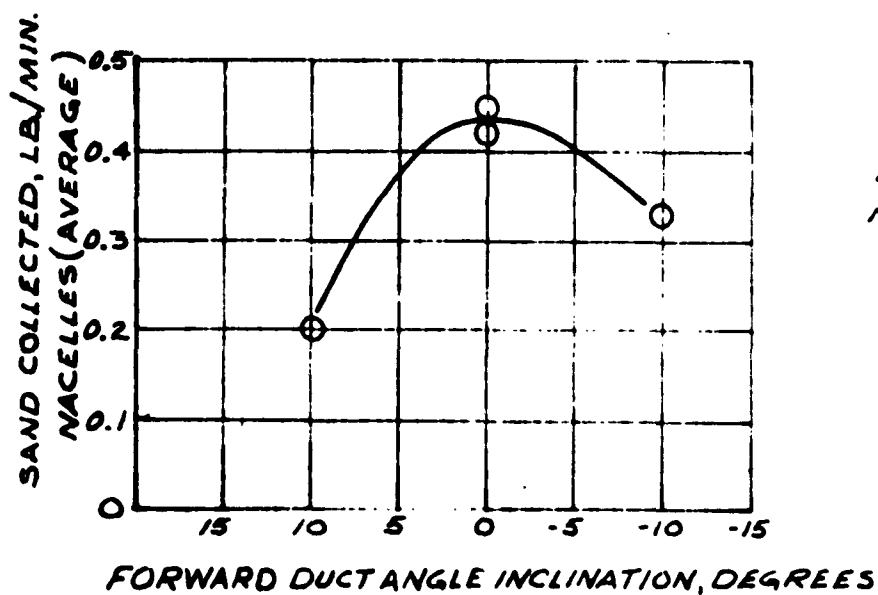


FIGURE 35. EFFECTIVENESS OF DEFLECTOR WING IN PREVENTING PARTICLE RECIRCULATION (DISC LOADING = 50 PSF)



**FORWARD DUCT ANGLE NOTATION**



**FIGURE 36. EFFECT OF LATERAL INCLINATION OF FORWARD DUCT ON PARTICLE RECIRCULATION (DISC LOADING = 50 PSF)**

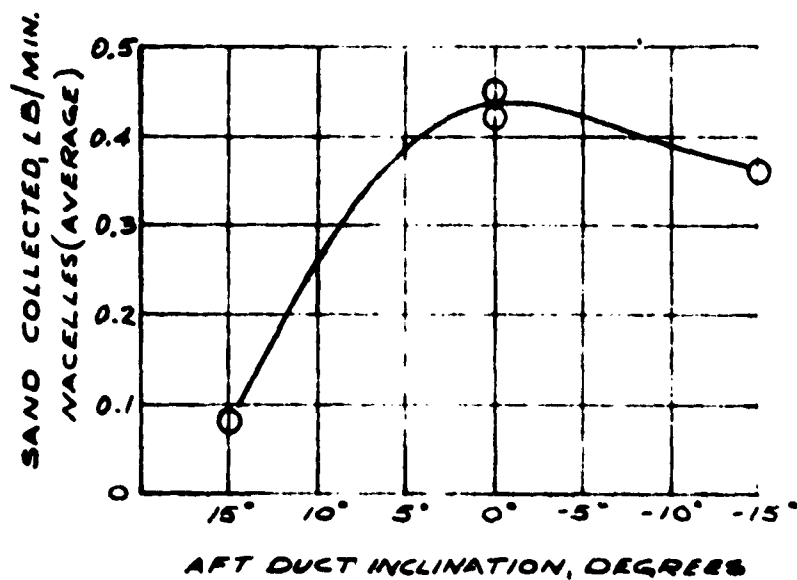
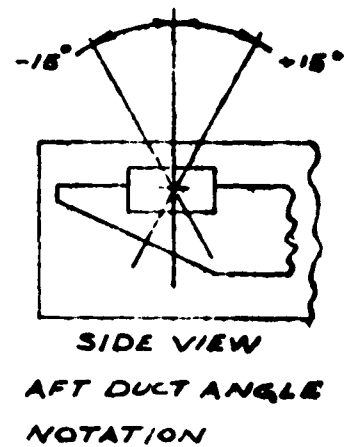
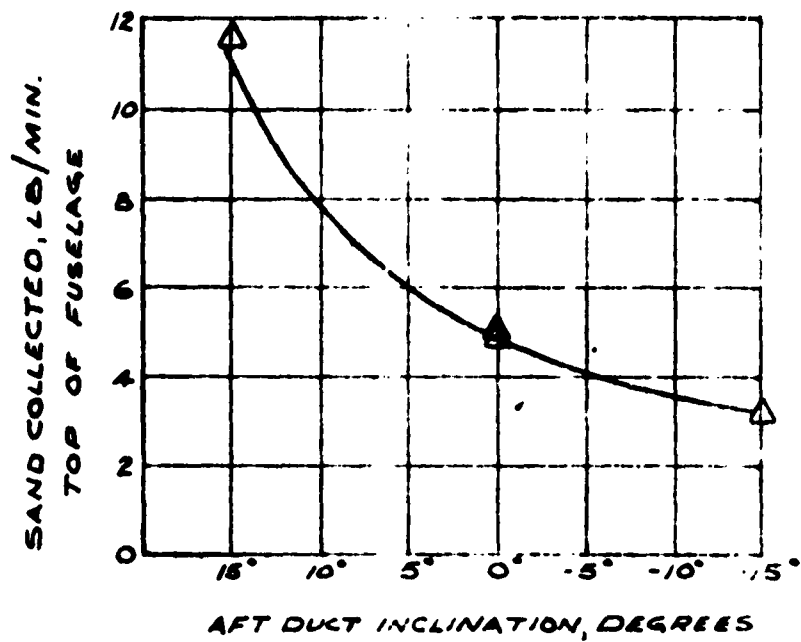


**FIGURE 37. EFFECT OF LONGITUDINAL INCLINATION OF AFT DUCT ON PARTICLE RECIRCULATION (DISC LOADING = 50 PSF)**



a) Vinyl Tape Leading Edge Abrasion Strip After One Minute Run At Maximum Power



b) Leading Edge Damage

FIGURE 38. PROPELLER SURFACE AND LEADING EDGE EROSION  
EXPERIENCED DURING TESTS OVER WET SAND.  
( $h/D_e = 1.48$ )

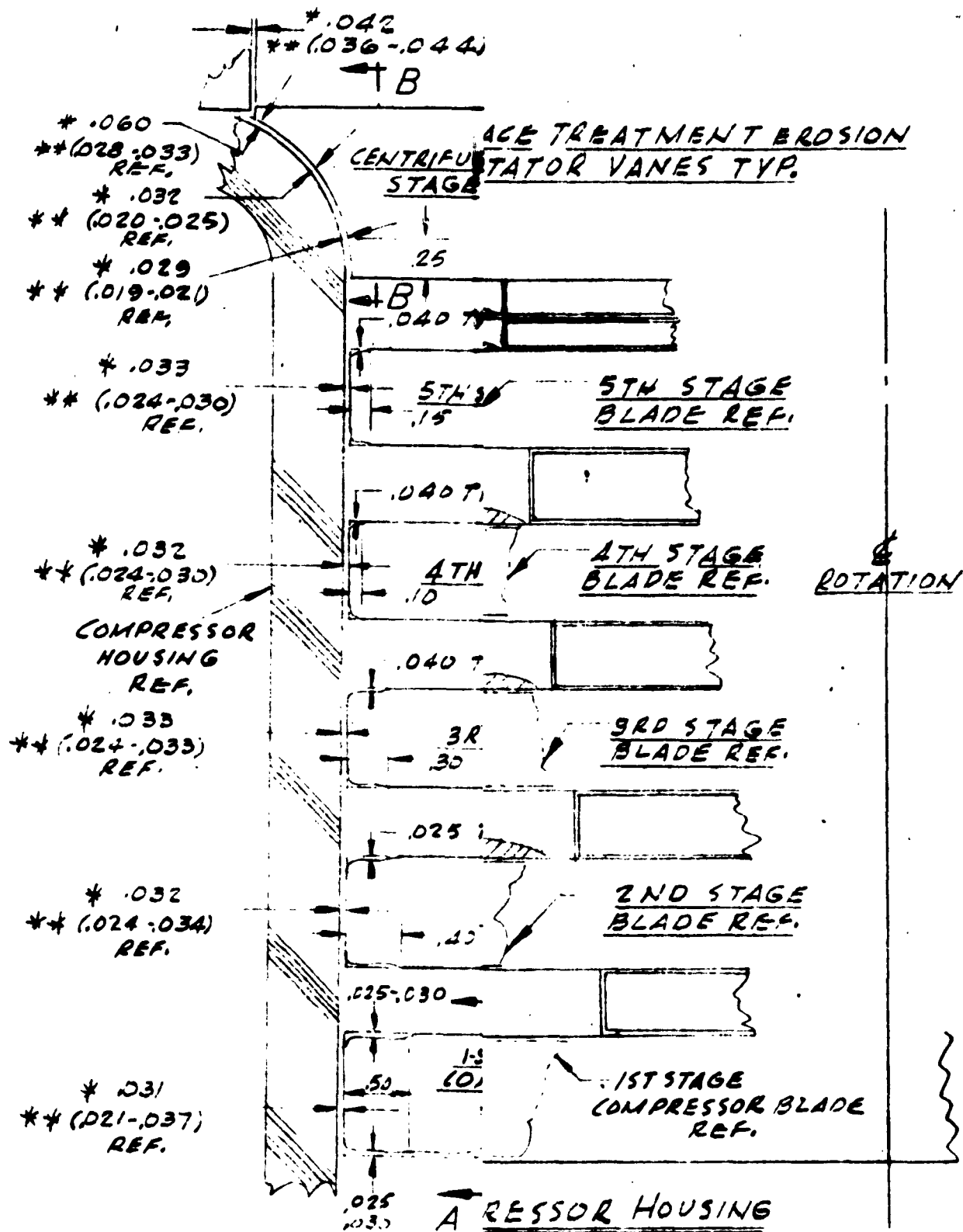


FIGURE 39. PHOTOGRAPH SHOWING EROSION OF STREAMLINE STRUT USED FOR SUPPORTING THE ENGINE WITHIN THE DUCT





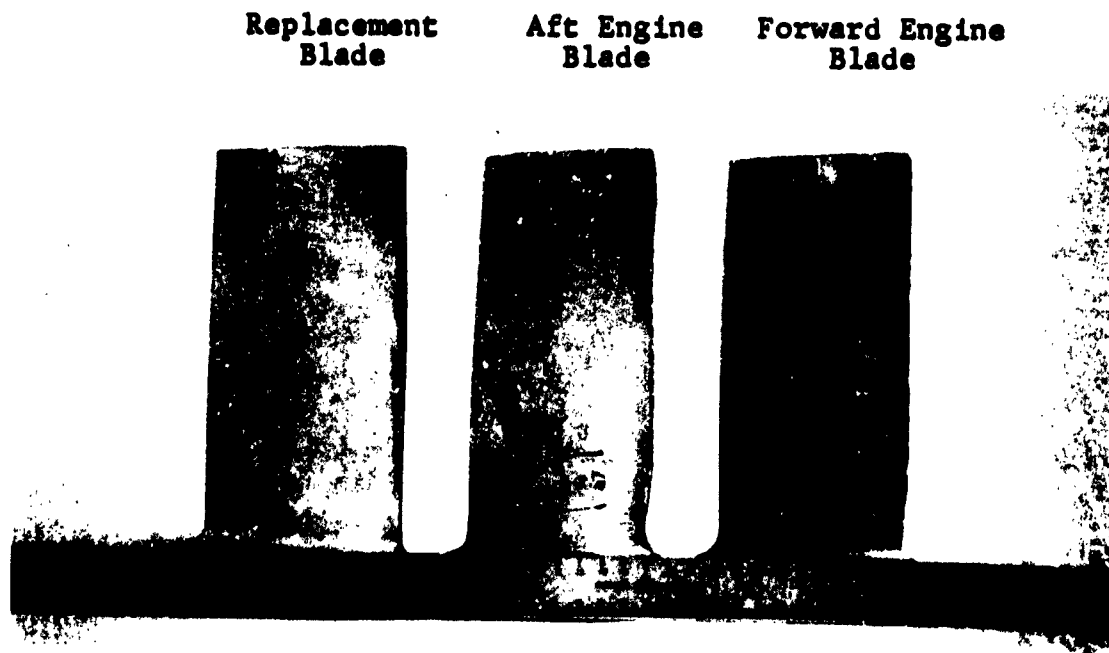
FIGURE 40. BOTTOM SURFACE OF AFT PROPELLER BLADE SHOWING FAILURE OF NEOPRENE ABRASIVE COVERING AFTER FIVE MINUTES OF MAXIMUM POWER OPERATION OVER SAND



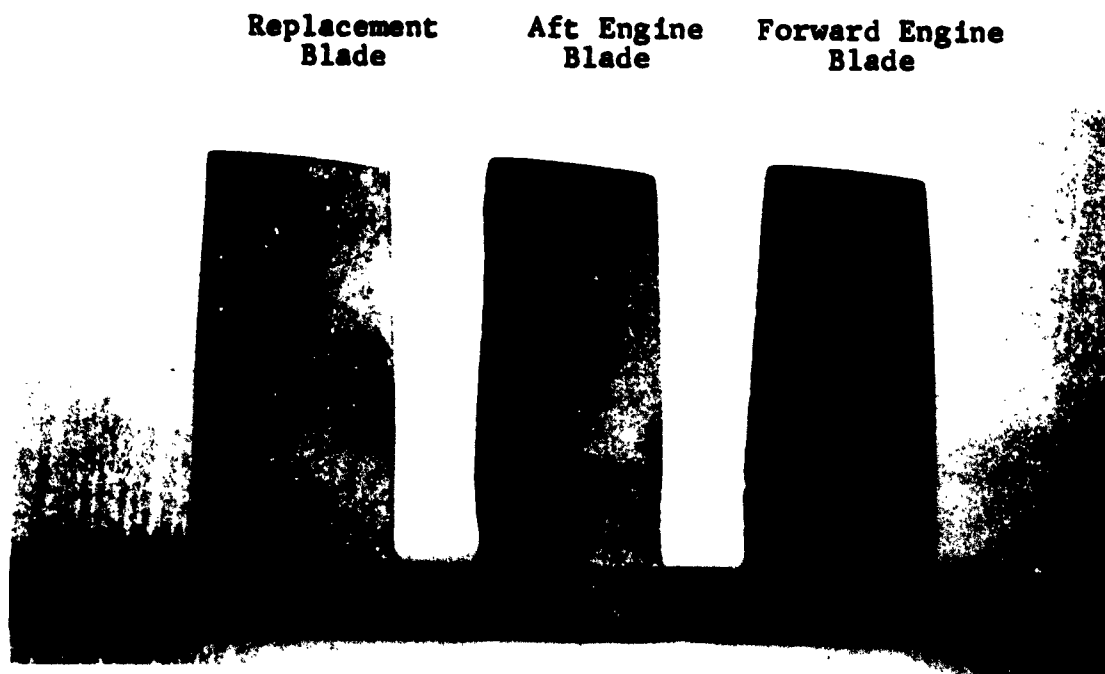
HOWING DAMAGE TO COMPRESSOR  
 \* ACTUAL CLEFT T53 ENGINE DOWNWASH  
 \*\* MANUFACTU



FIGURE 42. FIRST STAGE COMPRESSOR OF YT-53L3 TURBINE ENGINE USED TO POWER AFT DUCTED  
PROPELLER SHOWING DAMAGE DUE TO SAND INGESTION



a) Downstream Side Of Blades



b) Upstream Side Of Blades

FIGURE 43. COMPARISON OF FIRST STAGE COMPRESSOR BLADES OF T-53 ENGINES- SHOWING DAMAGE DUE TO SAND INGESTION

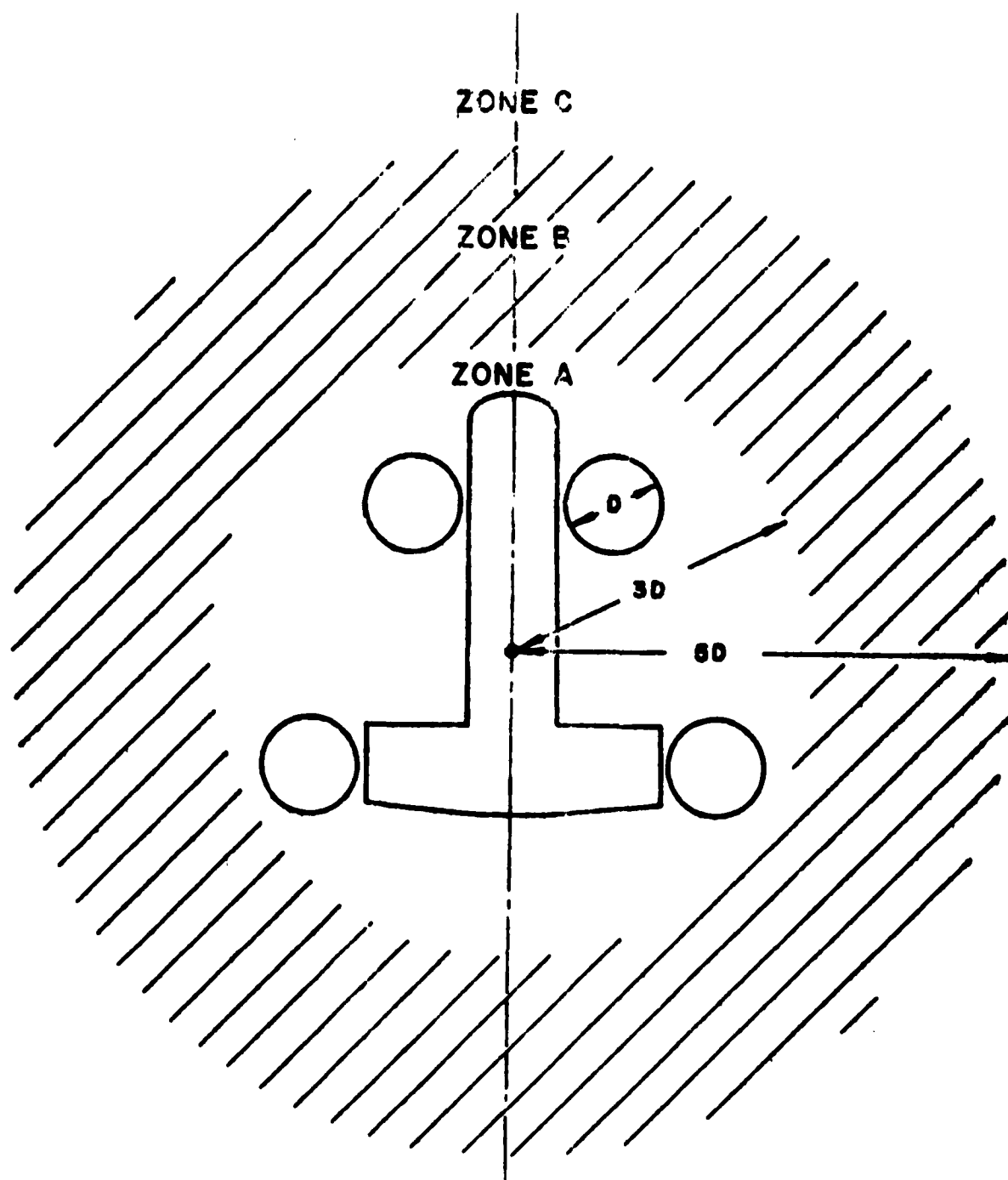


**FIGURE 44: ILLUSTRATION OF ZONES USED IN EVALUATING OPERATIONAL ENVIRONMENT**

$$C_{TH} = \frac{T}{\rho n^2 d_p^4}$$

$$C_{PH} = \frac{2\pi Q}{\rho n^2 d_p^5}$$

T = TOTAL THRUST  
Q = TORQUE  
n = RPM  
d<sub>p</sub> = DIAMETER OF PROPELLER

KAC TEST DATA  
+ SAND A/D = 1.5  
O SAND A/D = 1.0

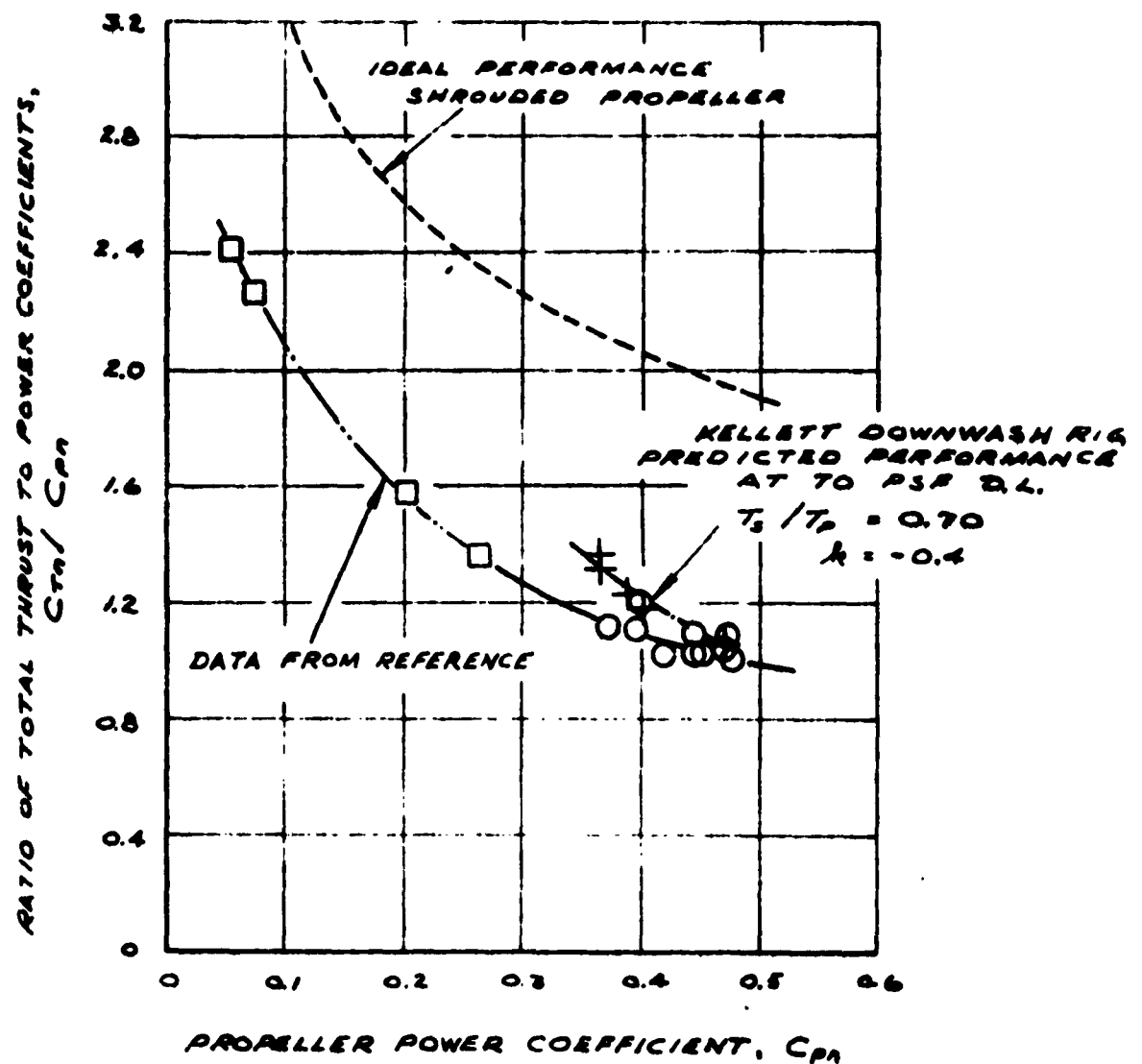


FIGURE 45. COMPARISON OF PREDICTED AND EXPERIMENTAL DUCTED PROPELLER STATIC PERFORMANCE DATA